SUMMARY OF

A STUDY OF JET FLOW AND REATTACHMENT IN CONTROL VALVES.

A thesis submitted to the University of Glasgow for the degree of Doctor of Philosophy

by

R.D.BEGG, B.Sc.

The Engineering Laboratories,
The University
Glasgow.

May, 1965.

NAME	ADDRESS AND AFFILIATION	DAT

Summary.

The work continues investigations into the characteristics of piston control valves; in particular it examines fluid flow through constrictions similar to the valve port.

The various flow phenomena associated with piston valves are reviewed, then a closer study is made of reports examining more specific aspects of the flow including separation, jet flow reattachment and turbulent entrainment. From these reports a mathematical model of the entrainment process inside valves is constructed for incompressible flow, and predictions of reattachment bubble lengths obtained for various port geometries.

Experimental results obtained using a two-dimensional model of the valve port show that the measured bubble lengths bear the same relationship to the predictions as is found in two other investigations of reattaching jet flow in similar configurations which are analysed on the same basis.

A further study of reports on compressible jet flow yields three methods to predict the jet angle of compressible flow through the valve geometry, and one is used to obtain theoretical values of jet angle and thickness over a range of geometries and pressure ratios.

Further experimental results, obtained from the same valve model, verify the predictions of jet angle and establish the characteristics of the compressible bubble throughout a wide

range of pressure ratios and orifice dimensions. During the test several distinct patterns of supersonic flow were observed using a schlieren light system and recorded by photographing them.

From consideration of the measurements and theoretical predictions some explanation is offered for the observed bubble behaviour and the various flow patterns. Finally the effect of these characteristics on the performance of piston valves is discussed and an attempt made to describe previously reported valve behaviour in terms of the measured bubble flow patterns.

UNIVERSITY OF GLASGOW

In respect of my thesis [title to be inserted]

'A study of jet flow and reattachment in contral valve'

1. I understand that no access to it will be allowed without my prior permission until one year has elapsed from the date of its deposit in the University Library.

2. Thereafter:-

   * a. I give permission for it to be made available to readers in the University Library or within another library.

   * b. I do not wish it to be made available to readers for a further two years without my written consent or (failing a reply from me within 3 months to a request from the University Library) the consent of the Library Committee in consultation with the Higher Degrees Committee of the Faculty.

3. Once any restrictions on access have expired:-

   a. I give permission for a photocopy to be made by the British Library for lending to other libraries.

   b. I * give/do not give permission for the University Library to make photocopies for other libraries or individuals without my specific authorisation. Note : Any prohibition on photocopying will lapse after five years from the date of deposit.

2552

Signed

Date ...25.. July ... 67

* Strike out the sentence or phrase which does not apply.

A STUDY OF JET FLOW AND REATTACHMENT IN CONTROL VALVES.

A thesis submitted to the University of Glasgow for the degree of Doctor of Philosophy

by

R.D.BEGG, B.Sc.

The Engineering Laboratories,
The University,
Glasgow.

May, 1965.

Contents

Page		
ii	Summary	
iv	Acknowledgement	
v	Nomenclature	
1	Chapter 1.	Introduction and reviews of previous work.
37	Chapter 2.	Theoretical study of incompressible flow.
53	Chapter 3.	Experimental study of incompressible flow.
78	Chapter 4.	Theoretical study of compressible flow.
97	Chapter 5.	Experimental study of compressible flow.
115	Chapter 6.	Conclusions and suggestions for further study
124	List of references.	
130	Appendices.	

Summary.

The work continues investigations into the characteristics of piston control valves; in particular it examines fluid flow through constrictions similar to the valve port.

The various flow phenomena associated with piston valves are reviewed, then a closer study is made of reports examining more specific aspects of the flow including separation, jet flow, reattachment and turbulent entrainment. From these reports a mathematical model of the entrainment process inside valves is constructed for incompressible flow, and predictions of reattachment bubble lengths obtained for various port geometries.

Experimental results obtained using a two-dimensional model of the valve port show that the measured bubble lengths bear the same relationship to the predictions as is found in two other investigations of reattaching jet flow in similar configurations which are analysed on the same basis.

A further study of reports on compressible jet flow yields three methods to predict the jet angle of compressible flow through the valve geometry, and one is used to obtain theoretical values of jet angle and thickness over a range of geometries and pressure ratios.

Further experimental results, obtained from the same valve model, verify the predictions of jet angle and establish the characteristics of the compressible bubble throughout a wide

range of pressure ratios and orifice dimensions. During the tests several distinct patterns of supersonic flow were observed using a schlieren light system and recorded by photographing them.

From consideration of the measurements and theoretical predictions some explanation is offered for the observed bubble behaviour and the various flow patterns. Finally the effect of these characteristics on the performance of piston valves is discussed and an attempt made to describe previously reported valve behaviour in terms of the measured bubble flow patterns.

Acknowledgement.

The author would like to acknowledge his gratitude to his supervisor, Professor G.D.S.MacLellan, for his continued encouragement and assistance throughout the investigation, to S.L.Bragg Esq. and Dr. A.E.Mitchell for several very helpful discussions, and to the Department of Scientific and Industrial Research for their generous financial support.

Nomenclature.

Symbol	Description	Figure or page
a	valve opening	Fig. 1.3.
a'	valve clearance	Fig. 1.3.
A	area of flow	Fig. 4.4.
A.R.	aspect ratio	Page 68.
C	contraction coefficient	Fig. 4.6.
f	force defect coefficient	Page 92.
F	force defect	Fig. 4.4.
k	$1.818/\sigma$	Page 132.
$\dot{m}$	mass flow per second	Page 138.
p	static pressure above atmospheric	
q	fluid velocity	Page 134.
r	pressure ratio	
R	radius of curvature	Fig. 2.1.b.
R_e	Reynolds' number	Page 68.
T	static temperature	Page 64.
$T_{(\ )}$	$\tanh \frac{\sigma Y_{(\ )}}{X_{(\ )}}$	Page 43.
t	jet thickness at vena contracta	Fig. 1.4.a.
u,v	fluid velocity components	Fig. 4.1.
w	clearance ratio (a'/a)	Page. 4.
X,Y	coordinate system based on jet C.L.	Page 132
ρ	fluid density	Page 138.
σ	entrainment parameter	Page. 39.

Symbol	Description	Figure or pag
ψ	stream function	Page. 134.
φ	potential function (chapter 4.)	Page. 134.
φ	jet inlet angle	Fig. 2.8.b
ϑ	angle between jet C.L. and plane (chapter 2.
ϑ	angle of velocity vector in hodograph plane (chapter 4.)	Fig 4
$\delta_{(\ )}$	jet width at point $X_{(\ )}, Y_{(\ )}$	Page 131.
Δp	pressure drop across orifice	
ν	function of velocity used in chapter 4.	Page8
U	centreline velocity of fluid	Page 39.
ℓ	bubble length	Fig. 2.1.a

Suffices

a	atmospheric
b	average within bubble
i	incompressible
o	stagnation
R	on radial reattachment plane. Fig. 2.1.b.
v	vena contracta Fig. 1.3.
w	any point on upstream wall
(1),(2)	components in directions (1) and (2) Fig. 4.4
O,R	conditions at points O and R Fig. 2.8

Chapter 1.

Introduction.

1.1. Jet flow in control valves.

1.2. Previous work on piston slide valves.

1.3. The object of the investigation.

1.4. A review of work on incompressible jet flow.

1.5. A review of work on compressible jet flow.

1.1 The problem of jet flow in control valves.

A control valve is a device which constricts a passage through which fluid flows. The extent of the constriction, or more usually the amount of flow permitted, is controlled by setting an external lever or plunger. In normal operation the valve partially blocks the flow so that the velocity through the constriction is greater than that in the passage and the fluid accelerates towards the con trol orifice and decelerates away from it.

The increase of the fluid velocity in the neighbourhood of the constriction causes (by Bernoulli) a decrease in the static pressure exerted by the fluid on the walls of the passage upstream of the constriction. The integral of this pressure reduction is proportional to the total increase in fluid momentum, and the thru on each wall is proportional to the flow through the opening.

For accurate and easy control the flow through such a cont valve should have only one consistent value at each position of th control lever, however some types of valve exhibit a double char - acteristic over part of their range when two distinct relationship can be measured between lever position and total flow, either of which is possible depending on the previous history of the lever movement.

The type of valve investigated in this report is a spool or piston slide valve, illustrated on Figure 1.1.a. Below the drawing of the valve are diagrams (Figure 1.1.b.) showing the two

types of flow found through the valve constriction. Depending on the arrangement of the supply and exhaust ports in the body of the valve the fluid may flow radially inwards or outwards through the constriction.

Figure 1.1.b illustrates that the difference between the tw flow patterns is in the behaviour of the fluid after it has passed through the orifice, when the stream breaks away from the boundary walls in the form of a jet, and reattaches stably to either of the downstream walls. At small valve openings the jet reattaches to th walls marked AB, and at large openings to the walls CD. However at intermediate openings the position of the jet depends on whether the valve has opened or closed to the position in question. The flow through the orifice for a given pressure ratio is different f the two types of flow; measurements have shown that it may be up t ten percent greater when the jet is reattached to the walls AB, due to the effect of the low pressure bubble enclosed between the jet and the wall.

Although the effect of a sudden change of such a size in th flow coefficient is in itself a serious drawback to an effective control system, the change in the static pressure distribution on the walls AB can be an even more serious hinderance, especially when the wall AB is a radial face of the moving piston as in the inflow diagram of Figure 1.1.b. In the case of outflow, the total pressure thrust may only vary slightly as the flow changes, but the thrust may increase by as much as double for the inflow model since the pressure in the bubble is low and it may extend over mos

of the area of the piston face. It was this change which spoiled early attempts to calculate reaction forces using assumptions whic neglect reattachment.

An accurate knowledge of the size of the reaction force is important in the design of control systems since this force may be the major part of the force required to operate the valve. If there is any elasticity in the system initiating the spool movemen then the reaction force can alter the spool positioning causing non – linearity and possibly instability. Sudden changes in the force caused by jet instability are therefore most detrimental to the operation of a practical control valve.

Another effect causing non – linearity is the change in jet angle caused by clearancebetween the spool and the valve body, which is necessary for operation of the valve, and may be enlarged by wear and erosion due to cavitation (caused by low pressures in the bubble). This effect, found at small valve openings, is illustr ated in Figure 1.2. When the valve is opened wide the ratio of clearance (a') to the valve opening (a) is small and the jet angle φ is 21° as shown in diagram 1. As the valve closes the ratio of a' to a increases and the angle φ also increases. At $a' = a$, φ is 45° and as a decreases to 0, φ increases to 69° as shown in 4. As the angle φ changes the jet reattachment shifts from wall AB to CD. These effects cause non – linearity in both the flow coefficient and reaction force around the position of zero flow, that is in the middle of the working range. Similar effects are produced if the corners making up the constriction become rounded through wear

corrosion or mechanical damage.

When the investigation was started there had already been many reports and comments on the existence of bistable flow in control valves. Turnbull (55.)* and later Mitchell (32a.) showed that the effect was dependent on the geometry of the downstream chamber for both the inflow and outflow configurations. They also produced methods for estimating reaction force which replaced an older analysis neglecting reattachment. The problem of devising a spool geometry which had a stable reaction force was also attempted by empirical methods, but although some geometries were found with the desired characteristics, there was no theoretical background to justify these shapes.

Since these other investigations a considerable quantity of research has been reported by workers in the field of fluid mechanics examining the characteristics of jet flow and reattachment to plane surfaces. The geometries of some of the flow patterns which have been analysed are very similar to the basic two-dimensional configuration found in piston valves (illustrated in Figure 1.3.) and it was thought that an attempt should be made to apply these new theories and experiments to explain the flow in valves. Such an attempt could provide a means whereby theories concerning the flow in valves could be theoretically and experimentally confirmed, and could also enable the theories themselves to be further tested.

Previous investigations of valve flow have been almost

* bibliography on page 124.

entirely restricted to incompressible flow, however an increased use of light pneumatic control systems in pressurised aircraft, and other technologies where weight must be reduced to a minimum, has caused a swing of emphasis towards the use of air as a working fluid. Already the designers of these pneumatic systems have reported unstable valve behaviour with symptoms very similar to the previous malfunctionings of hydraulic units.(29).

Another incentive to investigate the behaviour of compressible jets was the rapid rise in interest shown in the development of static switching devices, both as computer and process control elements. These switches consist of a two – dimensional fluid jet emerging between two symmetrical planes as shown in Figure 1.5.a. The jet can reattach stably to either of the side planes and the side to which it reattaches can be changed by applying either pressure or suction to the ports A or B. This provides a bistable binary memory unit, stable to quite large changes in both supply and delivery pressure, but which can be changed by small pressure signals applied to the control ports. Figure 1.5.a shows how similar the geometry of these switches is to the flow through valves illustrated in Figure 1.3.

These elements have an inherent power gain, the energy required to change the jet from one side to the other being small compared to the energy of the jet itself, and power amplifiers have been constructed with several elements in cascade to control large flows such as rocket motors and process flows in chemical manufacturing industries. The binary memory unit has also been considerably

developed as a digital computer element, and several attempts are being made to use such computers in the control of machine tools.

Preliminary tests with a valve model quickly showed the similarity between compressible and incompressible flow even at Mach numbers greater than unity.

Bearing these points in mind, it was thought timely to continue the investigation of the flow through valves along two main lines. Firstly to attempt to relate the investigation to the general field of fluid mechanics, and secondly to attempt to determine the basic characteristics of pneumatic flow, and try to relate these to those of hydraulic flow.

1.2. Previous work on piston slide valves.

As long ago as 1929 Tanaka (53) carried out a complet series of tests on fluid flow through a poppet valve,(actually an engine exhaust valve) and discovered four modes of flow which involved a reattached jet. He then found an incompressible poten tial solution and attempted to relate this to his results.

A serious study of control valve characteristics was not started, however, until some ten years ago. At that time an increase in the interest taken in control systems in general was accompanied by the problem of finding mathematical equations to represent the characteristics of components, and in particular of fluid control valves. This involved obtaining a knowledge of both the flow coefficient and the reaction forces exerted on the piston by the flow. As the flow coefficients were regarded as being easily measurable, attention was initially concentrated on finding a theoretical method of finding the reaction force, and on producing valve configurations with these forces either minimised or completely balanced out.

The first major attempt to calculate the size of the forces involved was made by Lee and Blackburn (28) in 1952. In their work the size and direction of the jet issuing from the control orifice was predicted using the potential solution of Von Mises (57) (for inviscid flow through the configuration as shown in Figure 1.4.a.) Using the solution, the change in jet momentum was calculated assuming that the turbulent jet found in the

actual flow had the same pressure distribution surrounding it as the inviscid jet. A glass sided model of a valve was used to measure the reaction forces, to confirm the jet angle and to test various spool geometries in order to find a geometry with minimal forces. The experimental results proved the jet angle prediction to be correct (21° for $w = 0$) and seemed to justify the assumptio made in calculating the reaction force. However it was noticed that at small valve openings the jet behaved differently, and that the abnormal behaviour (presumably reattachment to the pist end) caused large errors in the magnitude of the reaction effect

Another attempt to construct a spool with minimum force was described by Eynon (16) and yet another by Schaeffer (43). Both reported partial success but could not account for abnormal behaviour over certain ranges of valve opening.

Subsequent to the work of Lee and Blackburn, Harrison (23) carried out tests on another two – dimensional model of a slide valve and attempted to measure the reaction force. His results showed that reattachment took place at certain openings, and this was what made Lee and Blackburn's analysis inaccurate over parts of the range. From these facts he was able to make a spool (similar to the others) with a linear reaction force dependent on opening, and to demonstrate why it succeeded. He also obtained photographs of the flow showing the bubble, in som instances with cavitation showing inside it.

Harrison's special spool had the piston face cut back as shown on Figure 1.4.b. This effectively increased the angle

between thejet and the surface of the piston, so that the bubble length required for reattachment was large and the jet struck the opposite wall before it impinged back onto the piston. However at extremely small openings reattachment was still possible though nonlinear effects associated with completely closing the valve probably obscured the possibility.

Harrison's results were also partly obscured by the fact that most of the readings and photographs were taken while the piston in the valve was moving. A recent investigation by Foster (19) has shown that the flow patterns under dynamic conditions are most complex and vary considerably from those of the steady state. However Harrison's tests gave the first indication of the possible reason for the observed phenomena, and the photographs provided much useful information.

Turnbull (55) carried out another series of tests using a large scale model of a valve in two dimensions. Instead of measuring the reaction force on the piston directly, he measured the static pressure distribution along the radial faces of the piston and integrated this to obtain the total axial force (reaction) - making an allowance in the calculation for the momentum leaving the model.

During the course of the tests Turnbull isolated three distinct flow patterns, corresponding to 1 and 4 in Figure 1.2 with an intermediate stable jet position at 45°. Although he observed and noted the three types of flow and measured the orifice

dimensions at which each existed, he did not investigate the full nature of the flow patterns or of the mechanism which caused the stability of the patterns. He did note though that conditions existed at orifice dimensions intermediate to the stable condition when either of the two patterns might exist depending on the previous history of the spool movement.

Turnbull's findings, allied with those of Harrison, showed quite clearly that to base calculations of reaction force on a potential solution was too much of a simplification to be of any - thing other than limited practical use. More importantly, they demonstrated that little further progress could be made on the problem without a more exact knowledge of the flow conditions existing at the valve costriction.

Slightly later Stenning (52) reported similar findings for compressible flow using a valve model with air as the fluid. His results showed that the flow coefficient was also affected by reattachment (as much as 10 percent.) and also that the bubble persisted even though the velocity of the jet was increased beyon sonic speed. This was one of the first indications that the flow coefficient was also affected

As a result of these last three investigations the probl of finding out more about the flow patterns in valves was attempt by Mitchell (32a), in particular following up the work of Turnbul whose apparatus and methods provided a useful starting point.

The investigation described in this present report is

intended to complement and enlarge Mitchell's findings, and since the later chapters allude to and clarify some of his findings, it is necessary that his work should be described fully.

The first half of Mitchell's investigation dealt with two dimensional incompressible flow through the two configurations illustrated in Figure 1.1.b which differ only in the positioning of the additional downstream walls CD. Static pressure tappings along the boundary walls were used to determine the position and size of the reattachment bubble, and dye injected into the flow made it possible to obtain photographs of the jet path and the movement of the surrounding fluid. Using these techniques he was able to show that the ratio of bubble length to orifice width was constant for Reynolds' numbers from 2000 to 400,000. To achieve this wide variation of Re. with a limited pressure head available, Mitchell was forced to vary the orifice dimensions from 0.08 to 0.56 in. Since the depth of flow was only 1.25 in. the ratio of jet width to flow depth (known as the Aspect Ratio) was at times as high as 0.45. This and other points will be dis - cussed in Chapter 3.

Mitchell then went on in the same manner as Turnbull to find the limiting distances x_1 and x_2 (in terms of the orifice width) at which the jet detached from or reattached to the walls AB and CD. As before he found that there was a region where flow was possible attached to either wall, the position depending on the previous movement of the valve.

The second part of the investigation used an axially symmetric model which is the normal form of the spool valve. The three – dimensional flows observed and measured behaved qualitatively as in the two – dimensional case, but the bubble length and the various other distances x were affected by the radially increasing flow areas. Finally he carried out tests to determine the onset of cavitation in the reattachment bubble due to the subatmospheric pressures existing there when the outlet from the valve is at atmospheric. In both valve models he measured the minimum pressure drop across the orifice which would cause cavitation, and obtained photographs illustrating the onset of cavitation in the shear layer at the edge of the jet and in the centre of the bubble.

At the time of Mitchell's experiments little had been done in the general field of fluid mechanics to investigate the entrainment into two–dimensional jets and into the phenomenon of reattachment to plane surfaces. The only problem which had been thoroughly tested involving a bubble was that of an airstream, separated from an aerofoil at the leading edge, reattaching further down the wing. This problem, consisting of a semi – infinite flow rather than a doublesided jet, was investigated by Crabtree (12), Owen and Klanfer (38) and later by Moore and Kline (34), but is not immediately applicable to the valve flow problem whereas there have recently been several more appropriate studies which make Mitchell's analysis, based on Crabtree, unnecessary to describe. The modern studies of jet entrainment are reviewed in the next

section of this chapter.

Since 1960 several investigators have examined the possi - ility of the reaction forces providing a means whereby the output positionof the valve can be fed back to the input in such a way that it neutralises the natural damping, thus causing the valve spool to oscillate backwards and forwards without any external system to provide a feedback loop. A somewhat similar condition is found in spring loaded relief valves which are commonly known to oscillate spontaneously, and recently pneumatic spool valves used in aircraft pressurising systems have been reported as behaving in this way.

Although the possibility of valve instability from these causes was noted by Lee and Blackburn (28) and others, it was only recently that attempts were made to analyse and test this, and to obtain criteria for stability.

Among the first times that attention was drawn to this problem was in a report by Noton and Turnbull (56). Later Williar (59) derived equations to find the reduction in the gain of a spool valve system due to the reaction forces, and derived an approximate rule for estimating the stability of such systems. Backe (3) also examined the stability of valves in this respect when coupled to external loads which themselves provided feed - back loops causing instability.

The most recent and exhaustive investigation into the self oscillation of spool valves due to this internal feed-back provided by the momentum of the fluid, was carried out by Foster

In the course of his experiments he constructed a large scale model of a piston valve with an artificial means of damping the spool motion, so that the negative damping produced by the react force could be balanced out by a measurable positive quantity and thus be determined. While attempting to analyse the flow pattern in the model Foster obtained photographs (using a dye injection) of the jet shape in the reattachment zone while the valve was oscillating. These showed that the stable reattached flow was not fully achieved under the dynamic conditions, and that the je took up an oscillatory position somewhere between the fully attached and the separated states. This indicated that the inert of the jet and its surrounding fluid and the time constant of the reattachment process both play an important part in the analysis of valve performance under dynamic conditions. To proceed any further with such an investigation would require a fundamental study of the rate at which the reattachment occurs, a subject hitherto untouched.

This problem of the rate of attachment of a jet is also of great interest to the makers of fluid logic devices, since the speed of transfer of the jet from one wall to the other (see Fig. 1.5.a.) is a fundamental limitation on the speed of operation of any logical device built from such units.

The effect of these previous reports was to provide a considerable mass of sometimes conflicting evidence as to the performance and characteristics of slide valves. Although many apparently valid conclusions and theories were put forward to

explain the phenomena observed, a more complete understanding of the flow patterns existing within valves was needed before the characteristics could be confidently predicted. The experimen carried out by Mitchell were the first steps towards examining and explaining the flow phenomena involved.

Since then further reports on free jet flow and reattach ment have thrown new light on these subjects, and it has been the purpose of this present study to incorporate these new find - ings into a further investigation of the flow in piston valves.

1.3. The object of the investigation.

The objects of this investigation were:—

1.) To apply recent theories and models of jet entrainment to flow through the simplified piston valve configuration shownin Figure 1.3 in order to confirm and enlarge conclusions drawn from previous experimental results.

2). To extend the experimental data where necessary to test the new analyses, even though this involved geometries which would be impractical in a normal valve.

3). To obtain the characteristics of compressible flow through the valve configuration and relate them to the incompressible values.

4). To study the effect of compressibility on the reattachment of gas jets and to relate this effect to the behaviou of pneumatic control valves.

1.4. A review of work on incompressible jet flow.

Although the flow downstream of the control orifice in a piston valve is very dependent on viscosity, turbulence and entrainment, the flow upstream is smooth, starting from almost stagnation conditions. The velocities involved are low except in a small highly convergent region just before the orifice. These conditions are known to give flow patterns little different from those of an ideal inviscid fluid, so that the flow upstream can be analysed theoretically in terms of an ideal potential flow. The flow downstream is not suited to such treatment because of its complete dependence on viscosity and turbulence.

A potential solution for the geometry of the upstream flow was obtained in 1917 by Von Mises, and has been widely used in previous work on valve flow to obtain the jet angle, thickness and momentum of the separated flow. Von Mises (57) configuration is shown on Figure 1.4.a along with his predictions of angle and jet thickness as the ratio a'/a varies. Unfortunately the solution does not allow the pressure difference across the jet on the downstream side (due to the bubble being at a pressure below atmo pheric) to be brought into the calculation. This difference in th pressure drop across the control orifice at either side must cause a change in the jet angle and possibly the thickness, but the effect has not yet been measured. Since the pressure ratio on one side may be one third as much again the effect is sizeable A relaxation solution might be used to obtain an estimate of

the change of angle, possibly based on a method developed by Rouse (41) or on Norwood's technique, described in Chapter 4.

The flow downstream requires other methods of analysis to allow for the entrainment of fluid into the jet by turbulent mixing. When the fluid separates from the walls at the corners of the orifice it immediately entrains fluid so that by the time the Vena Contracta is formed the jet is already thicker than the theoretical prediction.

The entrainment of fluid from between the jet and the walls causes a decrease in static pressure in these regions, the decrease being most marked on the side nearest the wall. Thus the jet is deflected towards the nearer wall, which amplifies the pressure difference, and the process continues until the jet re-attaches.

Many attempts have been made to provide mathematical models for the shear layer existing between the jet and the surrounding fluid. These models have been used to try to describe the entrainment of fluid into the jet from the surroundings, which is caused by turbulent mixing in the shear layer.

An example of a solution for the growth of the shear layer was the work of Corrsin and Kistler (11), however the mathematical expressions which they derived to describe the process of entrainment are much too complex to be used in the present investigation.

Several empirical assumptions have been tried at various times to obtain simple (and surprisingly accurate) models of the

rate of growth and velocity profile of a free jet as it entrains fluid along its path. One such assumption, that the turbulent entrainment or mixing was equal to an extra viscosity term which was constant across the entire width of the jet, was developed by Prandtl and Gortler (44). This resulted in simple expressions for the entrainment and for the velocity profile in terms of an entrainment constant σ. It is on that assumption that the new analysis of the entrainment process has been based.

The analysis was derived from a thesis by Dodds (13) describing the use of suction to prevent unwanted separation of the air flow round wing sections. Later the theory was applied simultaneously to the reattachment of thin two-dimensional jets by Sawyer (42) and by Bourque and Newman (6). In all cases only incompressible flow was considered.

Sawyer investigated the flow of a two-dimensional jet issuing parallel to a plane surface as shown in Figure 2.1.a. Using the theory of entrainment (which is described in detail in Chapter 2,) he derived predictions of bubble length and pressure in terms of the entrainment parameter σ and the jet thickness. Then by measuring the length and pressure experimentally he was able to demonstrate that , provided the initial height of the jet above the plane was large in comparison to the thickness, the indicated entrainment parameter σ was constant; but as the ratio of height over thickness became smaller, the entrainment decrease markedly (i.e. σ increased.)

Bourque and Newman applied a simplified version of

this to the same configuration and also to the problem of a two-dimensional jet emerging from a flat plane at an acute angle and curving round to reattach to the plane again. This is illustrated on Figure 2.4.a. From their experimental results Bourque and Newman also found indicated values of σ for various height/thickness ratios and jet angles. Due to their approximation, however, the values of σ obtained did not correspond with those of Sawyer. A critical analysis of both of these papers is contained in Chapter 2 along with an attempt to rationalise them in order to obtain a relevant comparison. Also in the chapter is a similar analysis of the flow through the slide valve geometry of Figure 1.3, and a comparison of the experimental findings of the three investigations.

Another mathematical model of jet entrainment was suggested and verified by Rouse and others (1), which was an alternative to Gortler's assumption of constant turbulent viscosity. Instead Rouse assumed that the velocity distribution in a free turbulent jet was the same at all sections, and that the velocity profile was a Gaussian normal probability graph. Using this assumption he expressed the entrainment of fluid into a jet in terms of experimentally determined constants, which he measured accurately for both two-dimensional and axi-symmetric conditions. At the same time he verified that the velocity profile was repeated down the length of the jet, (the Gortler theory also leads to a constant velocity profile.) In the treatment of the inlet conditions Rouse took account of the change from a rectangular

inlet velocity profile to the fully developed Gaussian state further down the jet, whereas Gortler's analysis neglected this and assumed the jet to originate from a thin slit behind the real entry plane, positioned so that the jet width and momentum were correct in the plane of the real entry cross-section.

The concept of a transition region before the jet becomes fully established was examined by several investigators, in particular by Donald and Singer (14) who estimated (by measurement) the length of the region to be between seven and ten times the thickness of the jet on entry, and measured the rate of lateral expansion during this period to be almost half the subsequent rate. Their findings represent the average values for the various other reports.

Rouse's analysis was used by Olson (37) to calculate the length of a reattachment bubble using an iterative arithmetical method which is described in the next section on compressible flo

Experimental techniques to measure exactly the quantity of air entrained by an axi-symmetric jet were developed and reported by Spalding and Ricou (40). The difficulty involved in measuring the fluid flowing into a jet is that the edges are very indistinct and the velocities so small that a traverse to measure the total mass flow is inaccurate. Since the entrained air is the difference of two inaccurate values no exactness can be claimed. This is also the difficulty in providing an analytic expression to fit the measured profiles, although the central high speed region can be easily fitted the edges are difficult, and the

integration of such a curve is useless.

The apparatus designed by Spalding and Ricou to measure the volume entrained is illustrated on Figure 1.6. The air which the jet entrained between the planes A and B was supplied from a separate source through a measuring orifice. The flow of this supply was regulated so that the pressure in the enclosed volume between A and B was exactly the same as the pressure surrounding the jet outside the planes. Thus the flow into the jet was unaf - fected by the presence of the planes since the pressure at the edges was continuous, and the radial flow into the jet was not restricted by the parallel planes.

The results obtained using this apparatus were quite satisfactory and confirmed the general indication that entrain - ment decreased with increasing Reynolds' number up to a value of some 10,000, but there was little decrease thereafter. Most of the work reported dealt with burning jets and buoyancy effect which are unimportant in control valves. However, as a method of measuring entrainment into jets, the technique could be extremel useful to investigate the entrainment on either side of a curved jet - a measurement which would allow an improvement in all calculations involving reattached jets. A more detailed suggesti to this effect is contained in Chapter 6.

After reattaching to the wall in any of the configur - ations the fluid jet continues downstream, one side adhering to the wall as a boundary layer, and the other entraining fluid as before. This type of flow (a wall jet) was first studied in

detail by Glauert (22) who made several attempts to match the boundary conditions to existing jet theories.

Initially Glauert obtained a solution by using Gortler's assumption of constant turbulent viscosity throughout the jet, but although this gave a profile which fitted the measured value for the outside half of the jet, the theory predicted a much lower velocity gradient than was measured for the inner half, next to the wall. To correct this he imposed a turbulent viscosi profile on the inner half which was derived from Blasius' empiric expression for drag in pipes, and matched this with the uniform distribution on the other side. Unfortunately the resulting theoretical profile varied as the jet proceded downstream, how - ever the difference from a similarity solution was small over normal jet lengths, and the model has been found useful.

Bakké (4) provided further experimental confirmation of the model by accurately measuring the velocity profile of a large range of wall jets. His figures showed the model to be quite suitable over normal lengths, but showed that the actual profile was constant along the complete jet. Bakke also showed that both Gortler's and Rouse's models considerable overestim - ated the velocities at the outer fringe: his measured values indicated that the viscosity must rise sharply at the edges.

Sigalla (49) also carried out tests to verify some of Glauert's predictions of the tangential shear force exerted on the side wall to which the jet adheres, and found considerable

agreement with the calculated figures.

A complete and accurate study of a particular aspect of wall jets was made in 1961 by Schwartz and Cosart (45), who examined the transition section when a uniform jet impinges tangentially onto a flat plate. The experimental results, measured using a hot wire anemometer, give information about the veloci patterns in this zone, which would provide a good starting point for a study of conditions at the reattachment point of a separated jet flow. A similar study was reported by Mattieu and Taillard (31) who have also reported recently an investigation of the characteristics of both free and wall jets in a high speed fluid stream.

1.5 A review of work on compressible jet flow.

The flow characteristics of compressible jets at subsonic speeds are qualitatively similar to those of liquid jets. Reattachment takes place by the same mechanism, and the velocity and static pressure distributions around the bubble are similar. However compressibility does affect the flow through any orifice,(35), and in the case of an asymmetric orifice,such as the valve, Figure 1.3 both the contraction coefficient and the jet angle change with increasing Mach number. It was therefore necessary to calculate these changes in order to determine the inlet conditions to the downstream chamber.

This information was found for the incompressible case by the Von Mises potential solution, but the equations of compressible flow are non - linear and cannot be solved by the powerful methods using complex variable transforms. Such solutions are well known to be exceedingly difficult to obtain, and much effort has been devoted over the years in solving only a few simple cases.

Most of the difficulty in solving jet problems is due to the boundaries of the jet being unknown. Even relaxation methods are longer and more complicated since the boundaries have to be relaxed as well as the values at the points. This method of solving a problem was attempted by Emmons (15) who performed the entire process by hand, and obtained an answer after several years of work. For productive purposes this method was useless until the advent of high speed electronic computers.

Two main analytical methods have been evolved to deal with the non – linear equations of compressible flow. Both involve transforming the problem onto the hodograph plane – equivalent mathematically to changing the independent variables from x and y to their derivatives, the velocities u and v, in the X and Y dir – ections respectively. This transformation makes the equations linear, although their solution remains difficult.

One method of obtaining a solution from them was evolved by Chaplygin (44,57b). This consisted in finding a solution for incompressible flow through the same geometry in the form of a series of a special function, and then transforming this into the compressible solution by a standard mathematical process. Unfortunately the incompressible solution is as difficult to get in this required form as the compressible, and the validity only extends over the subsonic region.

Frankl (20) extended the method to cover purely super – sonic flow, but transonic flow is as yet unsolved. The question of the validity of these solutions in the transonic region was discussed by Sears (46), who reviewed the existing Chaplygin solutions and their inability to predict non – isentropic flows.

Another method of solving the equations approximately, known as the Karman – Tsien approximation, involved replacing the isentropic gas law $pv^{\gamma} = \text{const.}$ by a straight line tangential to the curve at the point of interest. This can only be applied when the pressure change throughout the flow is small, since the accuracy of the method decreases as conditions are removed from

the point of tangency.

The accuracy and validity of other, more accurate approximations to the gas law were considered by Chang (9), who effectively discussed a series of increasingly exact replacements for $pv^{\gamma} = C$, which were chosen to transform the linear hodograph equations into more manageable forms. These approximations ranged from a straight line (the original Karman – Tsien) through successively more accurate functions to an extremely close representation of the isentropic relationship.

The approximations had the effect of transforming the stream function equation into various well known forms, such as Riccati's, Bessel's and Whittaker's equations. For each of these equations Chang developed a solution in series with constants to be found from the boundary conditions. Finally in his report he applied his most accurate substitution to a problem already solved by Chaplygin, and managed to obtain the same answer, which justified the method.

An attempt was made in the present study to apply Chang's method to the flow through valves, described in Chapter 4, but with limited success.

As a result of the great difficulty involved in analytical solutions, other methods have been developed to determine discharge coefficients, jet thicknesses and angles. One such method was developed by Norwood (36a) based on the relaxation principle (as was Emmons') but using a digital computer to reduce the labour to a minimum. Its main advantage over the previous

method is that the relaxation is carried out in the hodograph plane where the boundaries of the flow are more completely known and are simpler than in the physical plane. When the process is complete the flow map is easily transferred back to the physical boundaries.

This is a powerful method of solution since both subsonic and supersonic flow can be treated, and once the computer is programmed an unlimited number of points can be obtained. The relaxation process is slightly different for the two types of flow and they have to be programmed separately, although in some instances (jet flow for one) a combined calculation can be carrie out.

Norwood initially applied the process to an investigation of flow through a flapper control valve illustrated on Figure 1.6 From the flow maps which he obtained he was able to calculate the jet boundary at various Mach numbers and to predict the pressure distribution along the surface of the flapper,(AB in the diagram) which, when integrated, gave the total reaction force.

At one time Mitchell (32b) had the idea of applying this method to the flow through the simple slide valve configuration, (1.3) and obtained one flow map for subsonic speed, however he did not pursue the matter and his programme is now obsolete. Had another way of calculating the various jet parameters not been found (described below) Norwood's method could have been used.

Another idea for calculating compressible jet dimensions that has attracted many investigators is the possibility of

applying a compressibility factor to the more easily obtained incompressible values. Originally most effort was concentrated on attempts to calibrate measuring orifices and nozzles for high speed air flow from tests made with water.

T.B.Morley (35) was among the first to investigate the use of nozzles and orifices as accurate measuring devices. He carried out numerous tests to determine the flow of compressible fluids through orifices and compared the results with theoretical predictions. In his tests he used three methods for measuring the flow of air. Firstly by the change in temperature of reservoi connected by the orifice being tested, secondly by the force caused by the jet impinging on a flat plate, and finally by a measurement of the reaction force on the walls of the orifice itself as the fluid accelerated through it. This last method was the basis for the work of Jobson and later Bragg (26 and 7a). Morley was also one of the first to note the change in the cont - raction coefficient due to compressibility.

Stanton (51) carried out further tests on air flow through similar orifices, concentrating his attention mainly on 'choked' conditions when the speed at the outlet is sonic or more During the tests he enlarged on Stanton's observations of the behaviour of the jet thickness due to compressibility, and also showed that the position of the vena contracta changed as well. Thus he demonstrated the difference between a nozzle and an orifi as a measuring device; a nozzle having a fixed minimum downstream dimensi and an orifice having a minimum jet thickness which continues to increase

beyond the sonic condition. This is clearly shown in the results of Chapter 4.

Continuing along the same lines Buckingham (8) also tested the contraction coefficients of orifices in long pipes and compared his findings with theoretical predictions.

In 1955 Jobson (26) succeeded in developing a theoretical method to determine the contraction coefficient of an orifice for compressible flow at any pressure ratio from the value at zero ratio (incompressible flow). To carry out the analysis Jobson introduced a Force Defect Coefficient, defined as the total reduction of the static pressure force on the up-stream side of the orifice due to the acceleration and velocity of the gas along the face. Then by assuming that this defect was independent of compressibility (i.e. that the velocity distribution was not affected by compression effects) he obtained the value of this defect from tests made using water and used it to find the compressible contraction coefficient over a wide range of pressure ratios. The assumption proved accurate for sharp edged orifices but as the edges of the aperture became more rounded and like a nozzle the calculated values were more in error. For coefficients greater than 0.7 the error was appreciable and Jobson set that limit on the use of his analysis.

Bragg (7a) suggested a modification to Jobson's theory which made it accurate over a much wider range. The change was to the assumption that the compressible and incompressible coefficients were the same. Instead of this Bragg assumed that the

mass flow everywhere at the walls was proportional to the average mass flow through the section. From this he derived the ratio of the compressible to the incompressible force defects in terms of the upstream conditions and the pressure ratio across the orifice. This in turn allowed an iterative solution for the contraction coefficient, and the accuracy was found to be good for all shapes of orifice or nozzle.

Under supersonic conditions the jet expands after it leaves the walls of the orifice so that the pressure is no longer uniform across the plane of exit as is assumed in the analysis. This produces an error in the predictions which grows as the jet becomes more supersonic and it is believed that Bragg (7b) is hoping to allow for this effect in a future analysis.

Although the analysis described above is itself a useful method for calibrating orifices for symmetrical two or three-dimensional flow, Bragg (7b) has indicated that it may be applied to two - dimensional asymmetric configurations to predict contraction widths and jet angles. This idea has been applied in Chapter 4 to the flow through the simple valve geometry

Experiments further confirming Jobson's analysis were recently reported by Benson (2) who measured the flow coefficient of the orifice formed when a piston exposes the exhaust ports in the cylinder wall of a two-stroke engine. The geometry of this system closely resembles that of the control valve except that the downstream walls are too short for reattachment to occur. Despite this, the tests show that the Jobson type of analysis hold

for the valve port. Benson completed his tests by an investigatio of the effect of high gas temperature on the flow and in particul on the discharge coefficient. Such effects would be important in the design of control systems working off hot exhaust gases, as in rocket engines.

Little has been reported on the reattachment of gas jets to plane surfaces, although straight supersonic jets have received some attention as engine exhausts. As previously stated Stenning (52) carried out a series of tests on compressible flow through a valve model, and established that the reattachment effect persisted stably long after sonic speed was reached in the vena contracta, thus indicating that this effect plays an important part in determining the flow patterns within pneumatic valves.

The only configurations with reattaching compressible jet flow which have been tested are those found in fluid logic elements of the type previously described (1.5.a). In such a system the speed of operation is of great importance and much effort has been applied to experimental studies of the flow patte existing within the elements. In particular emphasis was placed on discovering minimum element lengths to achieve stable bubbles, since it has been shown that the time taken for switching is a function of the transit time across the element. The thickness of the jets used is governed by considerations of air cleanliness so that speed of operation can only be achieved by high jet velocities and small element lengths.

In the study of the switching fluid elements Glaettli, Muller and Mitchell[33] have reported the findings of many experimental tests on the dynamic performance of the units, measuring rates of formation of the flow patterns and the mechanism of the pattern changes using high speed photography. The techniques developed will be useful if any investigation of dynamic flow conditions in valves is instigated.

However the tests reported were all experimental and no attempt was made to relate the results to any theoretical model or even to incompressible theory.

One mathematical model to predict the shape and extent of the bubble in a logic unit geometry has been attempted by Cohen and Tu (54) who treated the problem by mathematically transforming the fluid leaving the bubble onto another Riemann plane, thus satisfying the continuity condition, and the momentu lost is taken as being the effect of turbulent viscosity on the outside of the jet. The results of the analysis are not unrealis in the prediction of bubble dimensions, but, as the authors stat the problems involved in extending this type of solution to cove a more realistic representation of turbulent viscosity are very considerable.

Only one attempt has so far been reported to predict the bubble length by applying a compressibility factor to incompres sible results. This was made by Olson (37) who based his analysi on the findings of Rouse (1) concerning the entrainment of sub - merged water jets.

Olson analysed the flow through the geometry shown on Figure 1.5.b which is one half of the logic unit shown above it. In the analysis he assumed that the velocity distribution and entrainment were unaffected by compressibility and were the same values as were measured by Rouse. Then by assuming a constant bubble pressure and a semicircular jet centreline he was able to define the $\psi = 0$ streamline by a series of numerical integrations of the velocity profile. The intersection of this line with the plane he assumed to be the reattachment point. Although Olson allows for compressibility in his analysis to predict the bubble length, the initial assumptions regarding entrainment removes some of the value since the results quoted by Mitchell (32b) for experimental measurement of compressible bubble length, and the results of the present investigation show that entrainment reduces with Mach number. Without compressibility the calculation reduces to a parallel to those of Sawyer and of Bourque and Newman with a probability profile instead of Gortler's $\text{sech}^2 \frac{\sigma Y}{X}$.

His experimental results showed that the position of zero velocity (in theory the reattachment point), which he found by examining the distribution of lampblack on the plane, did not correspond to the pressure maximum measured by static tappings. This differs from the original findings of Sawyer and Bourque who both measured the null point to be close to the pressure maximum. Recent tests, as yet unconfirmed, indicate that both may be correct and that the relative position of the two points

varies slightly according to the angle with which the jet strike the plane. Both Sawyer and Bourque investigated geometries which had the jet striking the plane at large angles, whereas the logic unit has a shallow incidence angle. Unfortunately the apparatus used in the present tests was not large enough to allow this theory to be tested by measuring the velocity dist - ribution in the reattachment zone at various jet incident angles

FIGURE 1.1.

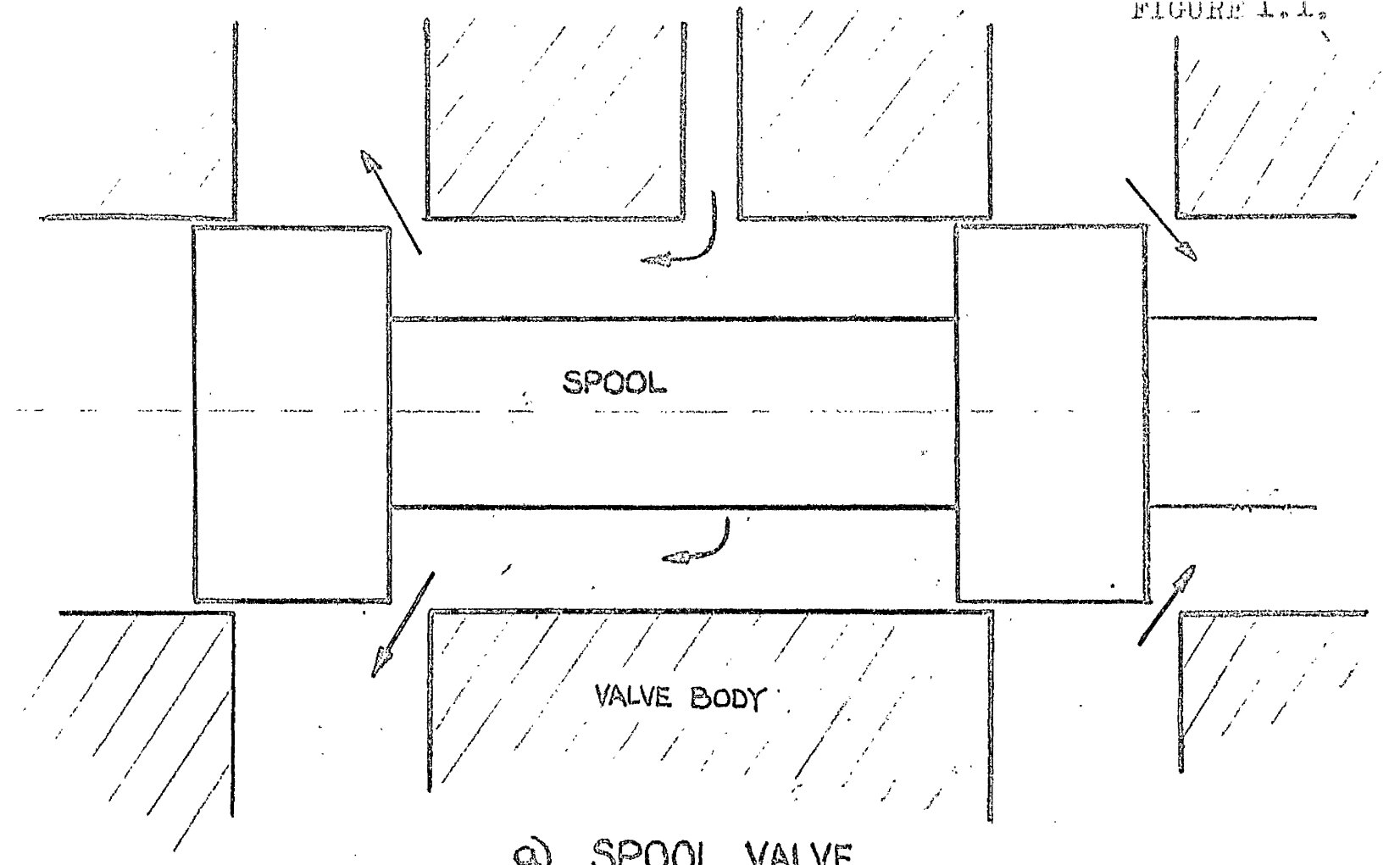

a) SPOOL VALVE

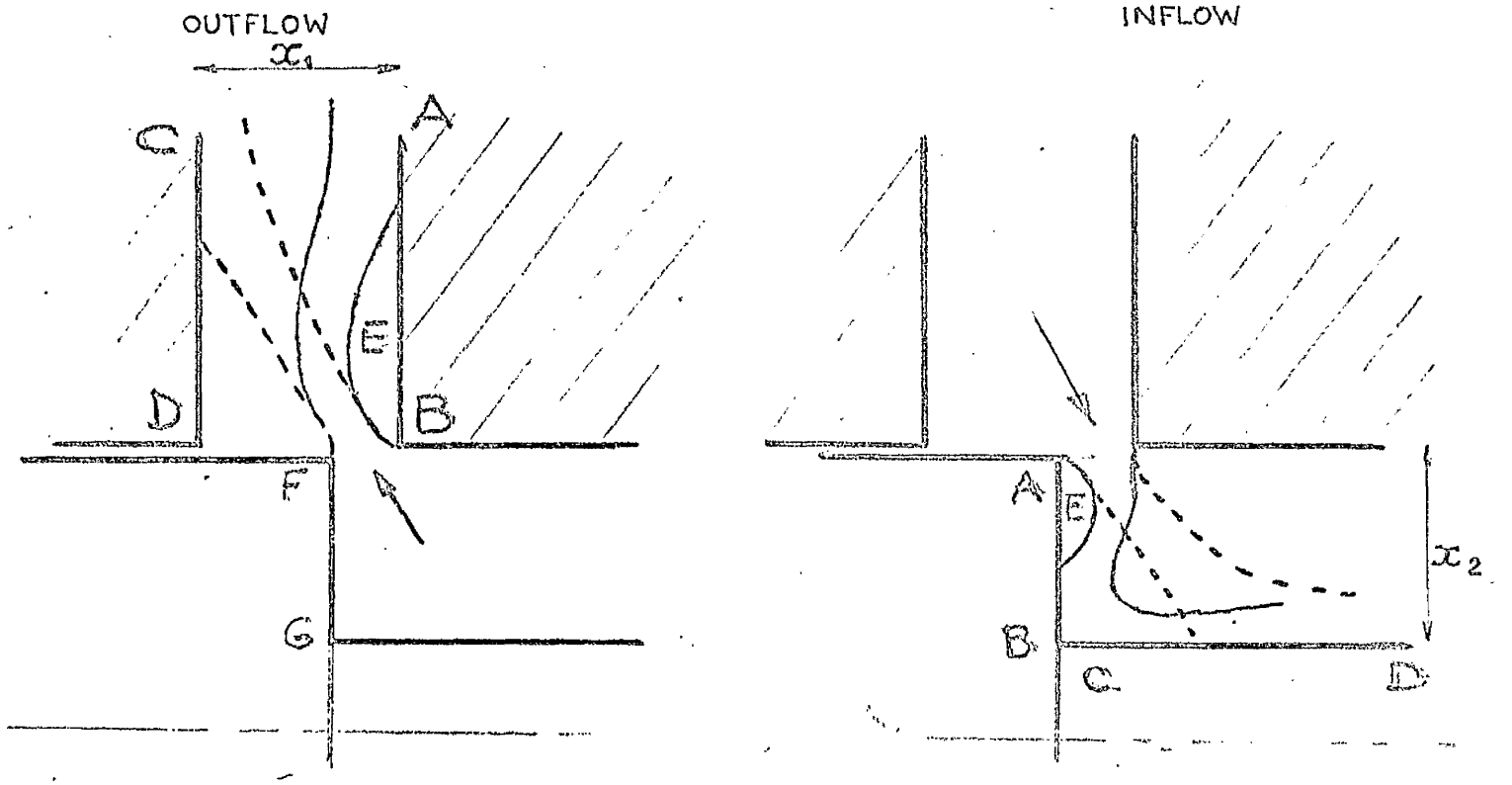

b) FLOW PATTERNS THROUGH PORTS.

FIGURE 1.2.

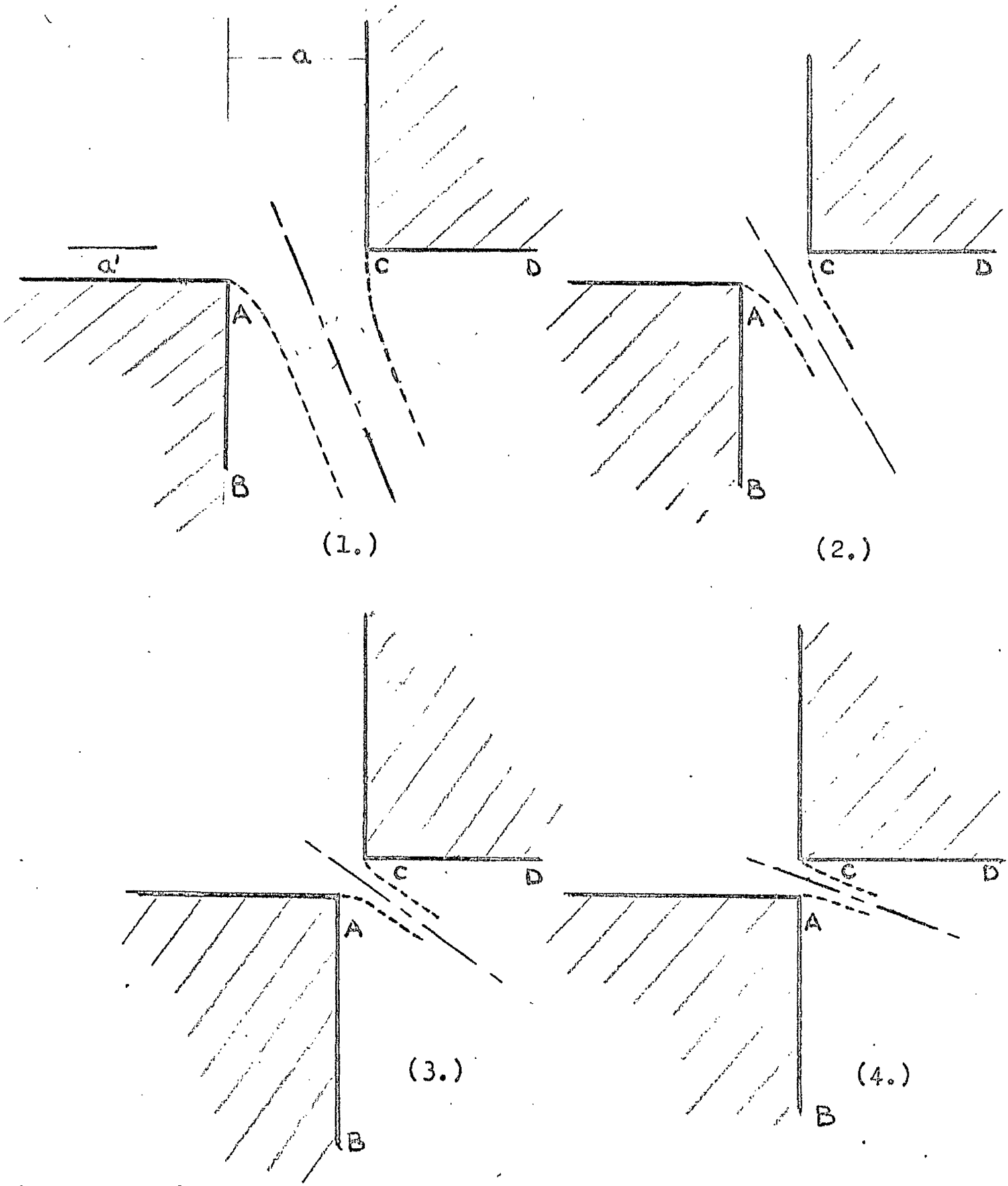

EFFECT OF VALVE CLEARANCE ON JET ANGLE.

FIGURE 1.3.

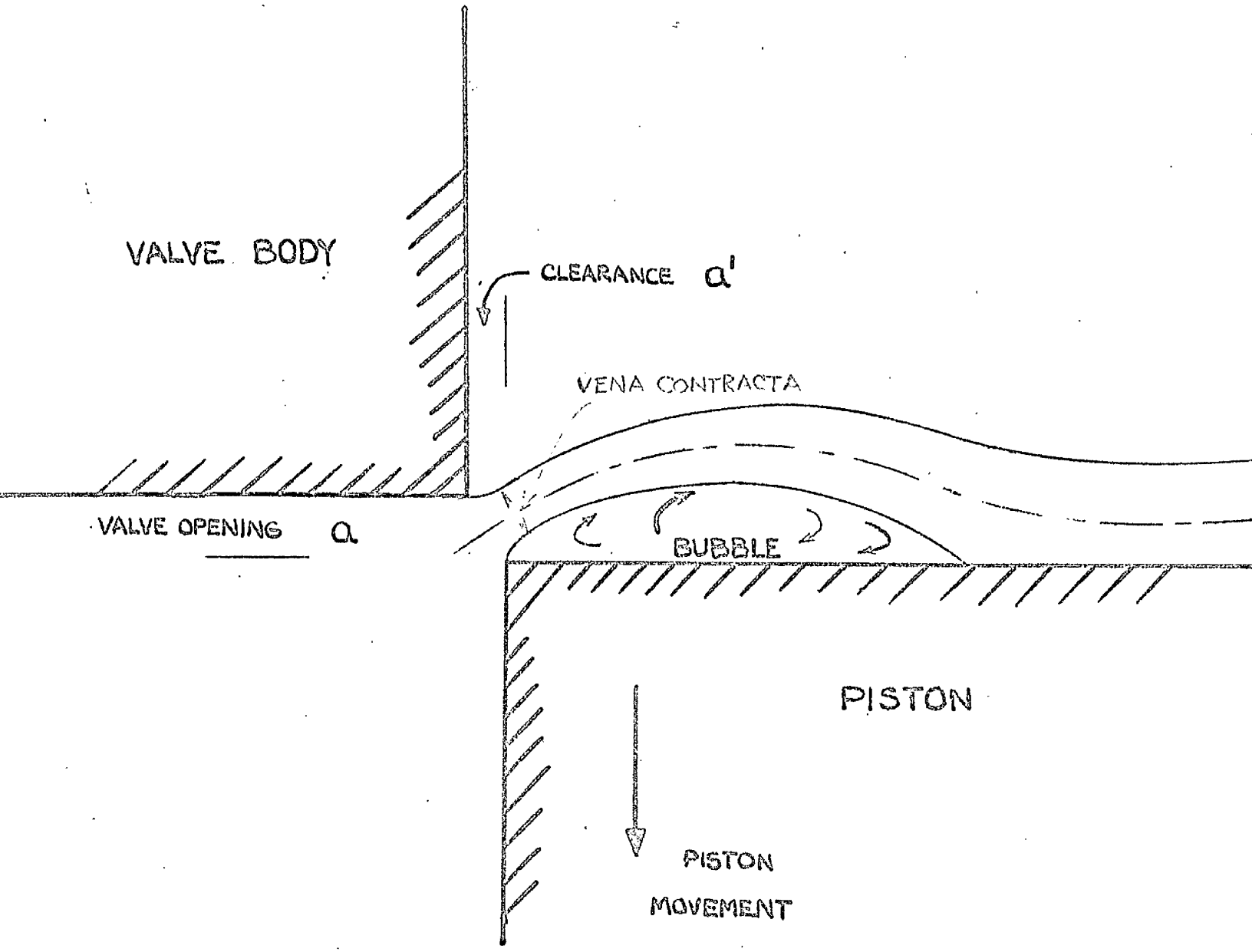

SIMPLE VALVE CONFIGURATION.

FIGURE 1.4.a.

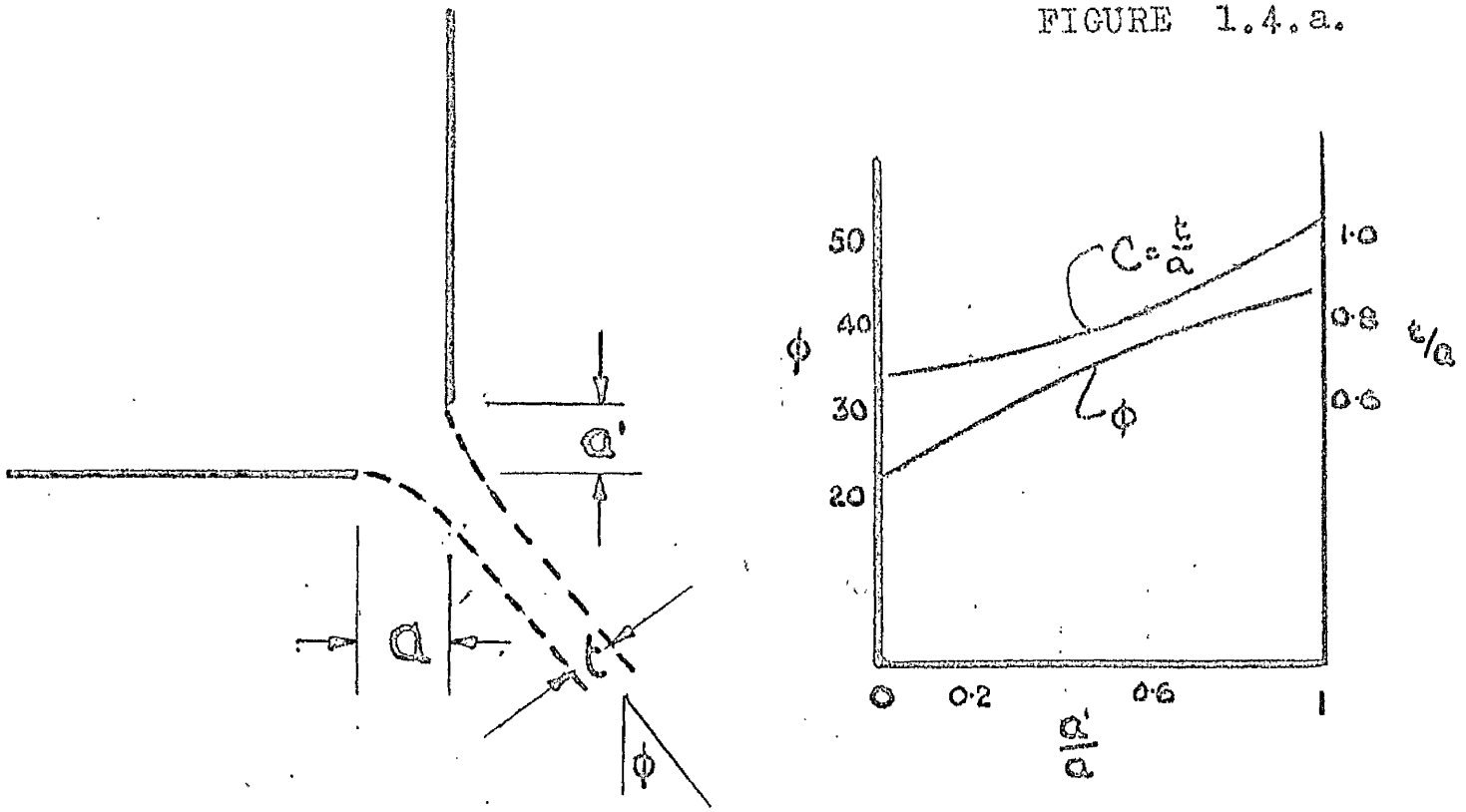

VON MISES POTENTIAL SOLUTION.

FIGURE 1.4.b.

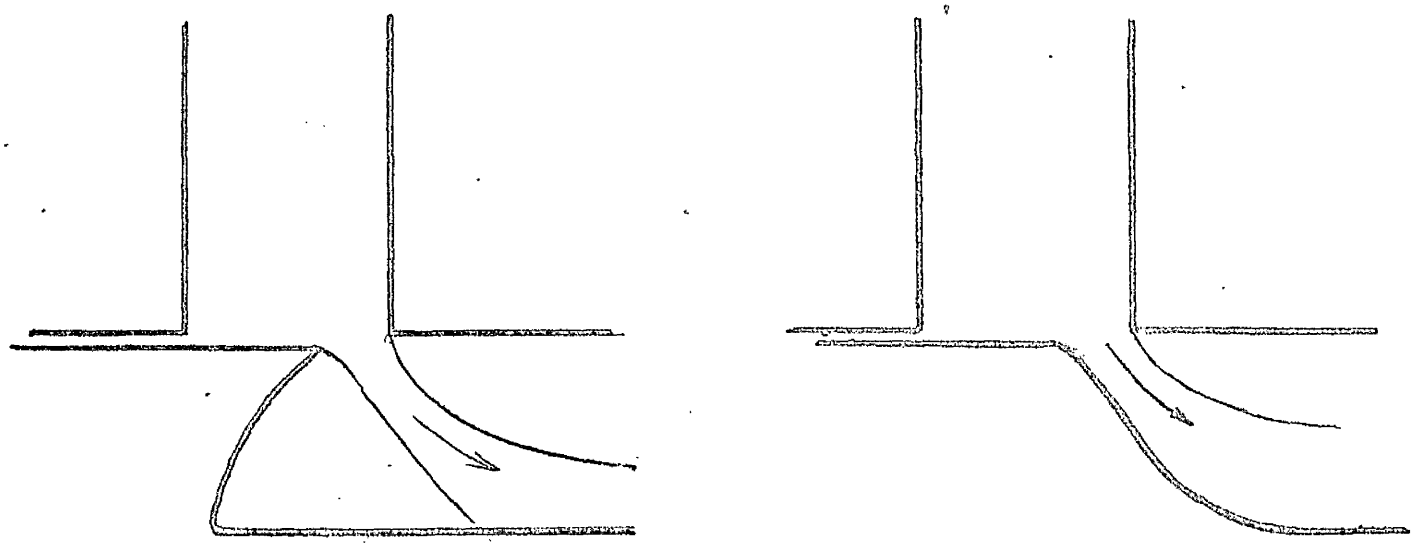

SHAPED SPOOLS TO AVOID REATTACHMENT.

FIGURE 1.5.a.

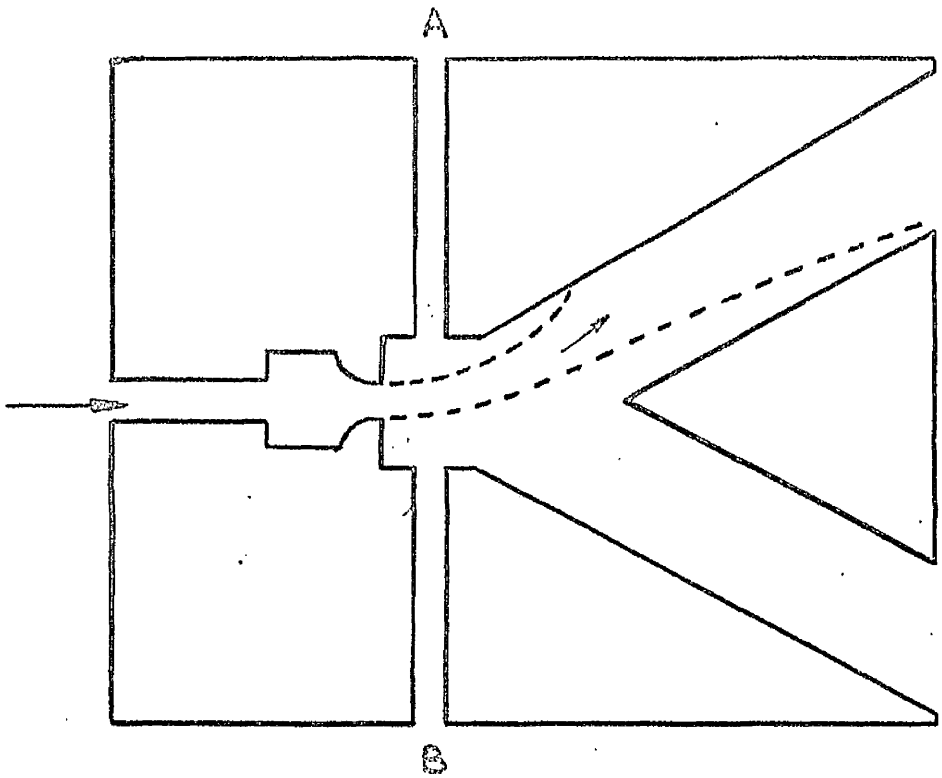

FLUID LOGIC CONFIGURATION.

FIGURE 1.5.b.

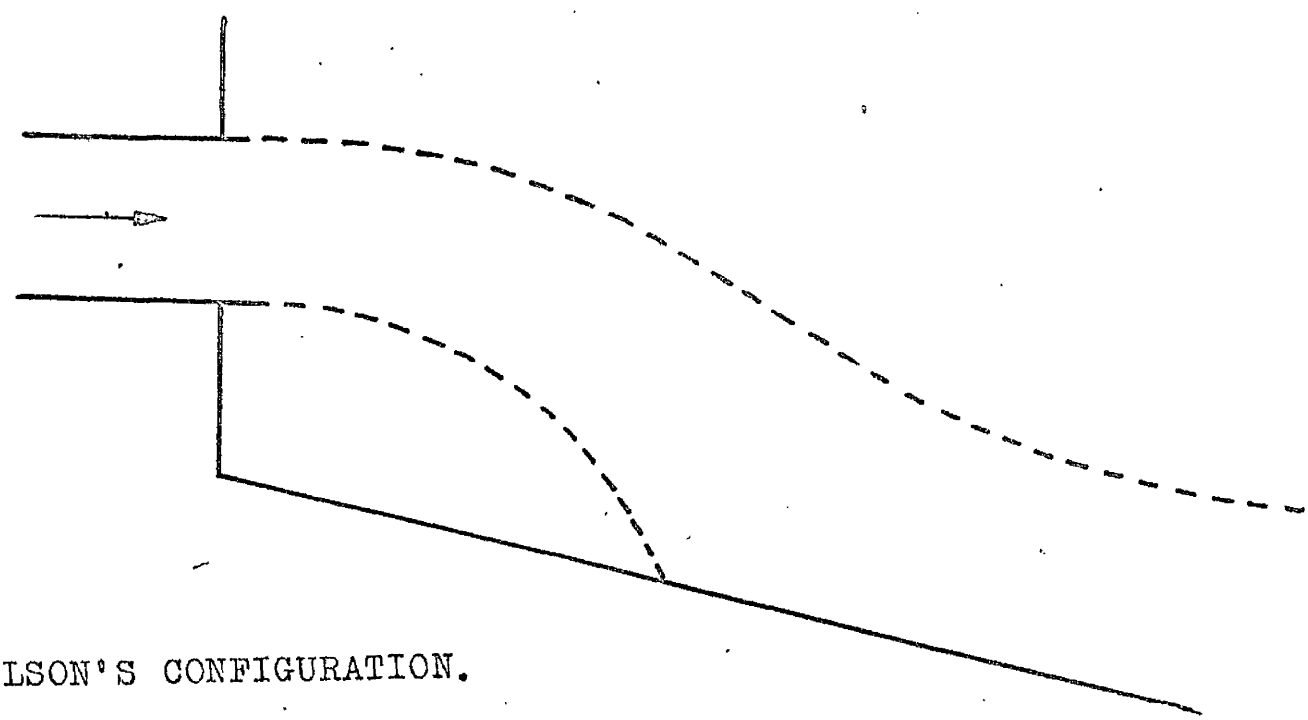

OLSON'S CONFIGURATION.

FIGURE 1.6.a.

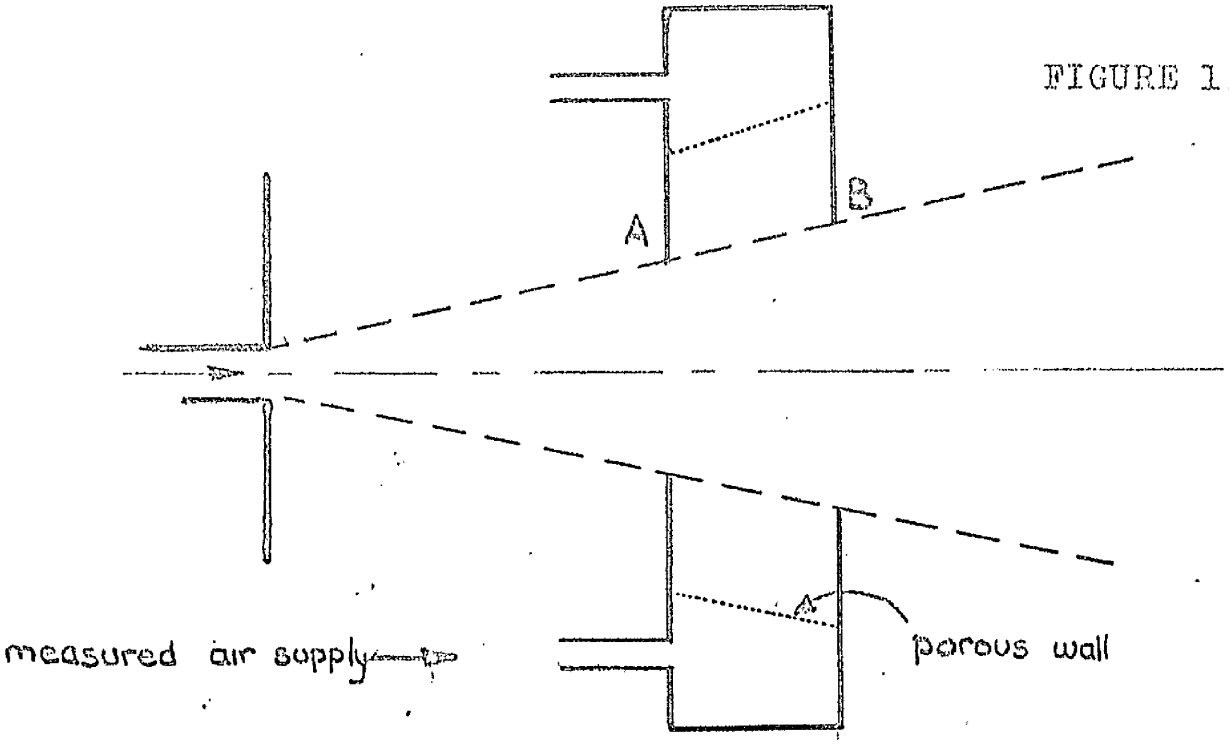

SPALDING AND RICOU METHOD OF MEASURING ENTRAINMENT.

FIGURE 1.6.b.

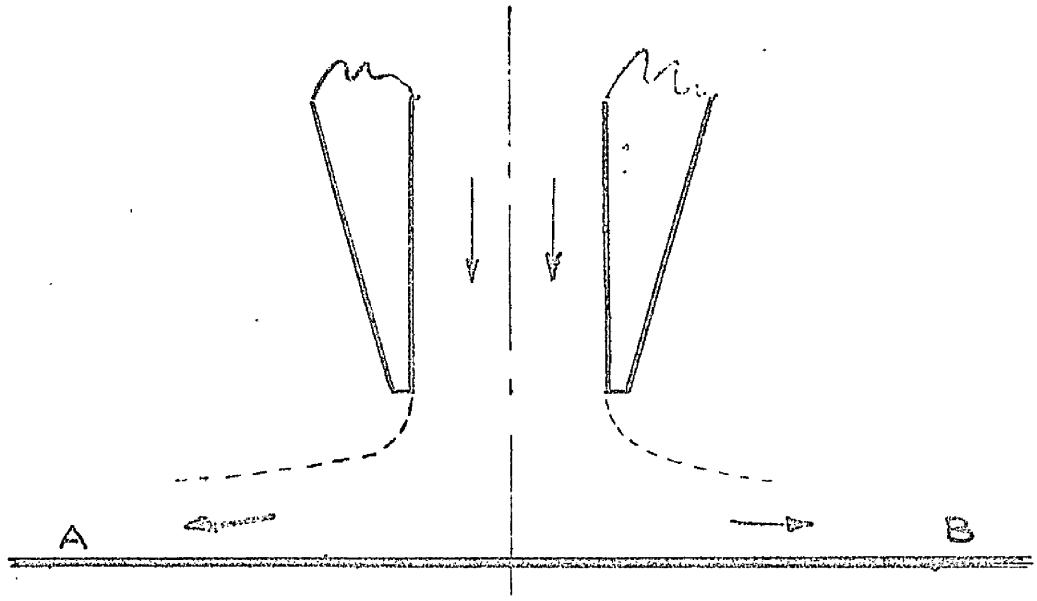

NORWOOD'S FLAPPER VALVE CONFIGURATION.

Chapter 2.

Theoretical study of incompressible flow.

2.1. An analysis of two investigations of turbulent jet reattachment.

2.2. Application of an entrainment model to the flow through a slide valve port.

2.3. A comparison of the three investigations.

2.1. An analysis of two investigations of turbulent jet reattachment.

One of the biggest problems in the theory of turbulent flow is the mathematical representation of the phenomenon of turbulent mixing. Direct analyses of the problem have only provided extremely complex expressions to represent the effects of this mixing on the flow. To overcome this, Prandtl (44) suggested that the mixing could be neatly (though empirically) represented as another viscosity term and went on to derive 'mixing length' theories which have been widely used in analyses ever since. This apparent viscosity, or turbulent viscosity as it is now called, is much larger than the normal shear viscosity which is usually omitted to simplify analysis.

The concept of turbulent viscosity can be usefully applied to analyses of free jet flows such as have been shown to exist in control valves, but it is necessary to make some assumption regarding the distribution of this new parameter across the jet.

Gortler (44) first made the assumption that the viscosity was constant across the jet, and went on to derive expressions for the distribution of fluid velocity across the jet. Experimental measurement showed these predictions to be accurate over the main body of the jet (but too high at the edges) and the assumption has been widely used in the analysis of fluid jets.

When the assumption is applied to the case of a two-

dimensional jet issuing from an infinitely thin slit the velocity distribution or profile at any distance X downstream of the slit is given by:- $u = U_{max}\,\mathrm{sech}^2 \frac{\sigma Y}{X}$ where Y is the distance from the jet centreline outwards, U_{max} is the velocity at the centreline at that X , and σ is an entrainment constant dependent on the turbulent mixing.

Chapter 1 contains references to other approximate and empirical methods of representing the velocity profile mathematically which have been used in other analyses and which could have been used in the following treatment of reattaching jets.

Both Sawyer (42) and Bourque and Newman (6) analysed the attachment of a two-dimensional incompressible jet to an adjacent surface using the Gortler assumption in a mathematical model first described by Dodds (13) in a report on an investigation of separation and reattachment in the flow round aeroplane wings.

Although both investigators used almost the same assumptions, when the experimental results were compared with the theoretical predictions there appeared to be a marked difference in the values of σ (the entrainment parameter) corresponding to the experimental results in the two investigations.

In order to find a suitable basis for comparing these two previous investigations with a new analysis of the control valve flow problem along similar lines, it was necessary to compare the two original analyses carefully to detect the reasons for their

disagreement. Once the reason for the discrepancy had been found, it was necessary to complete both analyses on a common basis before comparing them with the new control valve analysis on the same basis.

Sawyer's Analysis.

The configuration analysed by Sawyer is shown in Figure 2.1. and consists of a thin two-dimensional turbulent jet issuing from a slit in a direction parallel to a long flat plate. As the jet passes through the fluid the shear layer between the moving jet and the stationary surrounding fluid increases due to laminar viscosity. At a certain size the laminar flow in the shear layer breaks down into turbulence which causes momentum transfer and mixing along the jet edge. This effectively increases the viscosity causing the shear layer to expand rapidly out into the surrounding fluid and entraining more fluid into the jet. Passing through the fluid the jet entrains fluid from either side, but the removal of fluid from the side nearer the plate necessitates higher velocities as the replacing flow is restricted by the impervious plate. This causes a greater reduction in static pressure at the plate side and the pressure difference across the jet causes it to bend towards the plate, which in turn increases the velocity of the return flow and finally the jet impinges onto the plate and adheres to it, becoming a wall jet. When the jet strikes the plate it divides; one part reverses back into the bubble to replace the fluid entrained by the jet, while the other part continues

downstream adhering to the wall.

By idealising conditions at the reattachment zone and elsewhere the physical picture described above can be represented mathematically as shown in Figure 2.1.b.

The assumptions necessary for the model are:-

1. The fluid flow is two-dimensional and incompressible.
2. The inlet velocity distribution is uniform.
3. The static pressure in the bubble is uniform.
4. The velocity profile across the curved jet is the same as for a straight jet.
5. The tangential shear forces on the plane due to viscosity are negligible.
6. The point of reattachment is defined by the following -

   $\psi = 0$ and $\psi = Q$ are defined as two imaginary lines (on either side of the jet centreline) so positioned that the mass flow between either and the centreline is half the total mass flow from the slit at entry. Any part of the jet outside these two lines can be considered as entrained from the surrounding fluid. In particular, the fluid between the $\varphi = 0$ line and the jet edge is collected from the bubble during the transit of the jet along the boundary, and the same quantity of fluid must be returned to the bubble when the jet splits at reattachment.

The outside edges of the jet are defined as the lines through the points where the average fluid velocity

in the direction of the jet is one tenth of the velocity at the jet centreline (at the same position along the jet).

From these two definitions it follows that the jet will first touch the plane where the jet edge crosses it, and also tha the stagnation point on the surface of the plane will be where the streamline $\psi = 0$ crosses, some distance further along.

Sawyer obtains a model of the flow at reattachment by assuming that the radial plane through the intersection of the jet edge and the boundary plane marks the reattachment position where the jet instantaneously splits into two components, one flowing downstream and the other reversing back into the bubble. Although this splitting must affect the flow upstream of the radi plane the jet is assumed to have a free jet profile up to the section. The velocity profiles of the two separate flows existing after this will be discussed later.

The analysis considers a free jet issuing from an infinit thin slit at a distance X_o upstream of the actual physical inlet. (X,Y is a coordinate system based on the jet centreline) The leng X_o is determined by matching the width and momentum of the theoretical jet to those of the real jet.

Since the jet is thin and two-dimensional it bends into a circular arc under the action of a uniform pressure difference. This allows a geometrical relationship to be found between the coordinates of the intersection of the jet edge and the plane, (and hence of the $\psi = 0$ streamline and the radial plane) and the angle ϑ which both of these points subtend at the centre of curvature,

as is illustrated in Figure 2.1.b. There are now two unknown parameters in this equation, ϑ and a combination of X_R and Y_R which is given the symbol T_R, and is defined by $T_R = \tanh(\sigma Y_R/X_R)$. Another relationship between them is required for a solution.

Sawyer suggests two alternatives for this second equation; one is Dodds' original assumption, and the other is one of two suggested by Bourque andused in his analysis.

Dodds' originally obtained another equation by assuming that the jet splits into two streams at the reattachment point, one flowing back into the bubble with a velocity profile similar to half a Gortler profile and a maximum velocity equal to $\sin\vartheta$ times the maximum jet velocity before the split, and the other flowing downstream as half a Gortler profile and the same velocity as before the split.

Expressed mathematically and simplified this leads to the equation—

$$T_R = 1 - 2\left(\frac{1 - \cos\vartheta}{1 + \cos\vartheta}\right) \quad - \quad - \quad - \quad (A).$$

Bourque's first assumption, also used by Sawyer, was that the two flows after splitting retained the same velocity profiles as they had before, with only the directions of the flow changed. This leads to the equation —

$$\cos\vartheta = \frac{3}{2} T_R - \frac{1}{2} T_R^3. \quad - \quad - \quad - \quad (B).$$

Bourque' obtained his second equation by considering the momentum of the various flows into and out of the control volume ABCD and neglecting viscous shear forces on the boundary walls. The relationship obtained from these considerations is —

$$\cos \vartheta = \frac{3}{4} \left(\frac{2}{3} + T_R - \frac{1}{3} T_R^2\right). \quad - \quad - \quad - \quad (C).$$

Sawyer was then able to solve the geometrical equation with (B) to obtain T_R and ϑ in terms of the entrainment parameter σ. Using these values he calculated the bubble length for various entrainments and obtained Figure 2.2. Although his report deals only with (B) it was decided in this investigation to evaluate the predictions based on (A) and (C) for the sake of comparison with the other two analyses. The solution obtained from (A) is shown in Figure 2.3 and Sawyer's experimental measurements are marked on both figures. It can be seen from these that the experimental points indicate values of σ around 15 in 2.2, and 1·0 in 2.3.

A value for σ of 8 has been established for a two-dimensional uncurved free jet (44) and it is widely held that curvature inhibits entrainment so that σ greater than 8 is to be expected, making the predictions of figure 2.2 (equation B) the most acceptable. Equation (C) indicates σ to be less than 0·1 which is useless.

Sawyers findings are further discussed with those of the other investigations at the end of the chapter.

Bourque and Newman's analysis.

Again basing their work on the theories of Prandtl, Gortler and Dodds, Bourque and Newman analysed the problem of re-attachment in two configurations. One was the same as that treated

by Sawyer and the other consisted of a jet issuing at an acute angl from a two dimensional slit in a flat plane which is shown in figur 2.4.a. As before the jet entrains fluid from either side and the pressure difference caused by the presence of the plane bends the jet round until it reattaches.

In the analysis the first five assumptions are made as in Sawyer's treatment, but the definition of the point of reattachment is different. Instead of assuming that it occurswhere the outside edge of the jet strikes the plane, Bourque assumes it to be where the jet centreline cuts the plane, and the model of the flow isas shown in Figure 2.4.c. Figure 2.4.b shows the model obtained by using Sawyer's reattachment position.

Thus instead of a complex geometrical relationship as was found previously, the value of ϑ is immediately equal to the jet inlet angle φ. Although this appears to give a model very similar to that obtained before, the effect on the predicted bubble length is large for the smaller jet angles and considerable even as the jet angle exceeds 60°.

As in the previous analysis the second equation can be obtained using the same three assumptions, and the equations are the same as before. Bourque used both (B) and (C) in his analysis and both provided reasonable predictions of bubble length.For the purpose of comparison the solution using (A) was completed but the predictions which were obtained were unreasonable and have not been shown.

In order to test how the different assumptions for the reattachment position affected the predictions of bubble length, the same configuration was analysed using Sawyer's assumption (Figure 2.4 b) and the results compared with those of Bourque. The solutions obtained from Sawyer's method are shown on Figures 2.6 and 2.7, (equations B and C respectively) and from Bourque's on Figure 2.5 (equation B).

A comparison of the predictions of bubble length shown on these graphs shows that those of Figure 2.5 are considerably larger than the others. The difference is most marked at the smaller jet angles and is due to the assumption that the reattachment point is not affected by the spread of the jet (the point being the inter section of the jet centreline with the plane) whereas Sawyer makes the defining line to be the jet edge. At smaller angles the re - attachment is due more to the spread of the jet than to the curv - ature.

Another objection to Bourques assumption, and in a lesser degree to Sawyer's, is that the split in the jet (that is the reattachment plane) must occur before the jet strikes the plane, to allow space for the reverse flow to enter the bubble through the gap between the jet and the plane. Thus the actual point at which the jet divides must be slightly upstream of Sawyer's pos- ition and considerably upstream of Bourque's, making the first assumption preferable.

Consideration of these arguments and the graphs of

predicted bubble length led to the conclusion that the two analyses which have been described should be compared with the following treatment of the flow through a control valve on the basis of Sawyer's assumption for reattaohment and Bourque's equation (B)to determine the flow distribution after it splits.

2.2. Application of an entrainment model to the flow through a slide valve port.

The geometry of the flow through a piston control valve is a combination of the geometries considered in the two previous entrainment studies. As is shown in Figure 1.3., the straight sides upstream of the orifice cause the flow at the exit plane to have momentum in towards the jet centreline so that the jet continues to contract beyond the plane, forming a vena contracta. Thus the parallel-sided jet originates from a position both above and at an angle to the plane to which it eventually reattaches, a combination of the two previous geometries.

Von Mises' (54a.) potential solution predicts the width of the jet at the vena contracta and the angle it makes with the pla but it does not define the curvature of the free surface from the edge of the orifice to the vena contracta. An accurate field plot in Mitchell's report (32.a) allowed this to be measured and it was found that the distance from the orifice to the vena contracta is small and approximately equal to half the final jet width.

The final jet width is itself a doubtful value since the free surface of the jet entrains fluid as soon as it touches the downstream reservoir. Between the orifice and the contraction however the radius of curvature of the side of the jet is very small, which inhibits entrainment and permits this effect to be

ignored in the calculations.

With these considerations in mind an assumption has to be made to define the position of the jet entry in the mathematical model of the valve flow. In the following analysis two assumptions have been tried to indicate how varying the inlet position affects the prediction of the bubble length.

The two inlet positions used are shown in Figures 2.8.b and 2.9.b. In both instances the circular jet centreline is assumed to pass through the midpoint of the line joining the two corners which make up the orifice. Mitchell's potential map shows this to be a good approximation when the corners are in the zero clearance position (w = 0), and it is correct for the symmetrical case (w=1).

Figure 2.8.b illustrates the first assumed entry position with the jet emerging into the model from a line perpendicular to the jet centreline and passing through the midpoint of the line joining the corners of the orifice. The second position (Figure 2.9.b) has the jet centreline in the same position but the jet entering from a line perpendicular to the centreline and a distance equal to half the jet thickness up from the midpoint.

Having made these assumptions the analysis follows the previous two, using Sawyer's reattachment point .The geometrical equation is complicated due to the difficulty in defining the inlet position.

In Fig.2.8.b.

$$\frac{r - \frac{a}{2\cos\varphi}}{r - \frac{\delta_c}{2}} = \frac{\cos\vartheta}{\cos\varphi}$$

and in 2.9.b

$$\frac{r - \frac{a}{2\cos\varphi}(1+\sin\varphi)}{r - \frac{\delta_c}{2}} = \frac{\cos\vartheta}{\cos\varphi}$$

When these equations are simplified and expressed in terms of T_R and ϑ they become –

$$T_R = \frac{\cos\vartheta - \cos\varphi - k(\vartheta+\varphi)\cos\vartheta}{\cos\vartheta - \cos\varphi - (\vartheta+\varphi)\frac{a}{t}.\frac{3}{2\sigma}} \quad - \quad - \quad P.$$

and

$$T_R = \frac{\cos\vartheta - \cos\varphi - k(\vartheta+\varphi)\cos\vartheta}{\cos\vartheta - \cos\varphi - (\vartheta+\varphi)\frac{a}{t}.\frac{3}{2\sigma}(1+\sin\varphi)} \quad - \quad - \quad Q.$$

As before another equation is required for a solution and both equations (B) and (C) were tried –

$$\cos\vartheta = \tfrac{3}{2}T_R - \tfrac{1}{2}T_R \quad - \quad - \quad - \quad (B).$$

$$\cos\vartheta = \tfrac{3}{4}(\tfrac{2}{3} + T_R - \tfrac{1}{3}T_R^2) \quad - \quad - \quad - \quad (C).$$

The predictions of bubble length obtained are shown in Figures 2.10 (Equations Q and B), 2.11 (P and B), 2.12 (P and C) and 2.13 (Q and C). A more complete analysis is given in the Appendix at the end of this work.

The graphs on these figures show that all four solutions provide reasonable predictions when the experimental measurements are taken into consideration. As was expected the two different entry conditions affect only the bubble lengths at the smaller jet angles. When the jet angle is 45° the effect is small, but at 21° the effect is almost 25 per cent. The predictions of Figure 2.10 were chosen to be compared with the other investigations.

2.3. A comparison of the three investigations.

The three analyses and their associated experimental results were compared using Bourque's assumption regarding the momentum at the reattachment point and Sawyer's definition of the position of the point – this involved the graphs of Figures 2.3, 2.5 and 2.10.

From each set of graphs the variation of the value of σ indicated by the experimental results was plotted against the bubble length, and the findings are shown on Figure 2.14.a. This confirms a close agreement between the valve results and those of Bourque, however Sawyer's figures indicate much lower values of σ. If a correction is made for the effect of the radius of curvature – using the crude assumption that the value of σ varies inversely as the radius – then the valve results and Bourque's remain close as they have almost the same radius, but Sawyer's values of σ increase since his average radius was about 1.6 times that of the others. The corrected values are shown on Figure 2.14. on which all three sets of results correspond.

The remaining difference between Sawyer's and the othe two is in the angle which the jet makes with the plane at the poin of reattachment. In his geometry this angle is almost 90° whereas the others are more acute (between 15° and 50°). When the jet stri the plane at an acute angle the reverse flow back into the bubble affects the entrainment into the inner edge of the jet along a considerable length, but at larger angles the interference is quit

small. This possibly explains the reduction in entrainment at the more acute angles shown on Figures 2.5 and 2.10, and the less marked reduction at small jet heights on Figure 2.3.

At the other extreme, when the bubble lengths are large all three figures show a reduction in entrainment. This is linked to Bourque's finding that a stably reattached jet cannot exist when the inlet jet angle exceeds some 60° — corresponding to a bubble length of over 100 times the jet thickness. This is poss — ibly due to the effect of normal viscosity on the momentum of the jet — the velocity being dissipated before reattachment is complet The effect would be aggravated by any increase in turbulent visc - osity in the broad, low speed regions at the edges of the jet remote from the inlet — such non — linear behaviour has already been postulated to explain the rapid "cut—off" of the velocity profile at all jet edges.

From the point of view of the valve designer the comparis has shown that the mathematical model of the flow and reattachment provides a useful method of calculating bubble lengths over a slightly restricted range of inlet conditions. It has also shown that the jets found in control valves closely resemble those found and studied in other branches of fluid mechanics.

Using the theory developed it would be possible to cal — culate the average bubble pressure, thus enabling reaction forces to be determined empirically (Sawyer shows the calculation to be fairly accurate). However once the variation of entrainment due to curvature has been established (see Chapter 6.2.) the predictions of pressure will be less empirical and more accurate.

FIGURE 2.1.a.

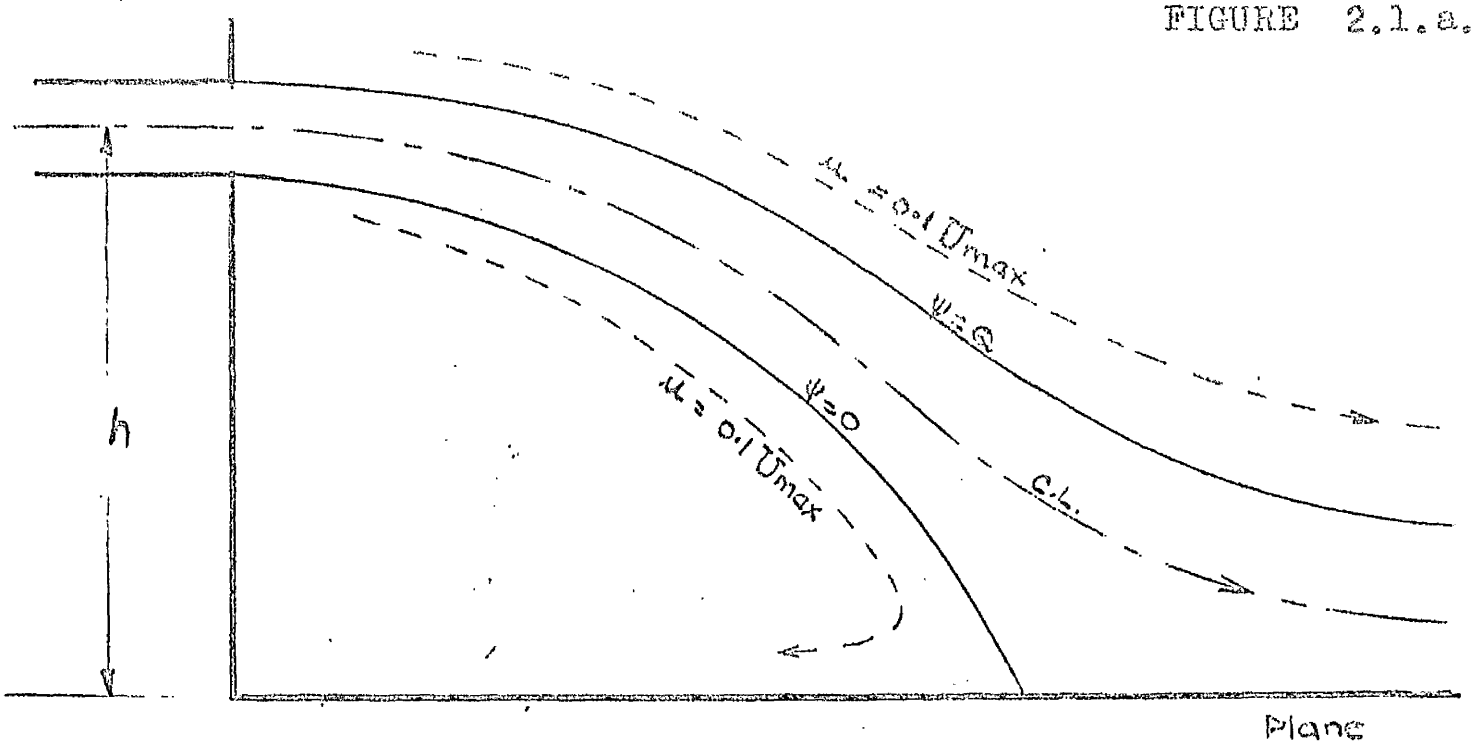

SAWYER'S CONFIGURATION.

FIGURE 2.1.b.

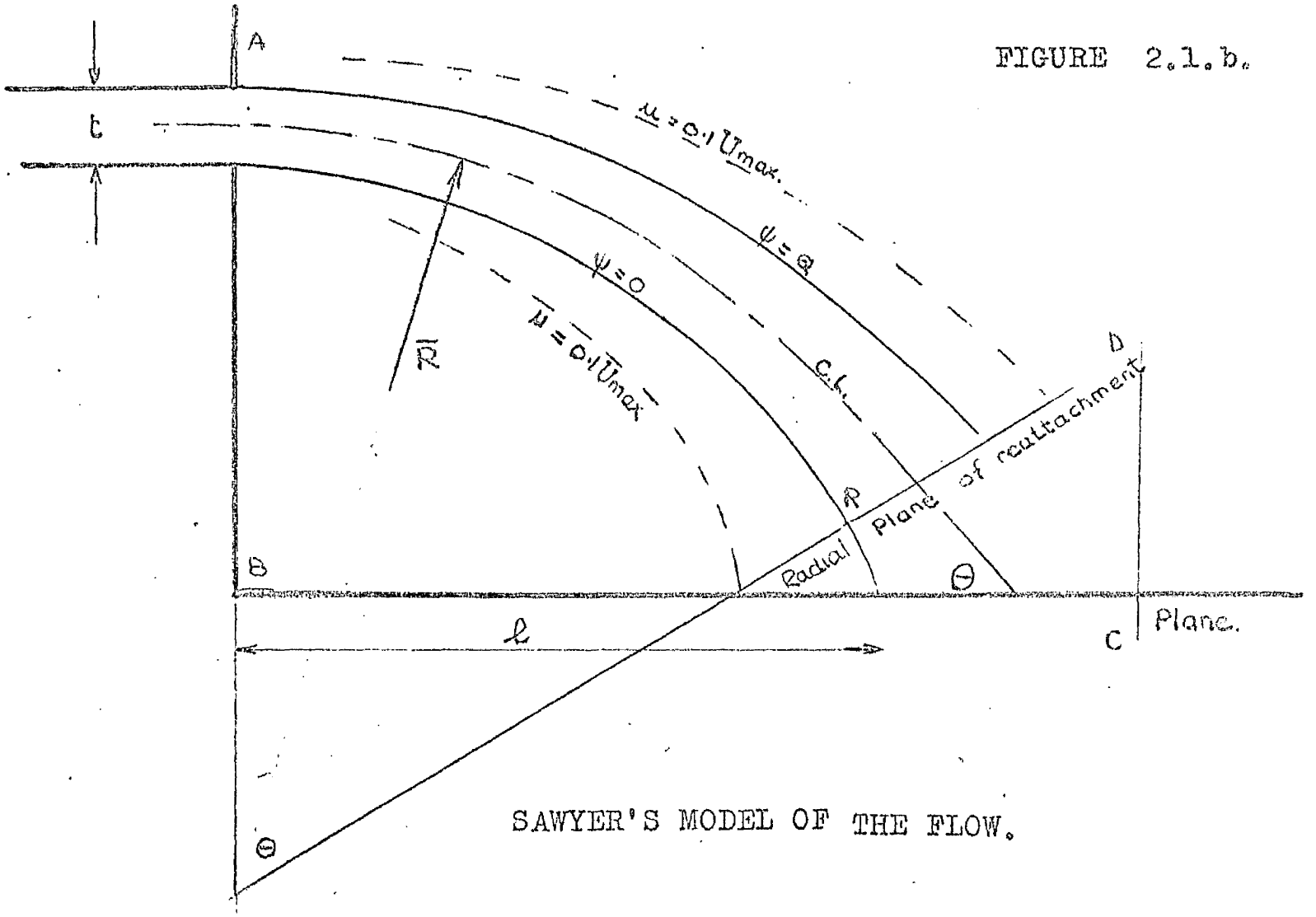

SAWYER'S MODEL OF THE FLOW.

FIGURE 2.2.

SAWYER'S CONFIGURATION AND ANALYSIS.

(BOURQUE'S MOMENTUM EQUATION B.)

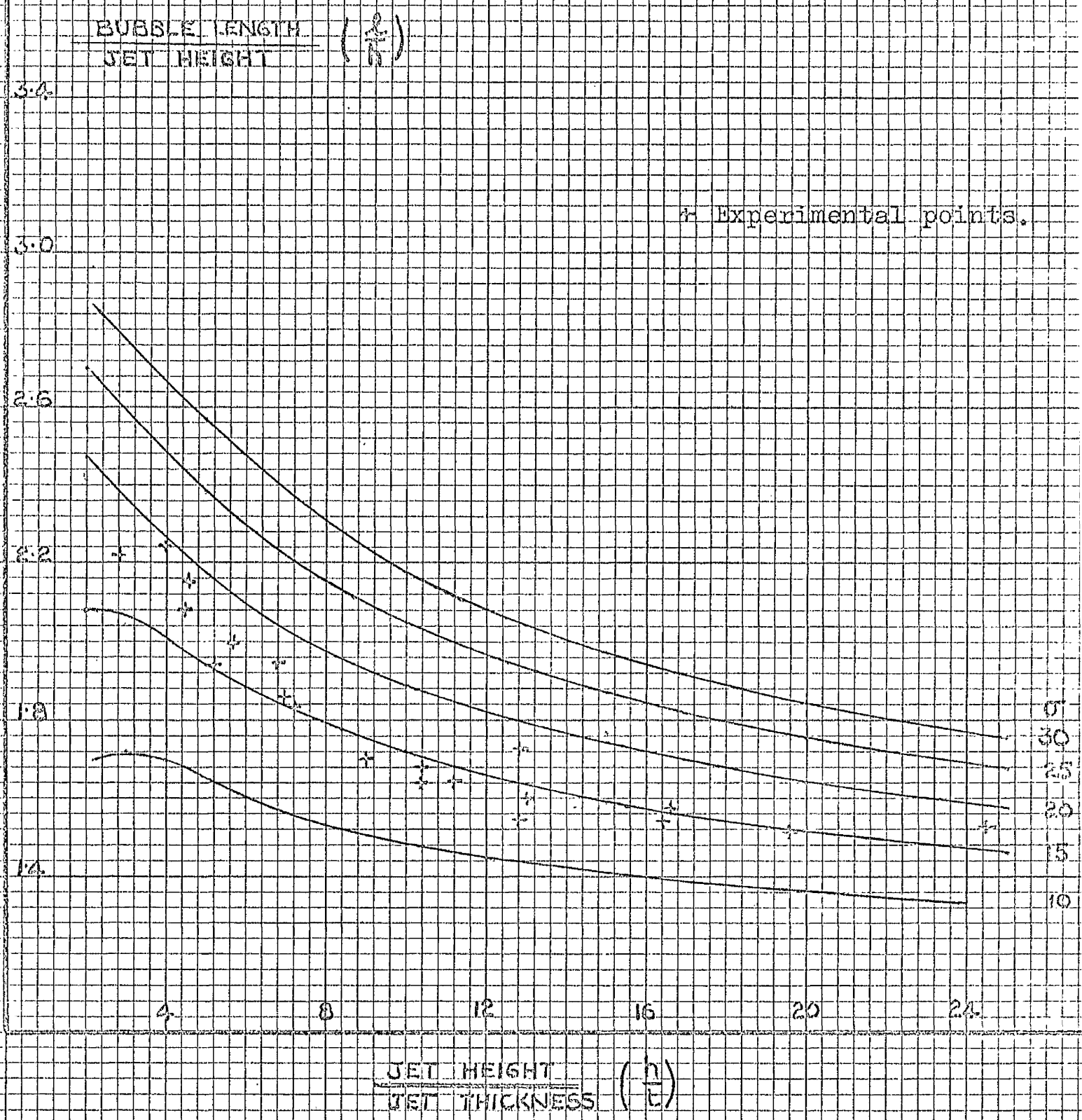

FIGURE 2.3.

SAWYER'S CONFIGURATION AND ANALYSIS.

(SAWYER'S MOMENTUM EQUATION A.)

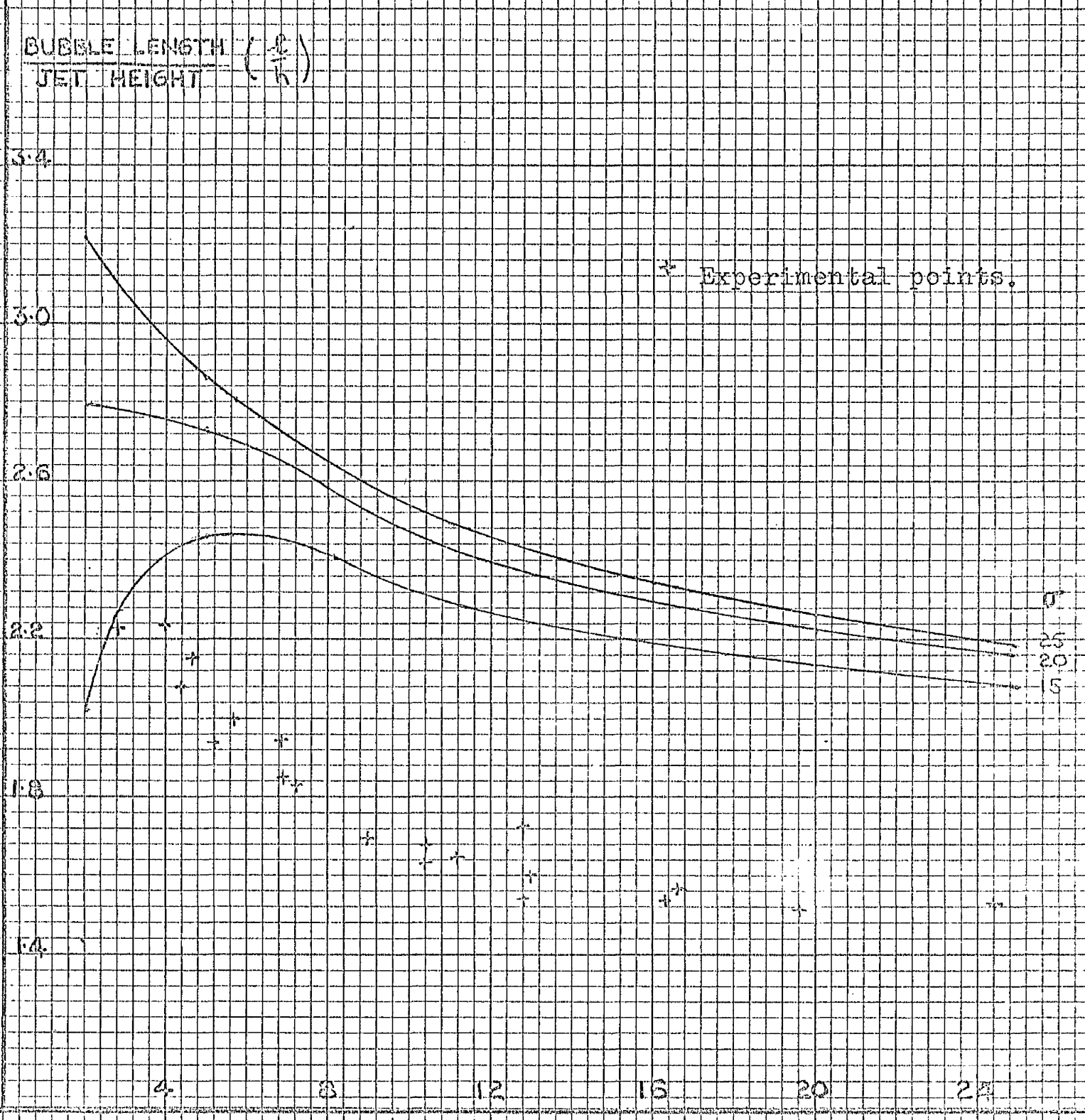

FIGURE 2.4.a

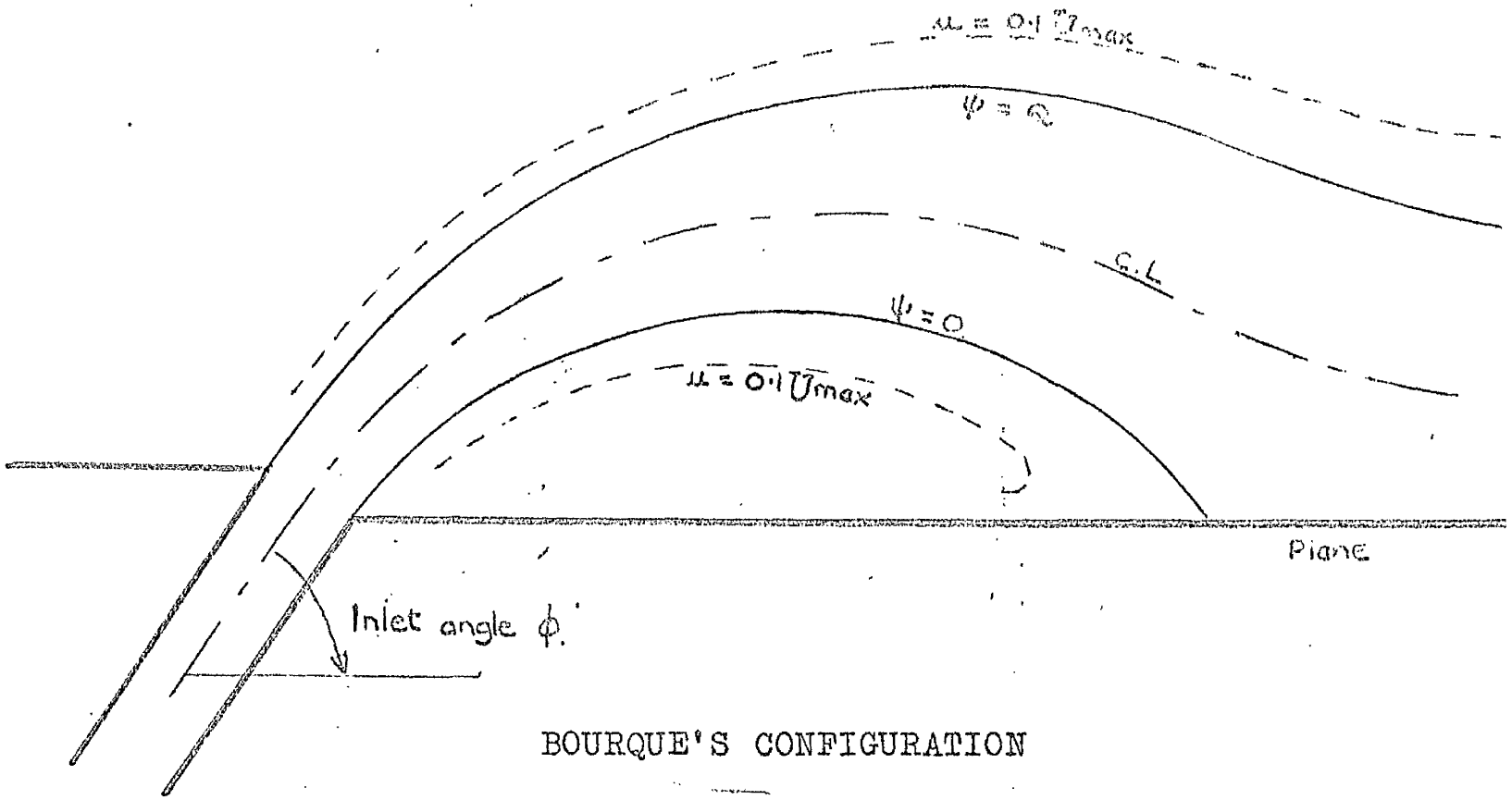

BOURQUE'S CONFIGURATION

FIGURE 2.4.b

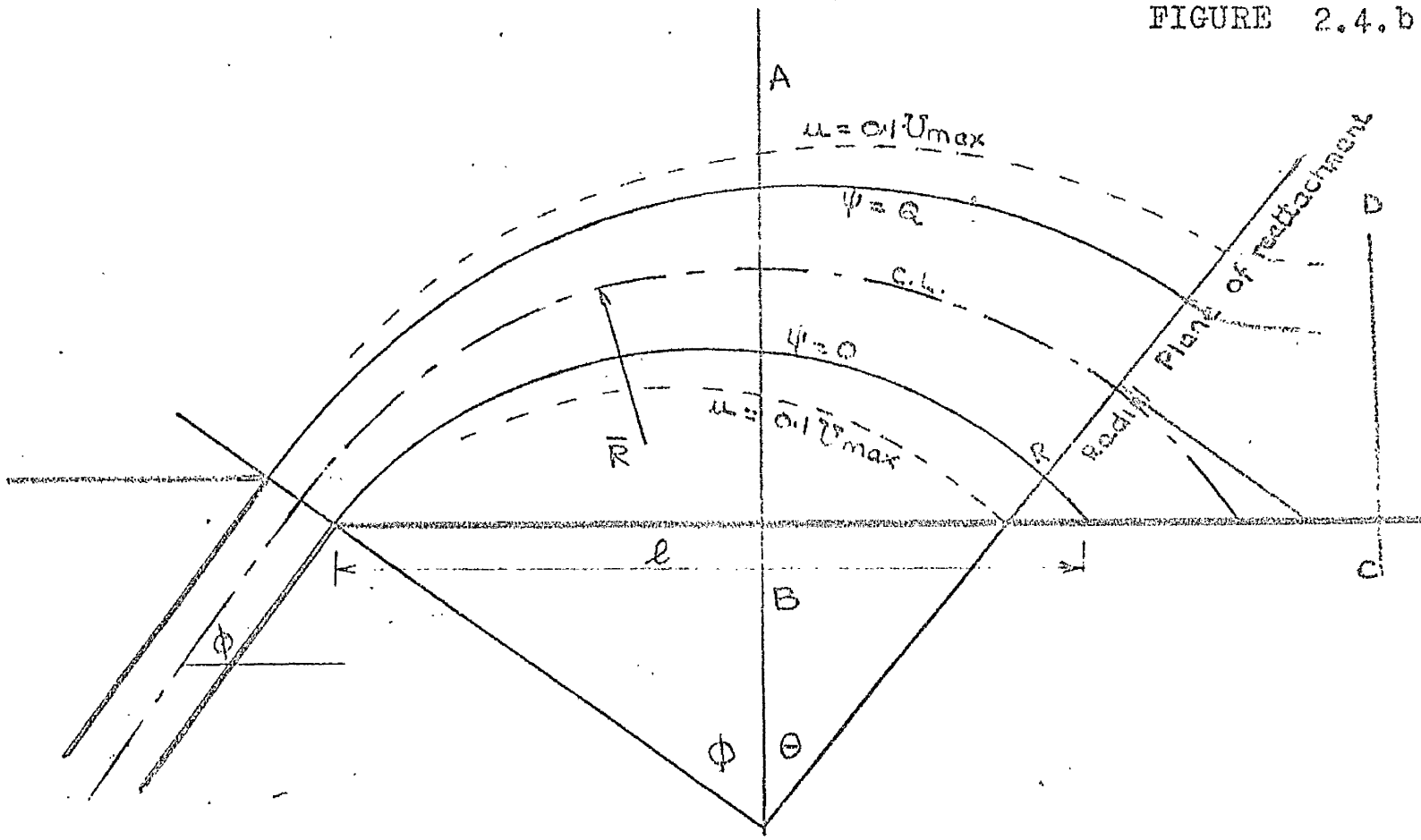

REVISED MODEL OF BO[illegible] FLOW.

FIGURE 2.4.c.

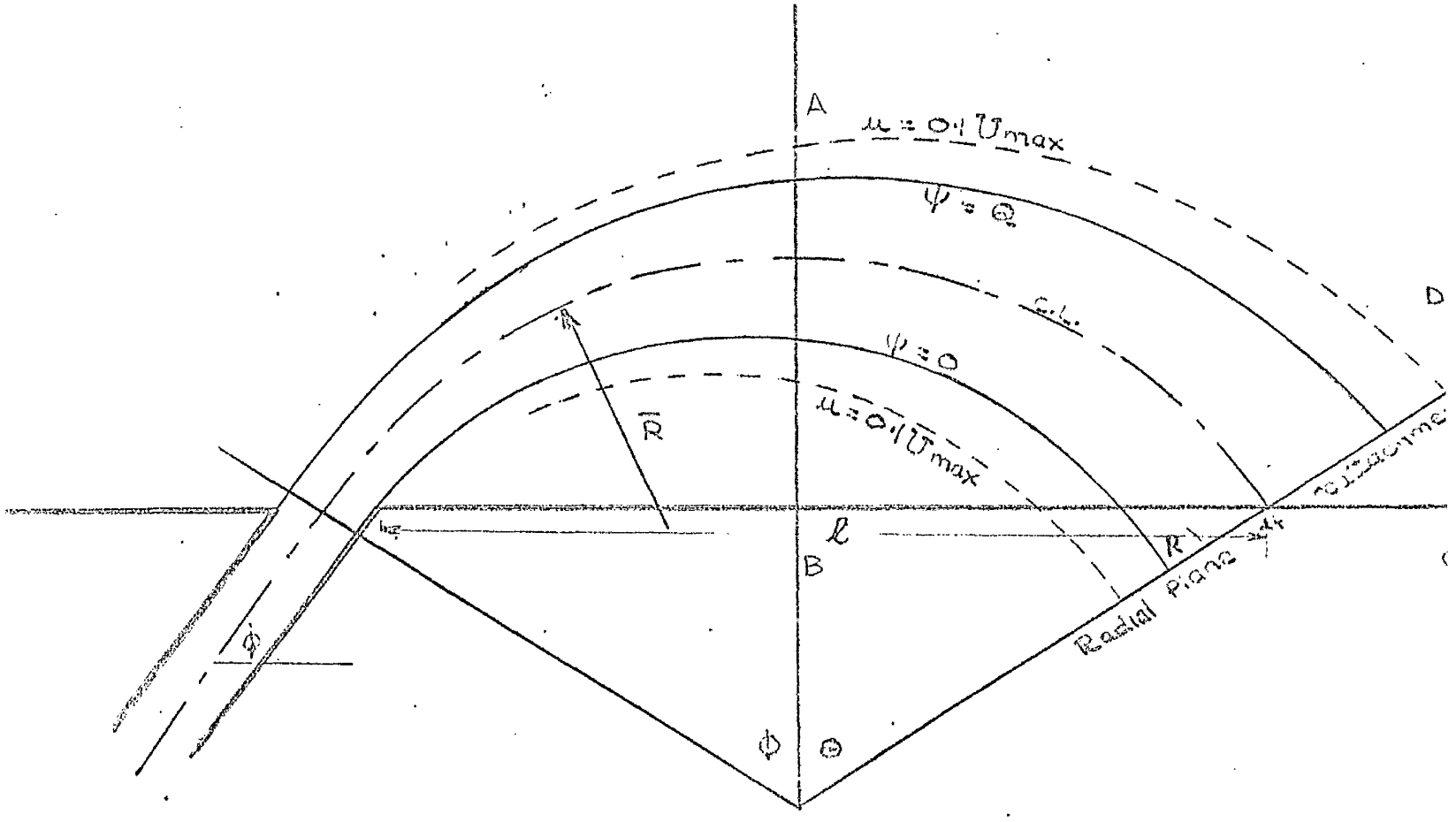

BOURQUE'S MODEL OF THE FLOW.

FIGURE 2.5

BOURQUE'S CONFIGURATION AND ANALYSIS

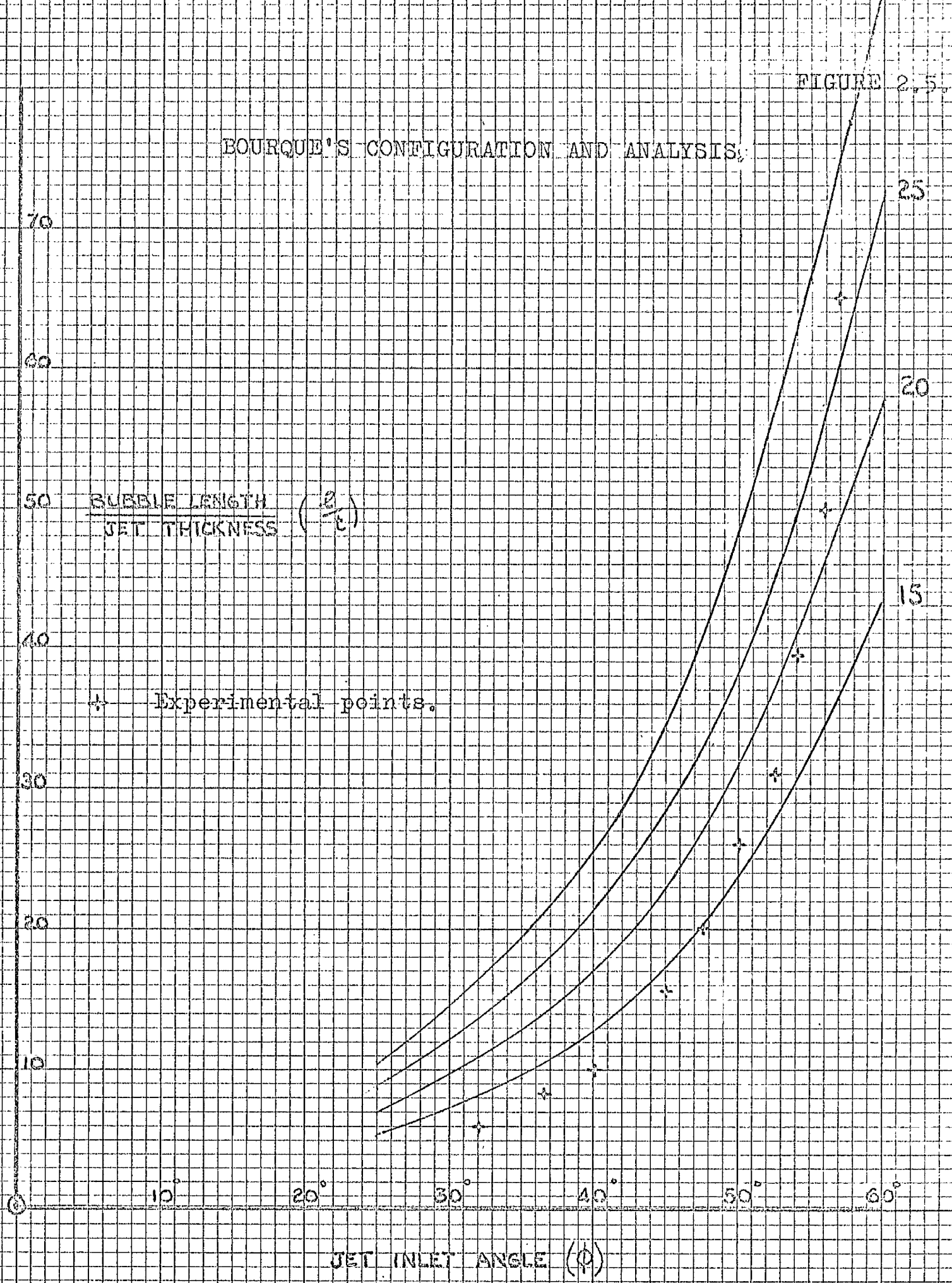

FIGURE 2.6

REVISED ANALYSIS OF BOURQUE'S CONFIGURATION.

(BOURQUE'S MOMENTUM EQUATION)

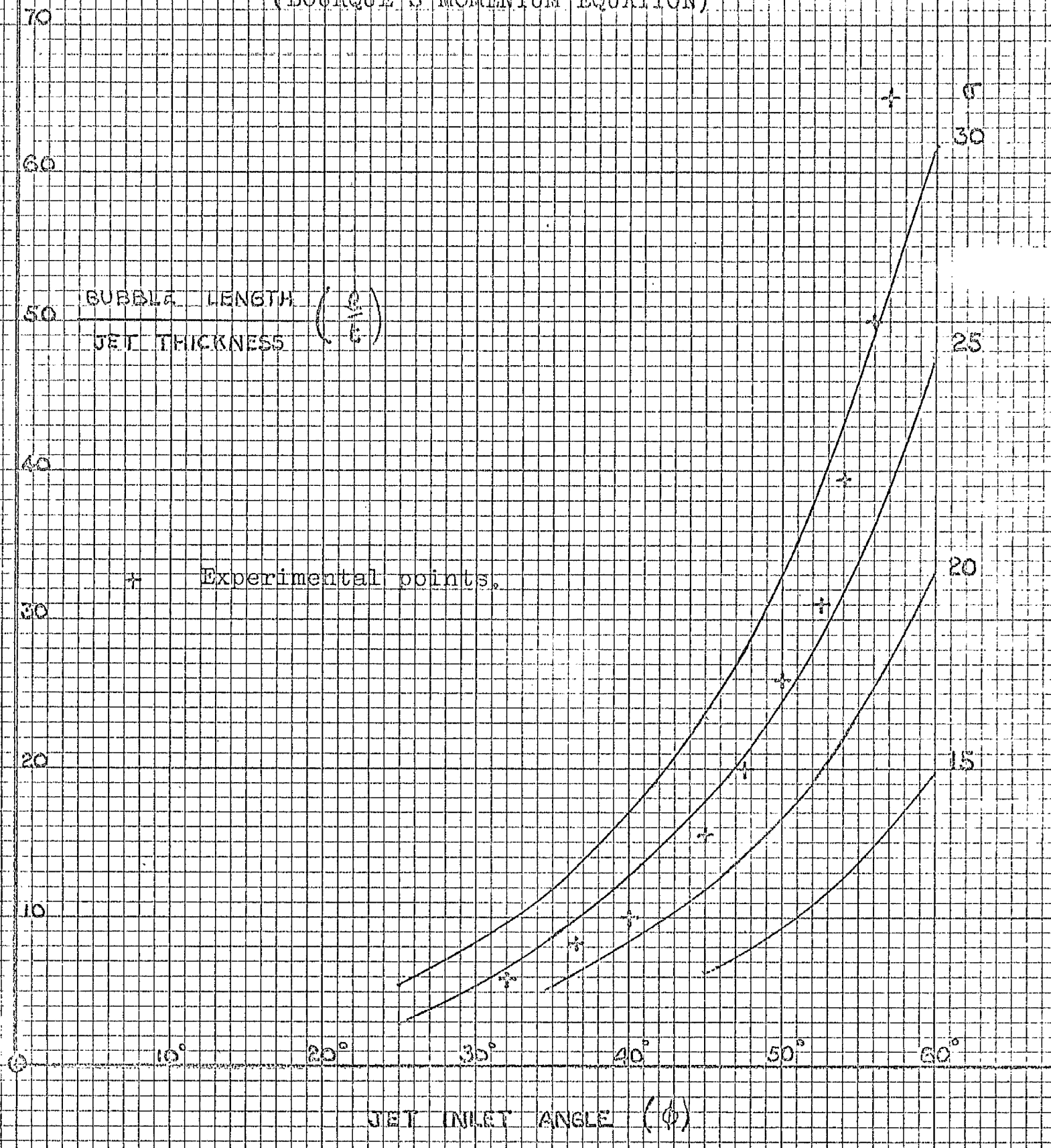

FIGURE 2.7.

REVISED ANALYSIS OF BOURQUE'S CONFIGURATION

(SAWYER'S MOMENTUM EQUATION).

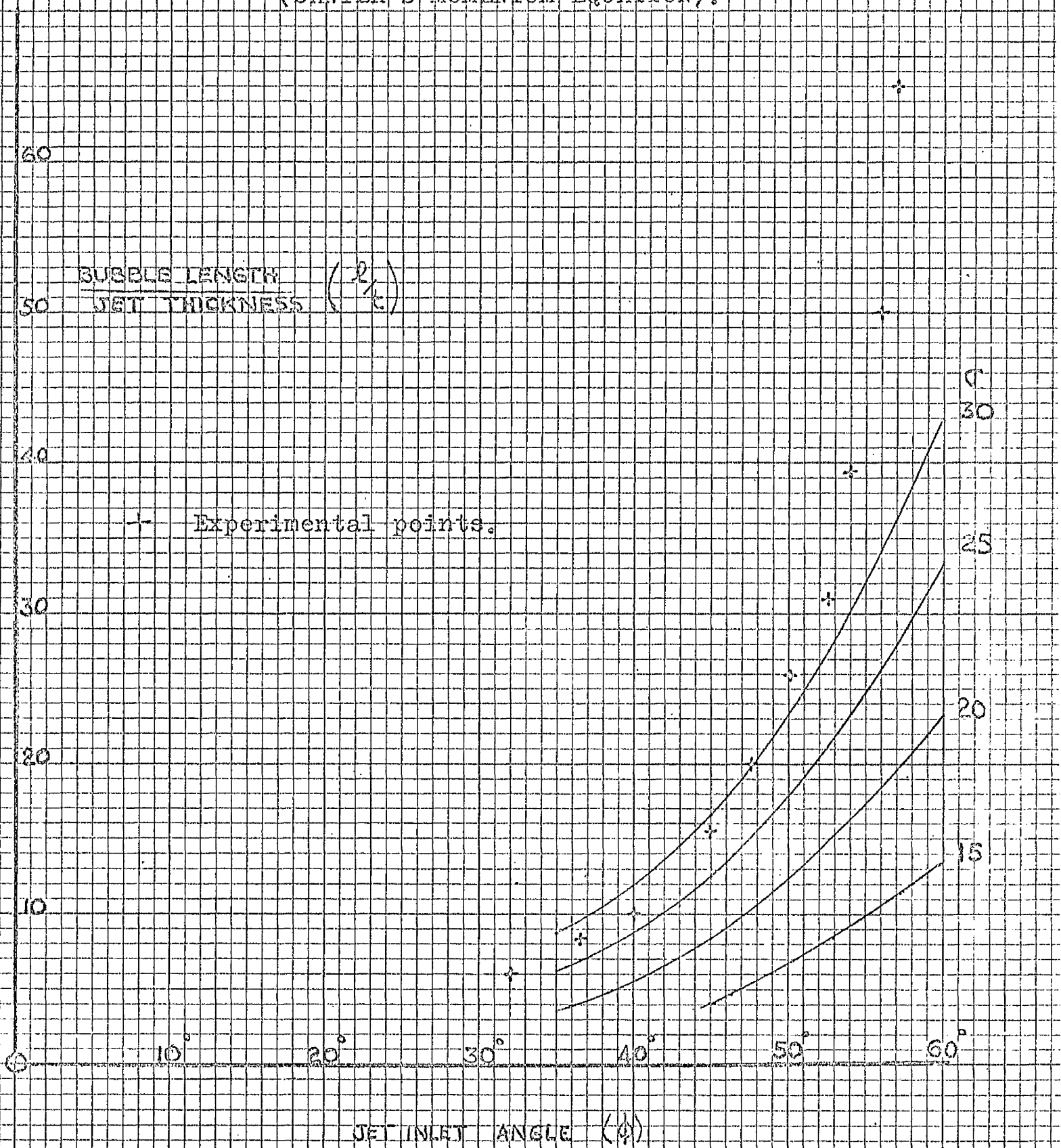

FIGURE 2.8.a.

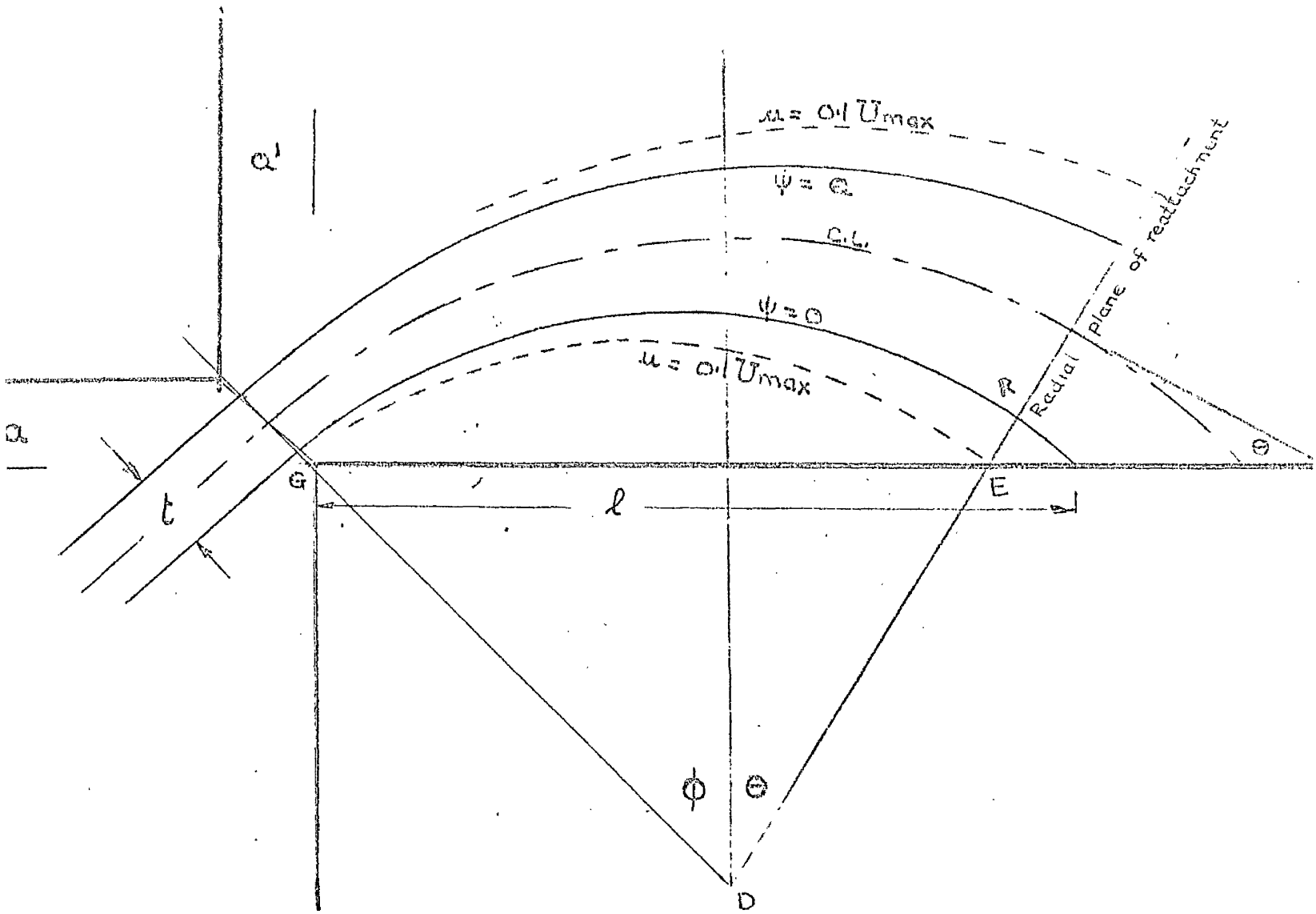

VALVE FLOW MODEL – 1st. ENTRY POSN.

FIGURE 2.8.b.

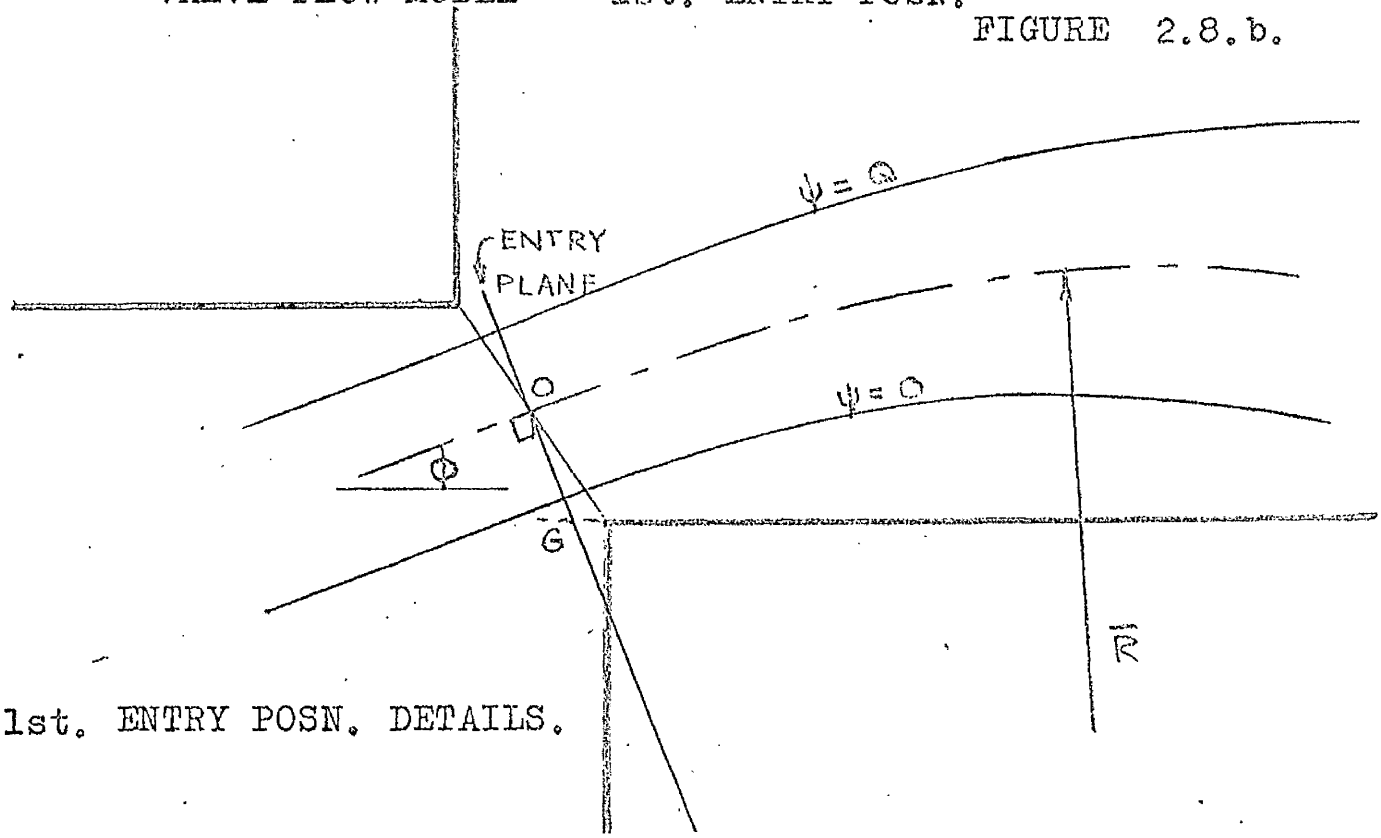

1st. ENTRY POSN. DETAILS.

FIGURE 2.9.a.

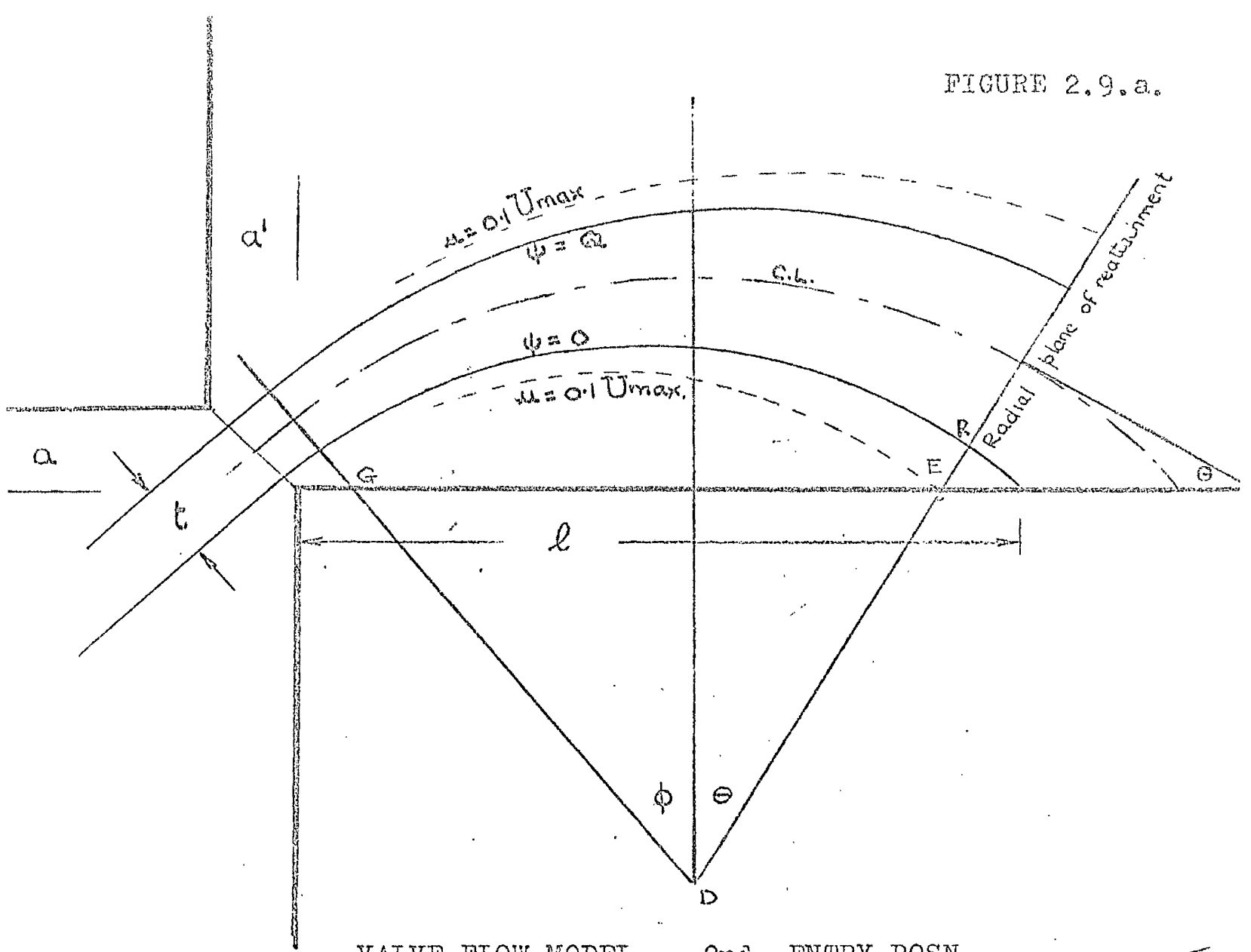

VALVE FLOW MODEL — 2nd. ENTRY POSN.

FIGURE 2.9.b.

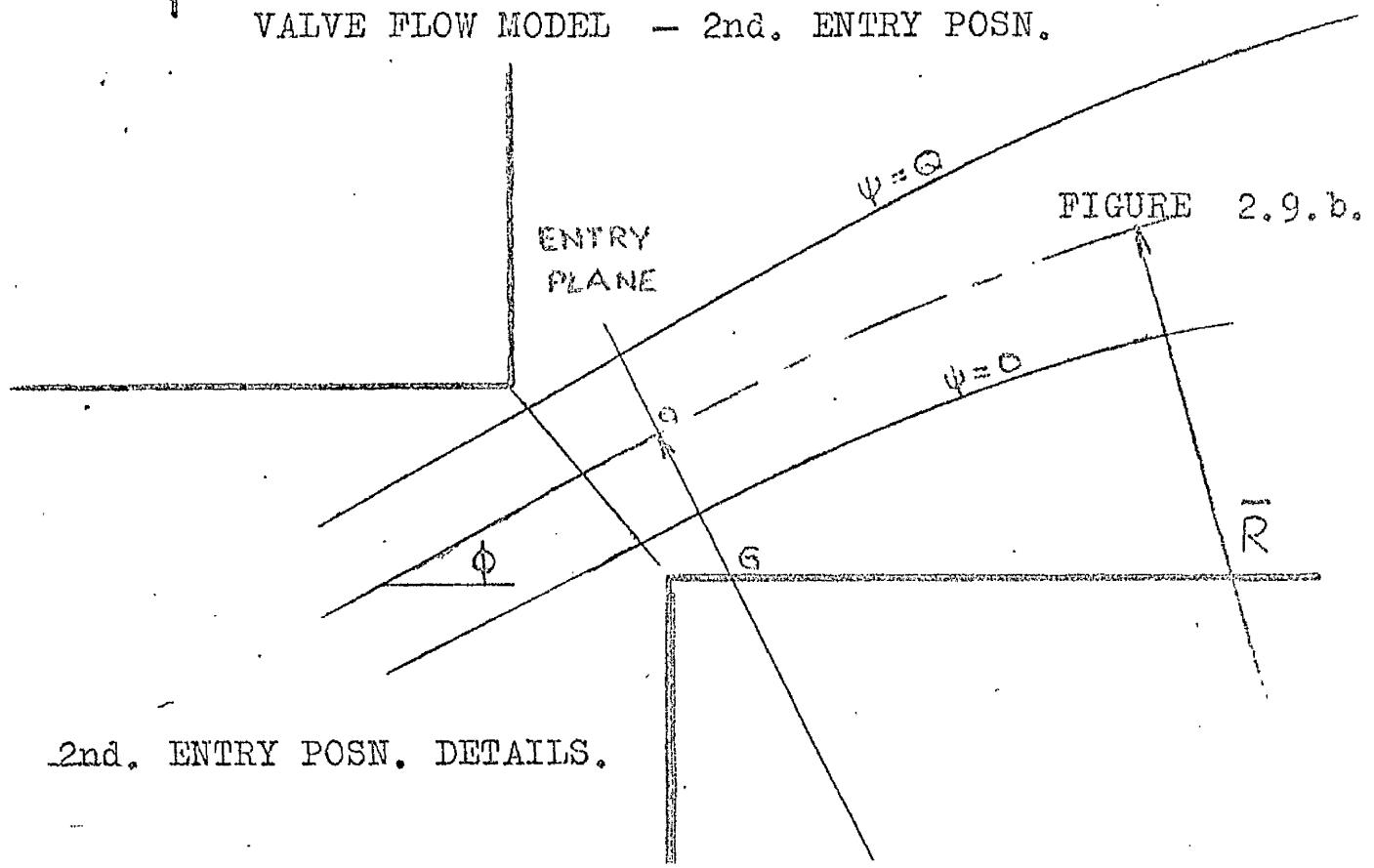

2nd. ENTRY POSN. DETAILS.

FIGURE 2.10.

REVISED ANALYSIS APPLIED TO THE VALVE CONFIGURATION.

((B) MOMENTUM EQUATION; 2nd. INLET POSN.)

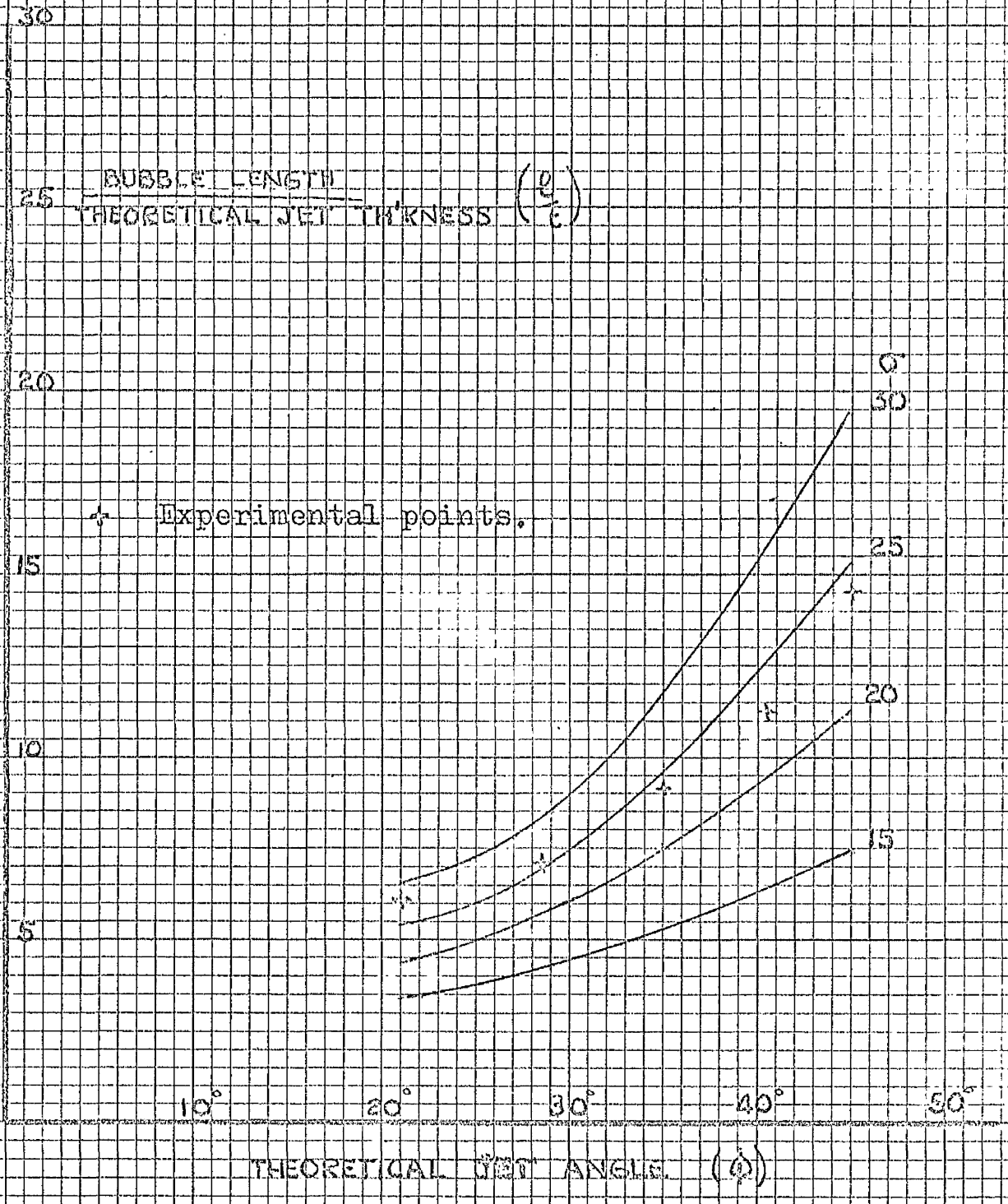

FIGURE 2.11.

REVISED ANALYSIS APPLIED TO THE VALVE CONFIGURATION.

((B)' MOMENTUM EQUATION; 1st. INLET POSN.)

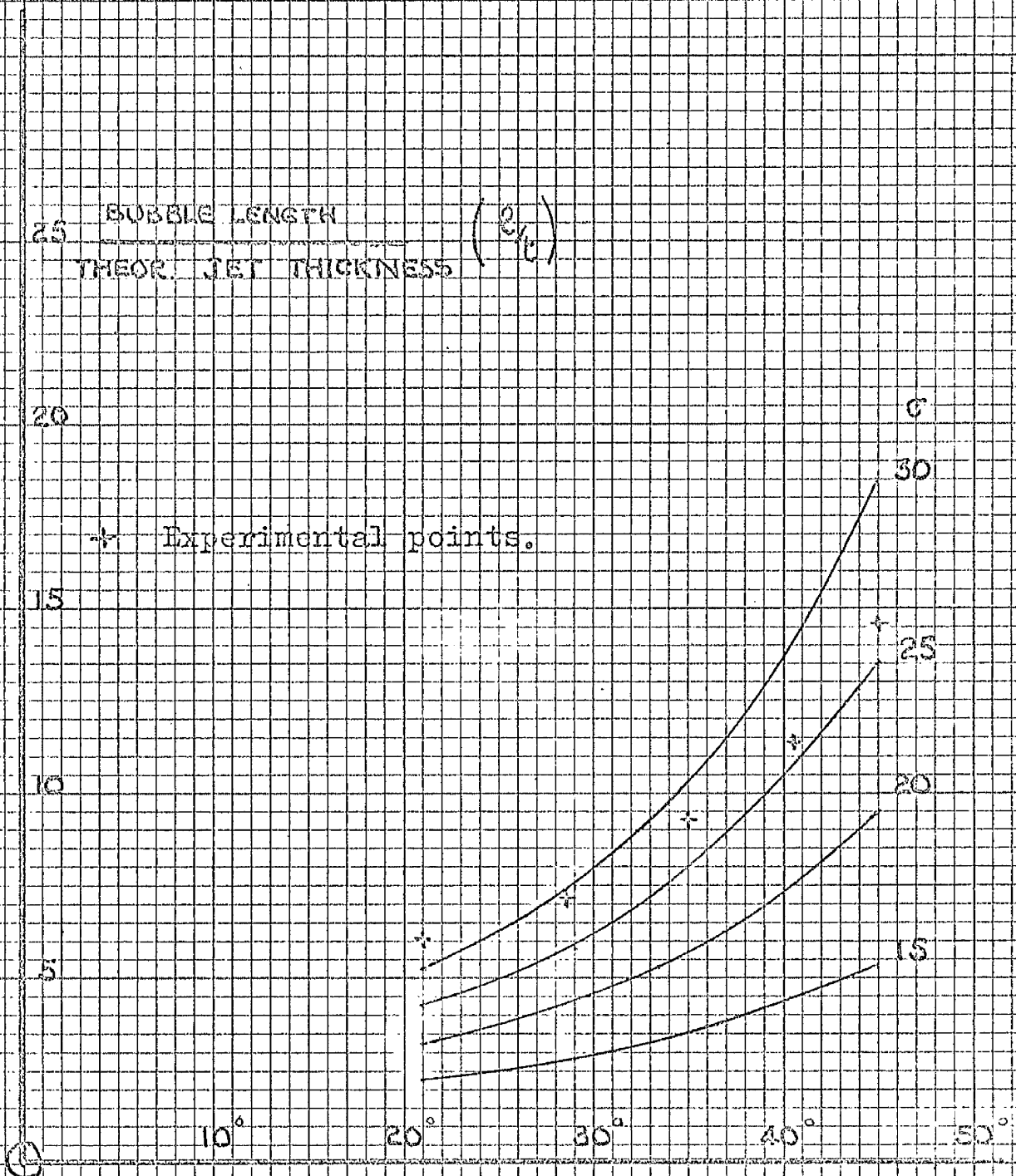

FIGURE 2.12.

REVISED ANALYSIS APPLIED TO THE VALVE CONFIGURATION.

((C) MOMENTUM EQUATION; 1st. INLET POSN.)

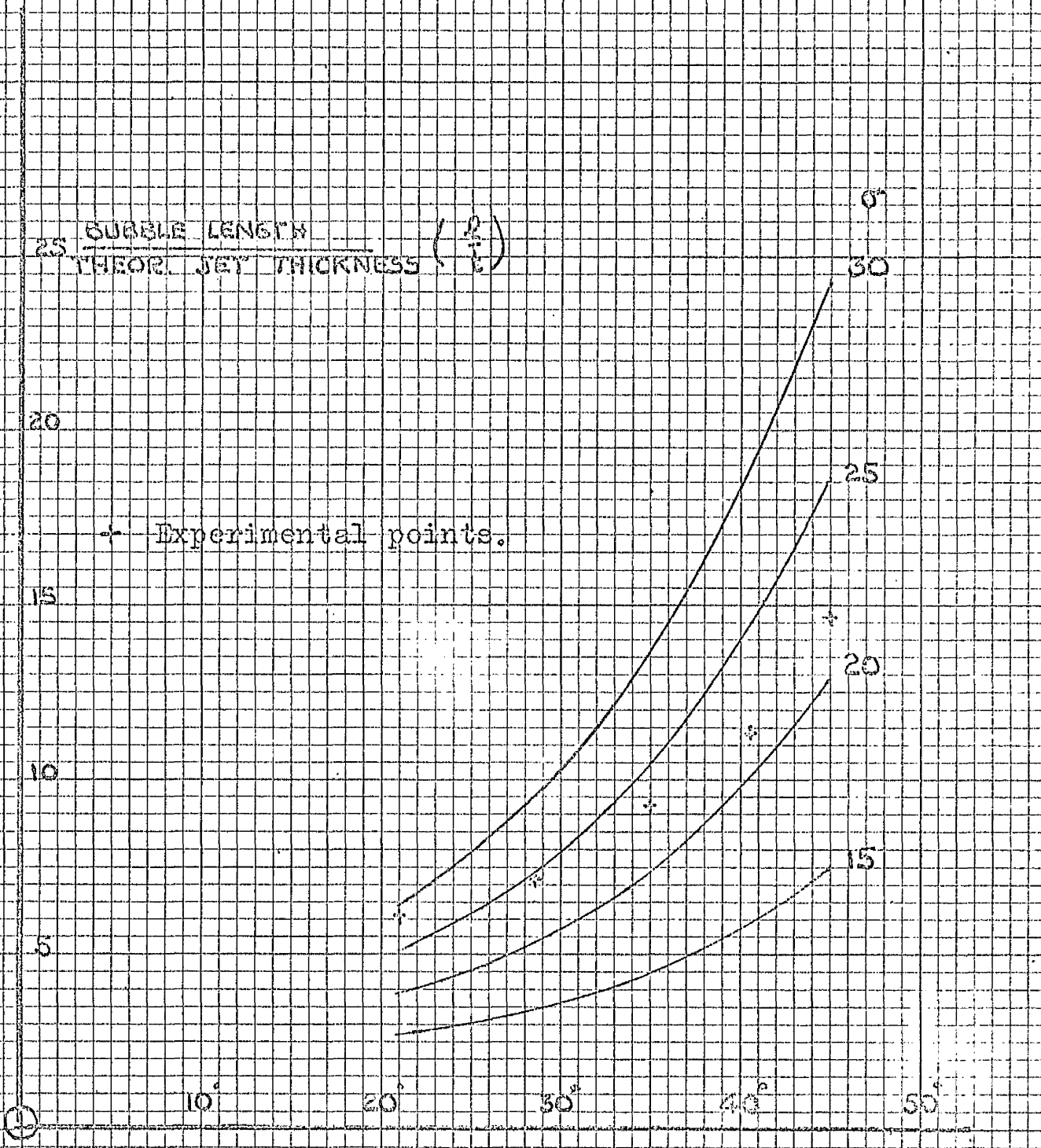

FIGURE 2.13.

REVISED ANALYSIS APPLIED TO THE VALVE CONFIGURATION.

((C) MOMENTUM EQUATION; 2nd. INLET POSN.)

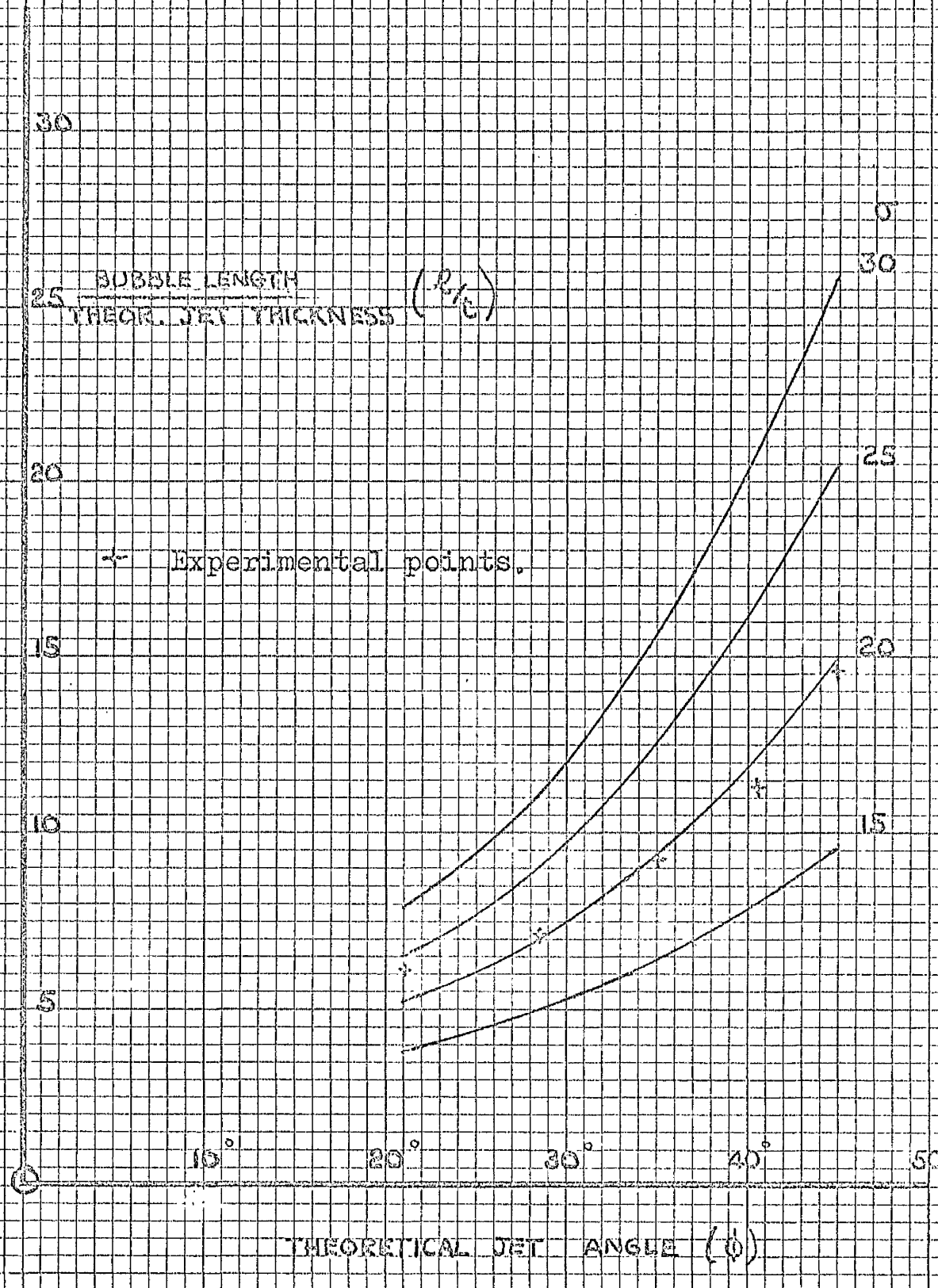

FIGURE 2.14.

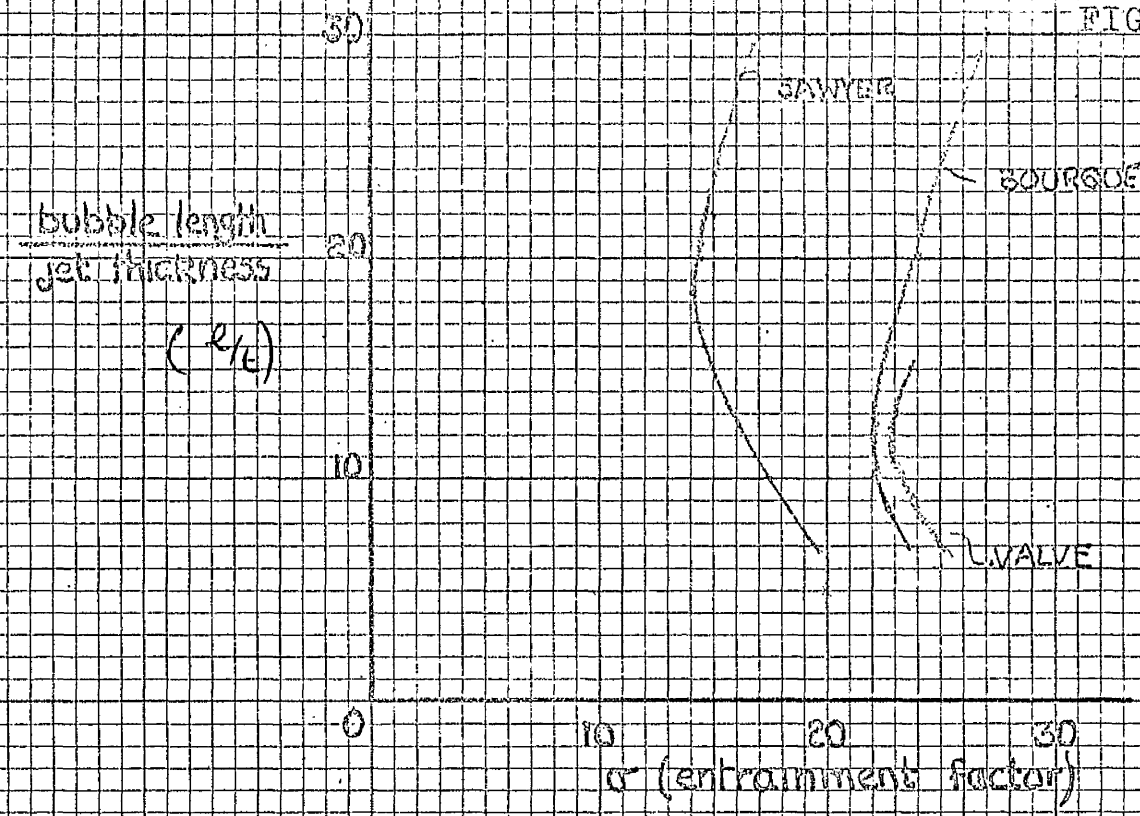

COMPARISON OF INDICATED VALUES OF σ.

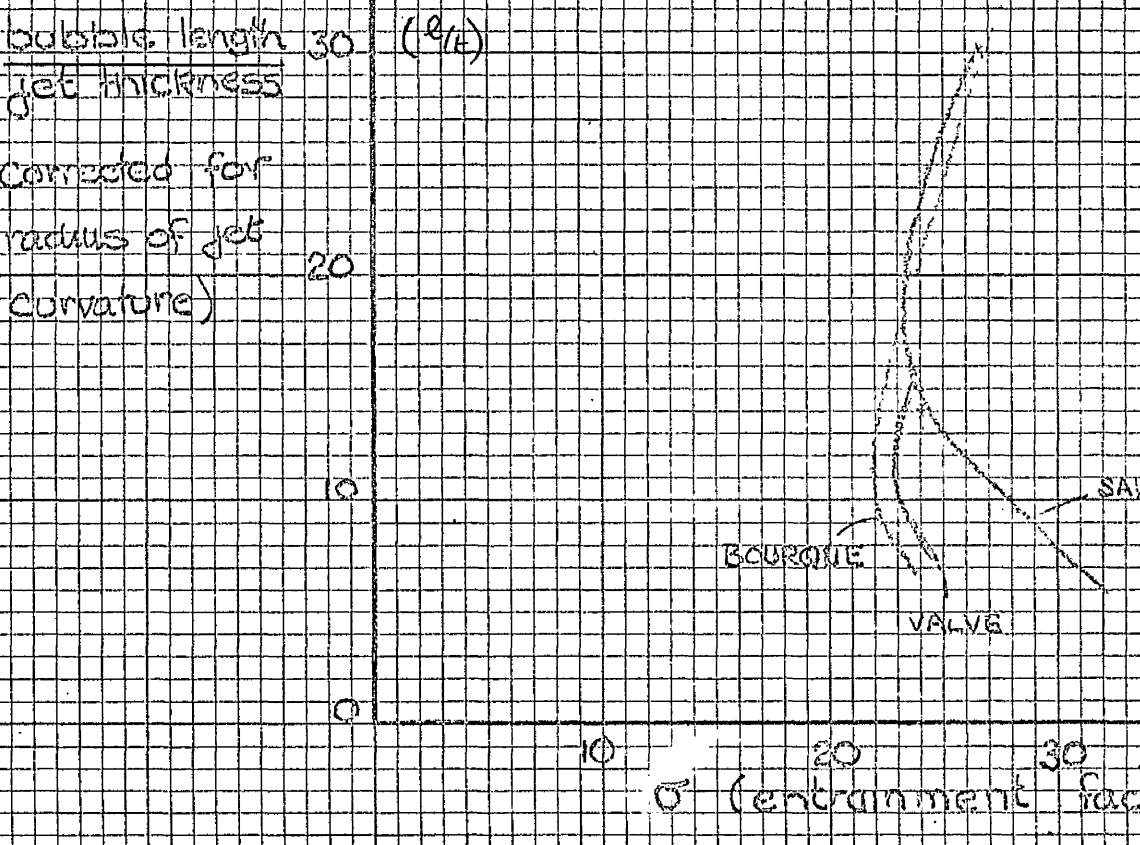

Chapter 3.

Experimental study of incompressible flow.

3.1. Description of apparatus and experimental techniques.

3.2. Experimental work and results.

3.3. Discussion of results.

3.1. Description of apparatus and experimental techniques.

The experimental work carried out used a two — dimensional model of the simple valve configuration illustrated in Figure 1.3.

The apparatus was designed for continuous operation with upstream pressures of up to 100p.s.i., corresponding to a pressure ratio of 0.123. However as a safety precaution factors were includ in the design to make the high pressure chamber rigid enough to withstand the full supply pressure of 250 p.s.i.Thus, provided precautions are taken and the bolts are gradually tightened as the pressure is raised, it should be possible to operate at the full 250p.s.i.(corresponding to a ratio of 0.056.).

To make up the valve configuration, boundary walls were sandwiched between two octagonal sheets of perspex, and heavy steel backing plates were used to reinforce the perspex over the up — stream areas subjected to high pressure. Figure 3.1 shows an outsi plan and a sectional elevation of the apparatus with the rein — forcing plates clamped in position, and Figure 3.2 shows the same plan view with the top backing plate and perspex sheet removed to show the disposition of the boundary walls and the arrangement of the measuring micrometers and positioning clamps.

The boundary walls making up the simple valve configu- ration were made up in the form of two rectangular pistons as show in the diagram. Since the area of the piston faces which were ex — posed to the high pressure of the inlet chamber was quite large

two struts were provided in each piston to brace the exposed wall against the opposite side. These rear piston walls were made to slide along substantial runners which were secured to the top and bottom perspex sheets, so that the movement of the pistons was restricted to two perpendicular directions. This allowed the orifice dimensions to be widely varied and the magnitudes of a and a' changed independently. The movement of the pistons was controlled by screws, and they could be locked in any desired position by two other screws which clamped the pistons to the runners.

Two micrometers, which butted on the outer ends of the pistons, measured the dimensions a and a' to an accuracy of one or two thousandths of an inch. The micrometers were fixed to the perspex sheets to ensure accurate and repeatable readings, and calculations indicated that the error due to the elasticity of the perspex might be one or two thousandths of an inch, which was tolerable with orifice widths of 0.2in. If necessary an allowance could be made for this effect.

The zero readings of the micrometers were obtained by moving one piston inwards over the centreline of the apparatus and then butting the other piston up against it when, theoreticall it was in the desired position. The pistons were reversed to zero the other micrometer.

The pistons were made 0.005in. less than the depth of the flow chambers (1.0in.) to help them to move freely even when the perspex sheets were lightly clamped together. Leakage between

the piston edges and the perspex sheets was avoided by having inflatable rubber tubes inserted in grooves along the top and botto edges of the pistons. These tubes, 0.125 in. diameter, were connect to an external pressurising device which could inflate them to a high pressure to complete the seal. The pressurisers were made to operate quickly so that the seals could be inflated or deflated in a matter of seconds, and a more complete description is given in an appendix. Both the tubes and the pressurisers were initially filled with water, thus when the tubes were trapped in the grooves between the pistons and the perspex a small displacement of fluid into them caused a large rise in pressure and the device worked quickly without any danger of the tubes fracturing. Since the pressure could be raised to 300p.s.i. without difficulty, the sealing was complete at the highest gas pressures.

Initially some leakage was noticed across the corners of the pistons, inside the sealing tubes, and this had to be stopped by building up the corners locally using adhesive tape, and by placing thin packing under the steel backing plates to depress the perspex onto the corners at the orifice. These measures somewhat interfered with the free movement of the pistons, but it was possible to position them without distortion and loss of accuracy.

The main advantage of this complicated arrangement was that the load on the pistons produced by the high pressure was taker in direct compression by the struts backing onto the heavy section runner. This reduced the elastic deformation of the pistons which

appeared in Mitchell's apparatus, and which would have been more in evidence had he gone to higher pressures.

The two remaining boundary walls of the inlet chamber had a hard rubber sealing strip inserted in a small groove along their length which sealed against the perspex when the backing plates were tightened down. These grooves were cut close to the inside of the walls so that the bolts (which passed through the walls) were outside the sealed volume.

Both side walls had a $^3/_4$in. diameter hole drilled through them which was normally closed by a brass plug. These holes gave access to the high pressure flow to allow smoke or dye to be pumped in to make the jet visible.

Since the pressure in the downstream chamber was almost atmospheric no very elaborate sealing was needed on the two non — moving walls. However a seal was needed on the two piston walls in this chamber since the pressure inside the reattachment bubble was known to be well below atmospheric and air might have leaked over the wall and into the bubble. Thus the sealing tubes were carried round along the top of the pistons to completely seal the edges right up to the junction with the runners, as is shown on the drawing.

The two other downstream walls were clamped to the perspex by screws, however for later tests involving measurement of the flow it may be necessary to complete the sealing with plasticene.

High pressure air was supplied to the apparatus through a 2 in. diameter copper pipe, and a connection piece was made to

effect the change in section from the circular pipe to the 3 x 1in. rectangular opening at the entrance to the apparatus. The flange of the connector was clamped onto the ends of the boundary walls by two screws and also by clamps attached to the backing plates. A soft rubber gasket was used to improve the sealing.

Originally it was intended to measure the flow coef - ficients of the various orifices, but when the Aspect Ratio effect was shown to be present and completely two-dimensional flow was unobtainable, no useful measurements could be made. To determine the flow quantities through the rig an exhaust tube was fitted on the downstream end with a measuring B.S.I. orifice midway along the tube. At the inlet to the exhaust a series of baffles and flow straighteners were fitted to ensure that the readings were not affected by the asymmetry created by the wall jet in the exhaust. The tube was clamped to the ends of the walls, and a soft gasket used to stop leaks.

Air was supplied at 250 p.s.i.from a supply with a stored volume of 220 ft^3 at the high pressure. Figure 3.3 shows diagram - matically the arrangement of the supply system. The air from the line passed through a gate valve to a Fisher diaphragm control valve which throttled the air down to the desired pressure and kept it constant by means of a Wizard controller. After passing through the rig the air flowed down the exhaust tube to atmosphere A tapping from the high pressure chamber was used to monitor the downstream pressure for the controller which was of the flapper type with full three term control.

Initially considerable trouble was experienced with the Fisher valve and controller, especially when the flow through the orifice was choked. This was presumably due to the very small down stream volume (about 150 cubic ins.) compared to the rate of flow which was around 2000 cubic ins. per sec. Below the critical pressu ratio the increase in outlet flow due to an increase of pressure somewhat reduced the rate of increase of pressure. When the flow was choked the outlet flow increased very little and the pressure rise was consequently more rapid causing instability in the control system. The instability could presumably have been stopped by pro — viding an air receiver between the valve and the rig, but before this was tried it was found that partially closing the gate valve (thus reducing the pressure drop across the control valve) stabilis the system, and allowed satisfactory working.

Static pressure tappings were used to measure the pressure distributions over the exposed boundary walls. These tapping con — sisted of fine holes drilled in the piston walls which were connect to multitube manometers by small bore polythene tubing (2 mm. bore) The details of the methods used to connect the tubes and the placin of the holes over the piston faces are given in an appendix.

Two multitube manometers were used to measure the static pressures — one filled with water for the low velocities (incom — pressible flow) and the other with mercury for high speeds (com — pressible flow). The mercury manometer was suitable for measuring the static pressures at the highest gas speeds used in this series of tests, corresponding to 100 p.s.i. across the orifice.

The overall pressure difference across the constriction

was measured by a 100 in. water column, a 100 in. mercury column and a 6 in. standard gauge where appropriate, while the slight rise above atmospheric of the downstream chamber was indicated on a small water gauge. Total difference was measured between tappings 26 and 52 (see Figure A.2.) preliminary experiments having shown that these were suitable.

Procedure and techniques.

It was originally intended that all the tests should use air as the working fluid. Preliminary tests with air showed that there was some discrepancy between the results obtained and those quoted by Mitchell (32a), so to avoid any possibility of this being caused by compressibility the apparatus was temporarily connected to a water main and an attempt made to repeat his results. Despite the fact that these tests quickly showed that there was no difference between the results obtained using water and air, all further tests on incompressible flow were made using first water and then air. The test verifying Von Mises solution was only possible using water.

The apparatus was easily modified for use with water. A flexible hose was used to lead the water in, and the exhaust pipe was replaced by a blanking plate to keep the downstream chamber full. Slots cut in the plate allowed water to escape, but were small enough to ensure that the chamber was slightly pressurised and that there was no free surface. Finally the water manometer was inverted so that the header and reservoir were open to the

atmosphere, and an allowance was made for the slight pressure in the lower chamber.

One useful feature of using water was that it provided a simple means of measuring the jet angle of discharge from the orifice. When the downstream chamber was full the jet reattached spontaneously to the wall, and no stable unattached flow could be obtained. However if the blanking plate was removed, letting the chamber empty, the jet issued as a thin wall adhering only to the top and bottom perspex sheets until it collapsed due to gravity a distance of 1 – 200 jet thicknesses out. Due to the surface tension there was no entrainment and the jet was parallel sided allowing the angle to be measured very exactly (to within $^1/_4$ of a degree.)

Normally during the tests the flow was adjusted to the desired value several minutes before taking the manometer reading to allow the levels to settle. Water increased the time constant of the system to some 30 secs. Because of the long time required to take all the readings, the overall pressure drop across the ri was noted before and after the readings and, in the initial stage midway during them. The midway reading was omitted as it was foun to be almost invariably the average of the other two.

When analysing the static distribution curves the bubble length was measured to the maximum positive pressure (in theory the intersection of the $\psi = 0$ streamline and the plane). Several investigators have reported that the actual position of zero velocity is on the upstream side of the pressure maximum, but exac information was lacking so the simplest criterion was used.

3.2 Preliminary experiments.

Before proceding with the main experimental measurements an attempt was made to test the apparatus, and to determine the effects due to the configuration of the boundary walls.

P.1. To determine the effect of the walls of the upstream chamber.

When the fluid leaves the entry pipe it separates from the walls and forms a turbulent jet as shown in Figure 3.4.a. To find what effect this had on the flow through the main orifice some special tests were needed.

A check on the effect was made during the water tests by allowing the downstream chamber to drain and letting the jet stream out unhindered as previously described. By leaving the pistons in a fixed position and varying the number and stations of various baffles in the upstream chamber, any change in the flow could be detected by a change of the jet angle. None of the baffle arrangements (Fig. 3.4.b,c,d,) caused any discernable alteration in the angle. This was the result anticipated from Von Mises theoretical solution which indicated that the angle would not be affected by conditions more than 10 x the orifice width upstream.

As a result of these tests no flow straighteners were placed in the upstream chamber in any of the experiments.

P.2. To determine the effect of the walls of the downstream chamber.

As shown in Figure 3.5.a the flow pattern in the down -

stream chamber is in the form of a vortex caused by the jet sweeping round the side walls after reattachment. At the exit the jet divides, part being retained in the flow to make up for the fluid entrained in the jet as it traverses the region, and part, equal to the mass flow through the orifice, passing out to the exhaust. The momentum of the retained fluid causes the swirl.

The velocities of swirl appeared to be high so it was decided to reduce them using baffles, thus making the region more nearly a semi – infinite volume as assumed in the theory. Fine mesh screens were placed in various positions, shown on Figure 3.5.b, and the bubble length measured for each configuration.

The effect of the various radial screen positions on the bubble length was scarcely discernable, but when they were placed along the length of the jet, Figure 3.5.c, the effect was marked. This can be explained in terms of the findings of other investigators, (14,1,and 40.) who established that the flow outside the jet is almost entirely radially inwards, with little or no axial component. Thus radial screens have less effect than axial ones.

As a result of the tests no screens were placed in the region for fear that the radial flow patterns might be upset.

Another finding from the same tests was that the pressure distribution along the other downstream wall (AB in Figure 3.5.b) seemed to be affected by the screen position. However since there was no apparent change in bubble length this effect was discounted

P.3. To determine the heat flow from the pistons to the gas.

The air supply to the rig was supplied from a two stage reciprocating compressor, and the air was partially dried by a silica gel unit in the supply line. A wind tunnel supplied from the same line was known to be affected by excessive condensation so it was decided to examine the cooling effects in the rig.

Condensation is caused by heat being conducted from the walls to the cold, high speed gas, thus reducing the temperature of the walls below the dew point of the water vapour in the gas.

In the test, air was blown through the orifice and the temperature of the walls measured using a fine wire thermocouple inserted down the first tapping from the corner. By observing the thermometer at a series of time intervals the graph shown on Figure 3.8.a was obtained. Then the air was turned off allowing heat to be conducted back to the corner and providing the second part of the graph.

A very much simplified calculation of heat flow through th piston showed that the heat lost was of the order of 5 B.T.U.s per hour which is small compared to the heat stored in the piston.

From these tests it appeared that condensation on the pistons was unlikely even after prolonged running, and this was later confirmed. However attempts to photograph the shock patterns were hindered by water condensing on the plate glass windows. This was expected due to the very low conductivity of glass compared to brass. (about one threehundredth).

P.4. To verify Von Mises prediction of jet angle.

Using the method previously described for measuring the jet angle, it was possible to obtain a graph showing the variation of jet angle with clearance ratio. The experimental results are shown on Figure 3.9 along with Von Mises theoretical predictions. As can be seen the points obtained compare well with the theory, indicating that the inviscid potential solution is a good approx - imation for the flow in the upstream region.

These tests were also used to find the accuracy of the piston positioning mechanism, which was found to be capable of fixing the dimensions to within two thousandths of an inch.

P.5. To determine the limitations of using air for incompressible tests.

To provide an adequate range of Reynolds'number in the main experimental work without opening the orifice too wide and spoiling the two - dimensionality of the flow, the fluid speed had to be high. It was therefore necessary to find what velocities could be used without compressibility affecting the bubble size.

The bubble length was measured for two values of w (0 and 0.25) at air speeds up to 600 ft./sec. and little change was noted in the lengths.This seemed to indicate little effect due to the compressibility, but subsequent measurements (chapter 5) showed that for w = 0.5 or more, the effect was much greater, and that two quite large effects were cancelling each other out.

In fact the air speed during the incompressible tests was kept below 150 ft./sec. and was much less at the larger values of w, so that the agreement between the air and the water results is not so strange as the figures of chapter 5 would indicate.

P.6. Tests on the reattachment of the jet at large angles to the plane.

During the tests with w = 1 it was found that inter - mediate stable positions existed between the fully reattached condition and the symmetrical central jet which did not touch either downstream wall.

These positions usually took the form of reattachment to the boundary wall beyond the end of the piston, thus enclosing a large bubble without seeming to tend to contract to the normal size. No reason could be found for this apparently stable mode of flow, but the problem may be related to the fact that there is a minimum length of wall to which a jet will spontaneously reattach. Bourque and Newman (6) investigated this effect and showed that the length required increased greatly with jet angle, and that reattachment did not occur spontaneously at angles greater than some 60°, no matter what length of wall was used. In all cases the minimum length was many times greater than the bubble.

The similarity to Bourque's condition was increased by the fact that the new large bubbles only seemed stable if the jet thickness was greater than 0.2 in., which would make the length of

the piston wall approximately equal to the minimum for reattachment

In his thesis Mitchell measured the minimum length of the wall AB (Figure 1.1.b,inflow) to allow reattachment to take place and also the critical length of DB (Figure 1.1.b,outflow) at which the jet changed walls. In both instances bistable flow was possible over a part of the range. However preliminary tests using a rough model (carried out before the present rig was made) seemed to indicate that this hysteretic region diminished as the effect of compressibility increased, and under certain conditions an oscillating flow was observed.

An investigation of this effect has not been possible up till the present since it would involve considerable modificatic of the existing rig, but such tests are included in the suggestions made at the end of Chapter 6.

Experiments with incompressible flow.

1. To determine the effect of Reynolds' number on the bubble length.

The reports of Bourque and Newman (6) and of Sawyer (42) indicate that the length of a reattachment bubble (expressed in terms of the jet thickness) is affected by the Reynolds' number of the flow, based on the jet thickness, from 2000, when turbulent reattachment begins to be possible, to values of 10,000 or more. On the other hand Mitchell's results (32a) show the length to be independent of Re. almost as soon as the turbulent bubble is formed, around 2000.

From a close study of Mitchell's thesis it was observed that he increased the value of Re. in his experiments not only by speeding up the jet , but also by increasing the thickness. Thus as he was making the Re. greater he was decreasing the ratio of jet width to thickness. This the Aspect Ratio (A.R.) of the flow and is taken as a measure of the two – dimensionality of the syste As the A.R. which he used was small compared to the values normall adopted to ensure two–dimensional flow (4 as compared to 20 to 100) it was thought that the two effects should be studied separately.

Thus the bubble lengths at various values of Re. were measured, the change in Re. being effected only through changes of jet velocity. This was repeated for different A.R.s and for two orifice clearance ratios. The results are shown on Figure 3.7.a

show clearly that the bubble length is affected by Re. up to high values, above 10,000.

2. To determine the effect of Aspect Ratio on the bubble length.

Since Mitchell's measurement of the effect of Re. was combined with a varying A.R., it was necessary to complement expt. 1 by determining the changes in length due to varying A.R.

In this instance the orifice dimensions were changed to alter the jet thickness (without changing the clearance ratio) but the Re. of the flow was kept steady by varying the jet speed. The results of this test are shown in Figure 3.7.b.

Figures 3.7.a and b, taken with Mitchell's report show that by increasing the jet thickness to obtain a bigger Re. he decreased the A.R. and the two effects cancelled out in terms of the bubble length. Points where the two effects did not cancel appear on his results as a rather excessive scatter in the results. During the present tests it was found possible to repeat values to within 5 percent, whereas Mitchell's variations were up to 20 percent.

The Figure 3.7.b also showed that the effect of A.R. extends beyond values of 5 to 10 which were to be the normal operating conditions of the present apparatus. Investigation of higher values than 10 was made impossible by the fact that the jet width was fixed at 1 in. by the boundary walls, and the minimum jet thickness by the spacing of the pressure tappings, which precluded acc-

accurate measurement of bubble length with jet thickness less than 0.1 in. (corresponding to a length of 0.4 in.– 4xthe tapping spacing) Thus it was apparent that the apparatus would not permit accurate determination of bubble dimensions and flow coefficients for two–dimensional conditions as was originally envisaged. However it was deemed accurate enough tosubstantiate and test the theories advanced in the various sections of the report.

3. To determine the static pressure change across the depth of the piston face.

When the apparatus was shown to be too shallow to ensure completely two–dimensional flow a test was made investigating the pressure distribution along the third dimension, to attempt to find the reason for the shorter bubble length at low A.R.

A piston was made (described in the appendix) with two rows of static tappings, one down the centre of the piston and the other $^1/_4$ way in from an edge. It was hoped that the bubble indicat by these extra tappings would provide a clue as to how the A.R. effects came about.

These tests were made over a range of A.R. from 5 to 2 and no difference was noted between the pressures shown by the two sets of tappings. From these results it appears that the three–dimensional effect alters the whole bubble, or the changes occur in the outer quarters of the depth. Since the A.R. was changed between such wide limits it seems that the latter conclusion is unlikely.

4. To determine the variation of bubble length with clearance ratio w.

The calculations of Chapter 2 provide predictions of bubble length for varying clearance ratios in terms of the entrainment parameter σ. The main object of the incompressible experimentation was to provide a graph showing the actual variation of bubble length with clearance ratio w. This curve could then be compared with the predictions of Chapter 2, and the apparent values of σ examined and compared with other investigations.

Bearing in mind the earlier tests the measurements had to be carried out at a constant Aspect Ratio and with a Reynolds' number greater than 10,000. Accordingly the jet thickness was calculated for each value of w (in terms of a and a', using the Von Mises solution) and values of a and a' chosen to keep the jet thickness constant. Then with a constant pressure ratio throughout the tests both the Re. and the A.R. remained constant.

For each setting of a and a' the static pressure distribution along the piston face to which the jet reattached was measured using a multitube water manometer. At the low mass flows used in these tests the supply pressure remained constant and the manometer was read in the usual way. Figure 3.6.a shows a typical pressure distribution, and the graph of w against bubble length is shown on Figure 3.6.b. The experiment was repeated at various values of Re. without finding any difference in the results, but when a different A.R. was tried a change was noted in the measurements in line with Figure 3.7.b.

5. To determine the effect of the downstream boundary wall opposite the bubble.

As the jet emerges from the orifice and reattaches to the nearer of the boundary walls it entrains fluid on the outside as well as the inside, and the fluid path to replace that absorbed into the jet is restricted by the second wall. Thus considerable fluid velocities must be attained in the corner bounded by the wall and the jet which, by Bernoulli, lowers the pressure and may there by reduce the pressure ratio across the jet. This would result in smaller curvature and longer bubbles.

To assess the effect another piston was used which had the downstream wall removed, thus reducing the fluid velocity and exposing the outer edge of the jet to atmospheric pressure. In the course of repeating the tests of section 4 in part, even at $w = 1.0$ when the effect would be worst, no difference could be discerned, and it was concluded that it has no effect in the simple valve configuration.

Subsequent to these tests Glaettli (21) reported to the author that in the configurations of fluid logic devices where the angle between the two downstream walls is as low as 30°, (the valve angle being 90°) the opposite wall has a marked effect on the bubble characteristics. Following from this the effect must be present in the valve case but is unmeasurably small. If special spools are made with reduced downstream angle to gain other desired characteristics then this may become important.

3.3 Discussion of results and conclusions.

The preliminary experiments were tests to determine the suitability of the apparatus for measuring the bubble characteristics and examining the jet behaviour.

The first two tests showed that the dimensions of both the upstream and downstream chambers were large enough to avoid the boundaries affecting the flow through the orifice joining them. A more accurate method of measuring the changes in the flow pattern caused by the walls would have been to find the velocity distribution directly, using some kind of pressure probe, and then compare the flow maps of the region. A method similar to this was originally envisaged and surface static pressure tappings were arranged in the upstream piston faces. Unfortunately the fluid velocities in the upstream chamber were found to be very small except in the immediate neighbourhood of the orifice, and such a method would have required extreme accuracy and repeatability. These problems, allied with the small size of the region to be investigated, caused the idea to be abandoned for the much simpler if less informative, method of measuring the jet angle.

In the case of the downstream chamber some high swirl velocities were observed in the preliminary tests and it was feared that these might have interfered with the flow of fluid into the jet at the outer edge, causing false readings of bubble length. The fact that no effect was measured due to the swirl bears

out Mitchell's findings when he investigated boundary wall effects in the downstream side. According to the theories of Chapter 2 the entrainment of the outer edge of the jet has little effect on the curvature, but it has been reported (31) that jets re-attaching in a moving stream can be considerably affected by the flow past the bubble. Although in this instance the magnitude of the effect appears to be small, the problem needs further exam - ination before it can safely be ignored in actual valves.

The heat flow tests indicated that the heat lost to the gas from the pistons was negligible, however later troubles with condensation on non - metallic boundaries indicated that continuous running of pneumatic spool valves over long periods could be troubled in this way, especially if the air supply was not dry enough. Similar troubles have been experienced in attempts to use exhaust gases from engines to operate pneumatic logic and control systems (29).

As well as confirming Von Mises' solution for jet angle, the tests with the empty downstream chamber served to measure the accuracy of the piston positioning arrangements. During the jet angle tests slip gauges were used to check the orifice dim - ensions. At the same time the micrometers were used to determine a and a' and it was found possible to position the pistons using them alone to within two thousandths of an inch. They alone were used in subsequent tests.

The preliminary investigation of the limitations on using air as an incompressible fluid was later shown to be incon -

clusive since both the bubble length and jet angle are affected by compressibility at quite low speeds, although the bubble lengths measured at w = 0 and w = 0.25 were unaffected. This is more fully dealt with in Chapter 5, but it should be noted that air speeds which might be tolerable in other systems may well cause quite large effects in reattaching flow.

Although the preliminary tests showed the apparatus to be suitable for accurate measurement as far as the positioning of the boundary walls was concerned, the first two tests in the main series showed clearly that it was not deep enough to remove three – dimensional flow effects.

The design of the apparatus was based on reports of pre – vious experimental work on valve models, especially on Mitchell's, which all seemed to indicate that the Aspect Ratio effect was negligible. As the experimental measurements progressed, however, it became increasingly obvious that the bubble length was not independent of A.R. and extra tests confirmed this. At this point the publication of both Sawyer's and Bourque's reports made the conclusion certain.

The effects of A.R. and Reynolds' number on entrainment and bubble length are of great importance in the functioning of the computing pneumatic elements described earlier (Figure 1.5.a). To economise in bulk and shorten the gas transit time across the element (a measure of the computing speed) the designers of these devices are using values of A.R. from 1.0 down to as low as 0.3 whereas the values considered in these tests were between 5 and 10.

While investigating the reattachment mechanism in their configurations they have measured that with A.R. less than 1.0 the bubble length slowly increases with decreasing A.R., and it seems that the complete graph of bubble length against A.R. would resemble the dotted continuation of Figure 3.7.b. However as their geometry is more complicated than the simple valve, since there is an additional downstream wall, it is not possible to be certain that the graph is the same for both cases. The comparison is strengthened by the fact that the variation with respect to Reynolds' number is the same in both cases.

Thus the bubble lengths measured throughout these tests were not true lengths for two - dimensional flow but were slightl shorter. As shown in Figure 3.7.b, the effect of A.R. is levellir off at a value of 10, so that the errors involved in taking an A.R. of 5 as standard throughout the following tests was not expected to be greater than 10 percent. When comparing the result with those of other tests 10 percent has been added to allow for the effect.

The principle object of the incompressible experimentatio was to measure the bubble length at various orifice clearance ratios. These figures were to be used in confirming the theories of Chapter 2 and in attempts to explain some of the inconsistencies of other reports.

Figure 3.6.b shows the change of bubble length (at a fixed Re. of some 20,000 and an A.R. of 5) as the clearance ratio is changed. The upper dotted graph shows the values extrapolated

for infinite A.R. (10 percent above that for A.R.=5) and used in all comparisons. In Chapter 2 these corrected values are shown to line up well with those of other investigators.

In addition the various tests indicate explanations for some of the effects reported previously by other investigators and some of the precautions to be taken when comparing their figures.

Finally the experiments showed possible improvements in the apparatus and techniques which were incorporated before the more difficult tests on compressible flow. These are described at the beginning of Chapter 5.

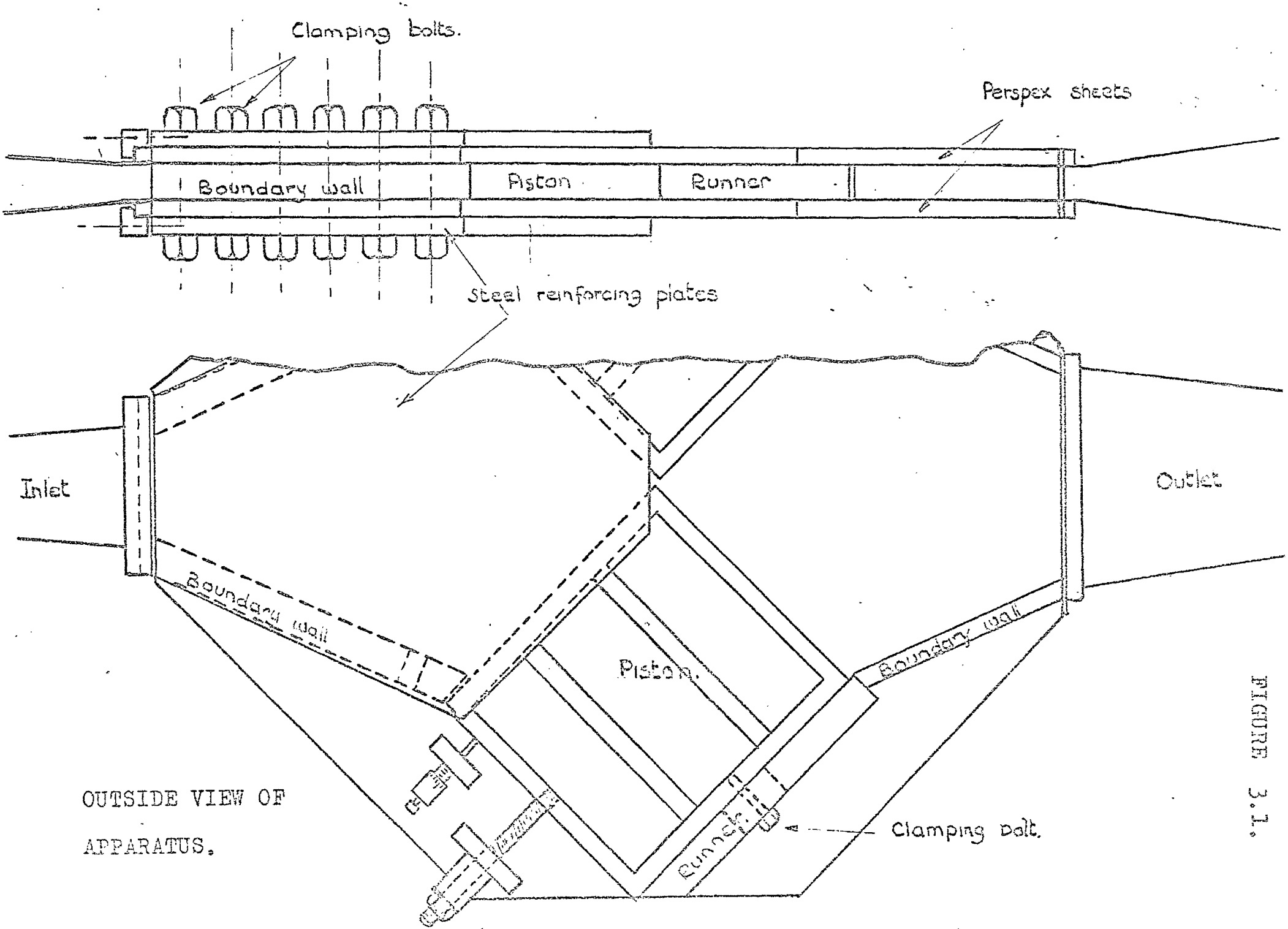

OUTSIDE VIEW OF APPARATUS.

FIGURE 3.1.

FIGURE 3.2.

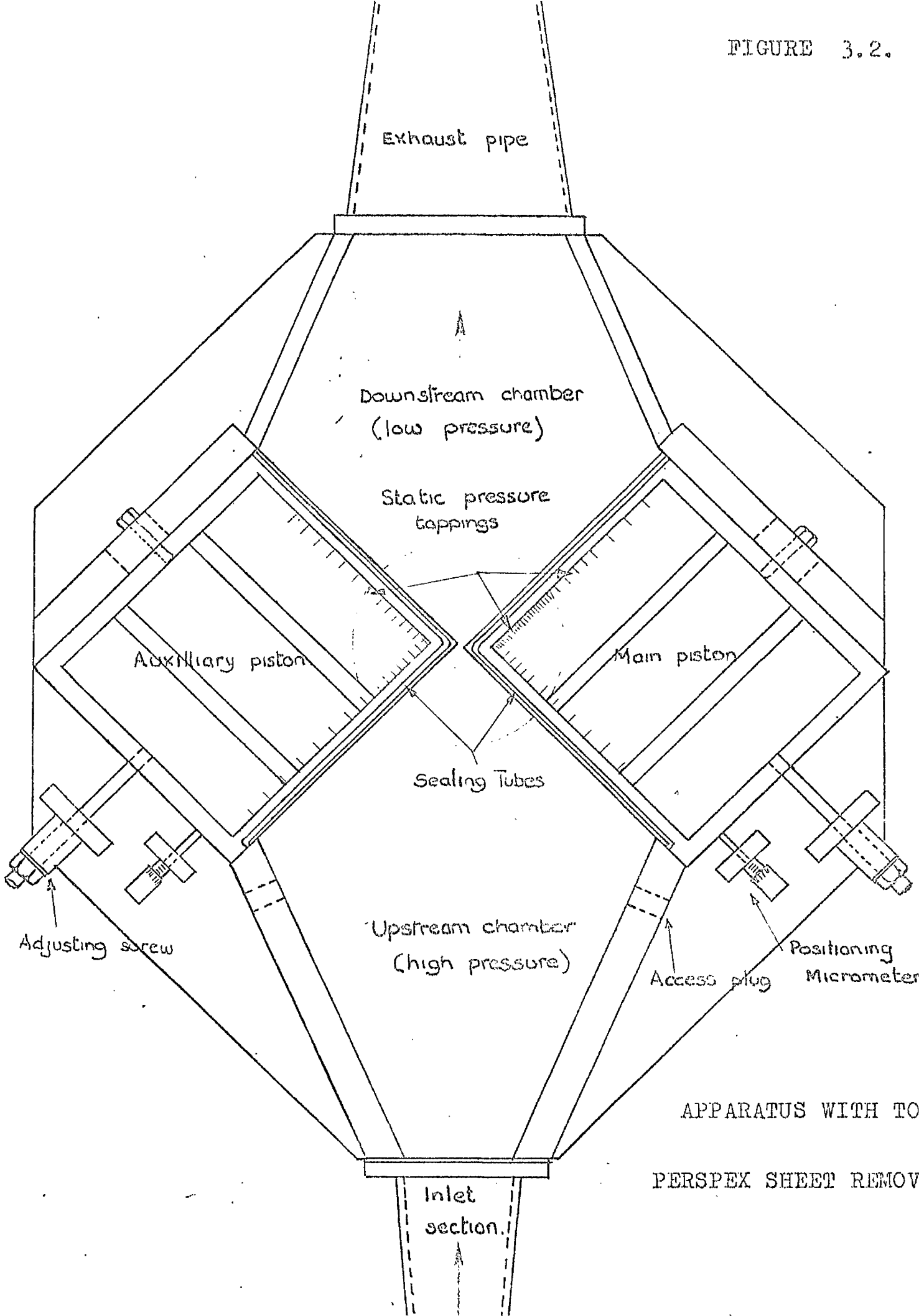

APPARATUS WITH TOP

PERSPEX SHEET REMOVED.

FIGURE 3.3.

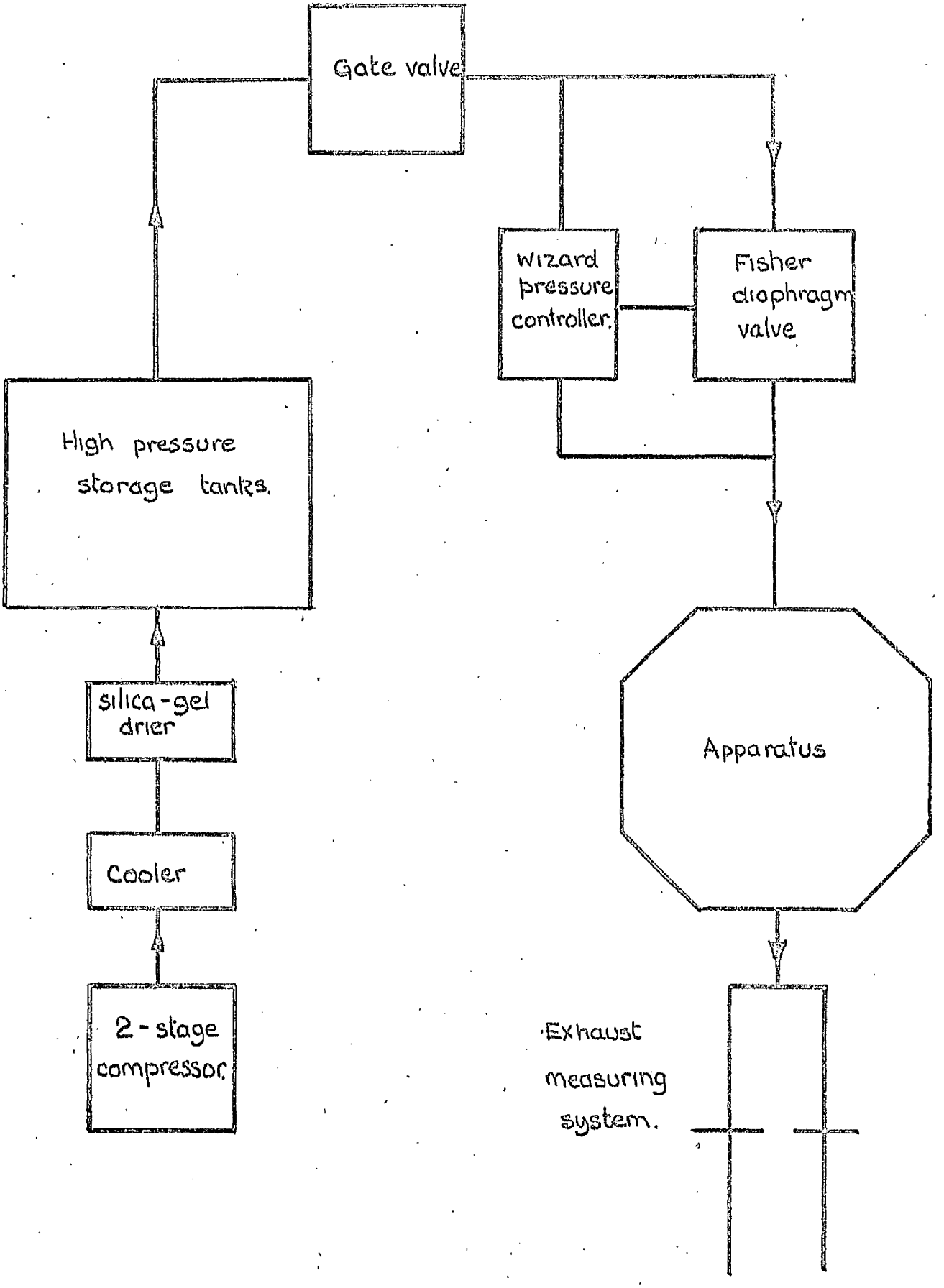

DIAGRAMMATIC ARRANGEMENT OF GAS SUPPLY SYSTEM.

FIGURE 3.4.

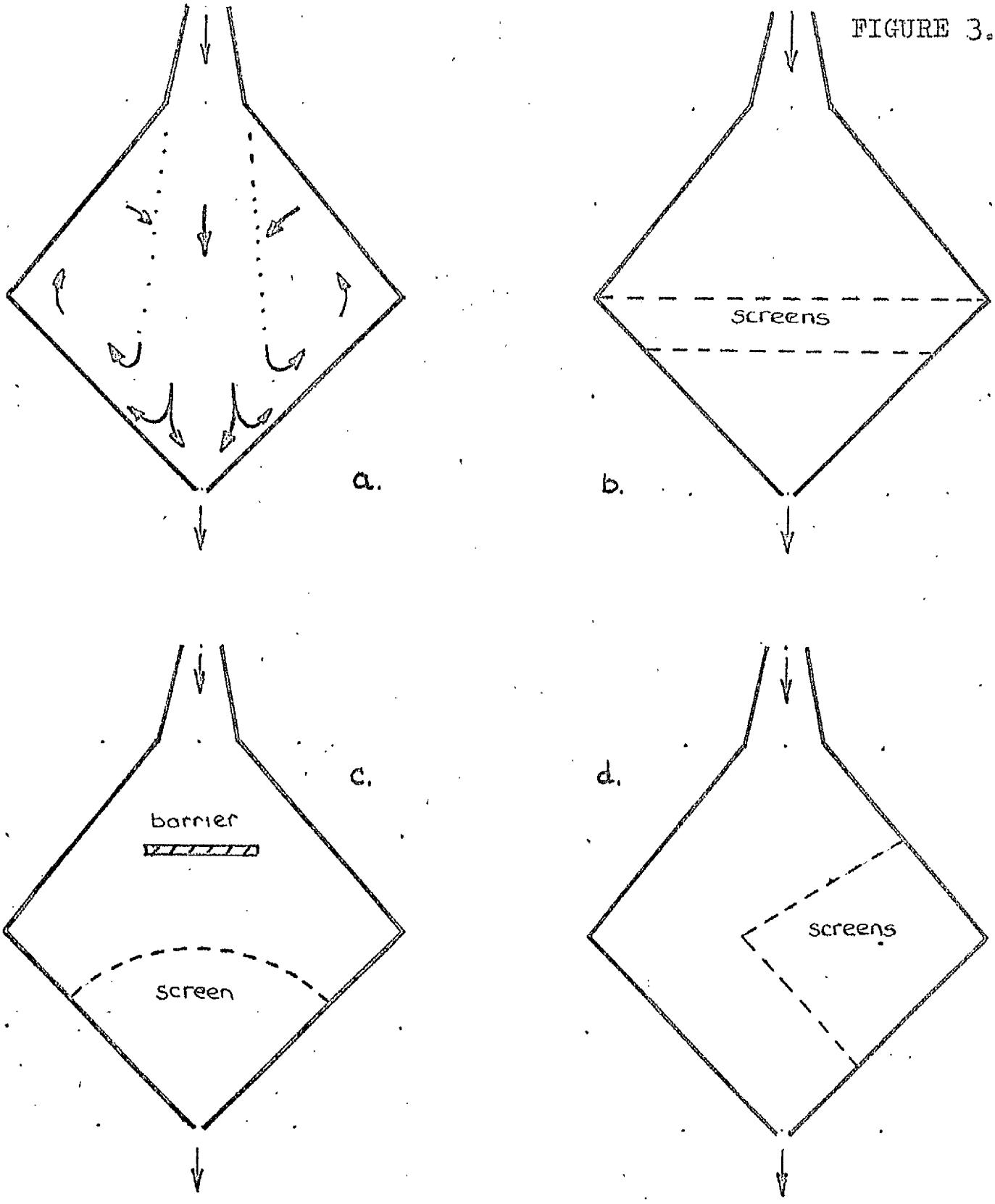

POSITION OF SCREENS IN TESTS ON UPSTREAM FLOW.

FIGURE 3.5.

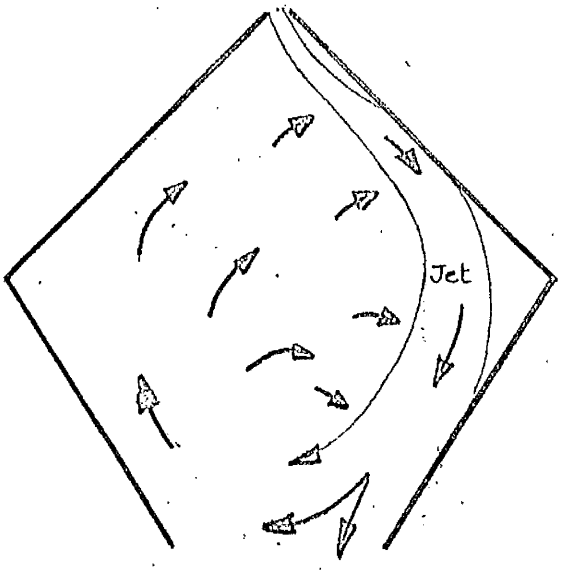

a. Flow with no screens.

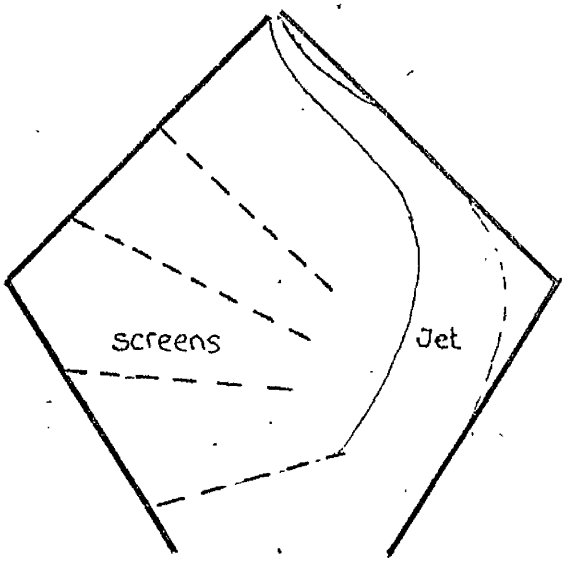

b. Radial screens

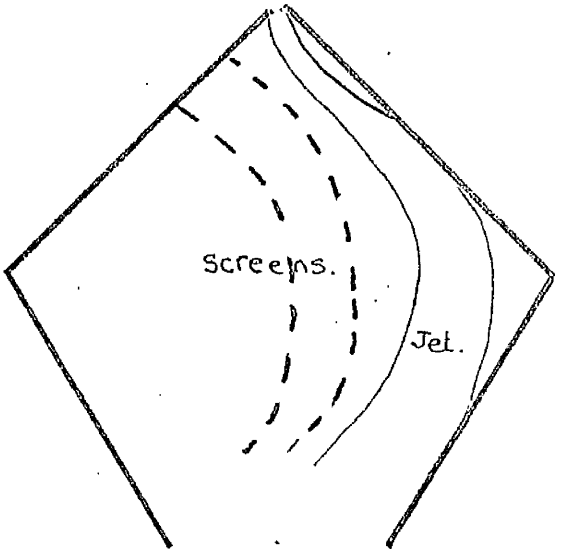

C. Parallel screens.

FLOW IN DOWNSTREAM CHAMBER WITH TEST SCREENS.

FIGURE 3.6.a.

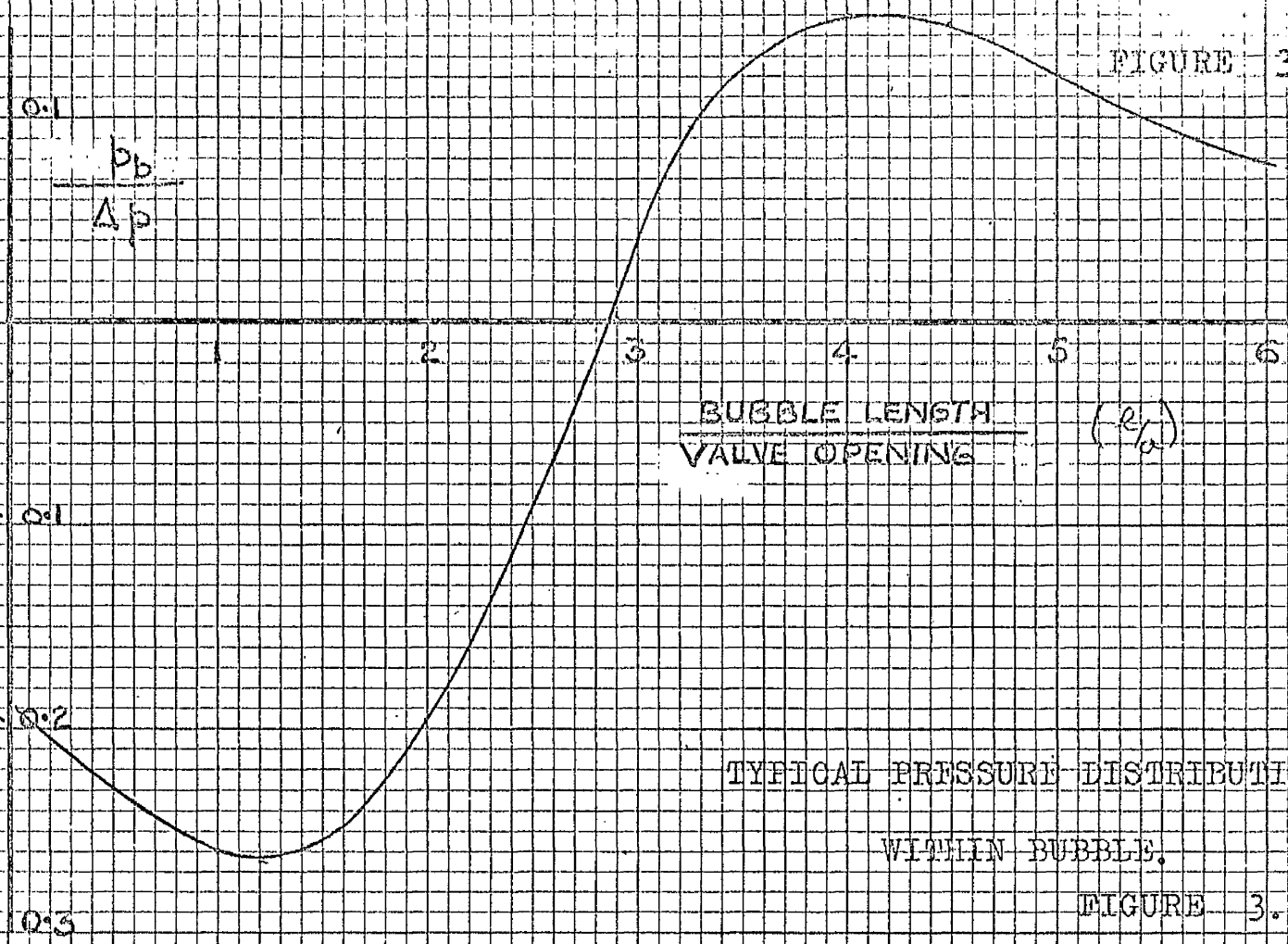

TYPICAL PRESSURE DISTRIBUTION WITHIN BUBBLE.

FIGURE 3.6.b.

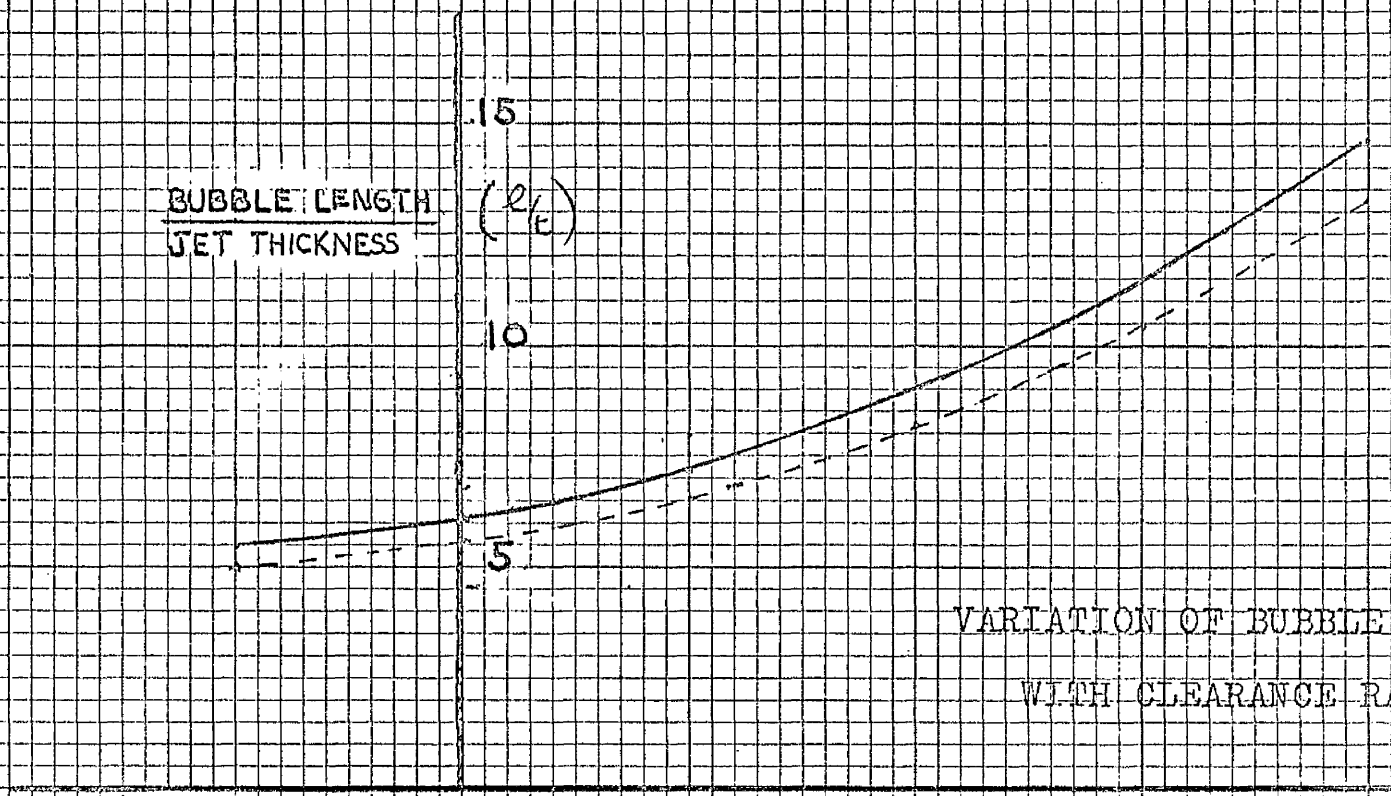

VARIATION OF BUBBLE LENGTH WITH CLEARANCE RATIO.

FIGURE 3.7.a.

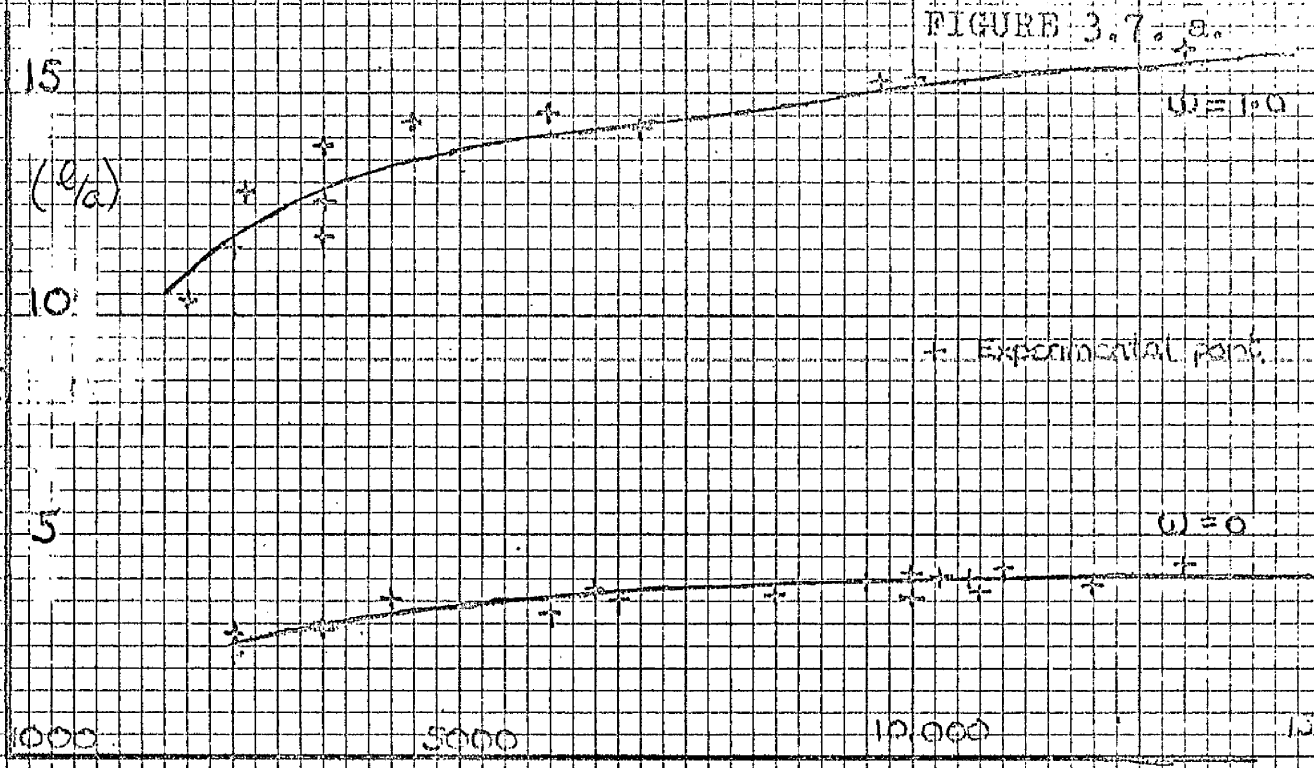

BUBBLE LENGTH / VALVE OPENING a

REYNOLDS NUMBER (R_e)

VARIATION OF BUBBLE LENGTH WITH REYNOLDS' NUMBER.

FIGURE 3.7.b

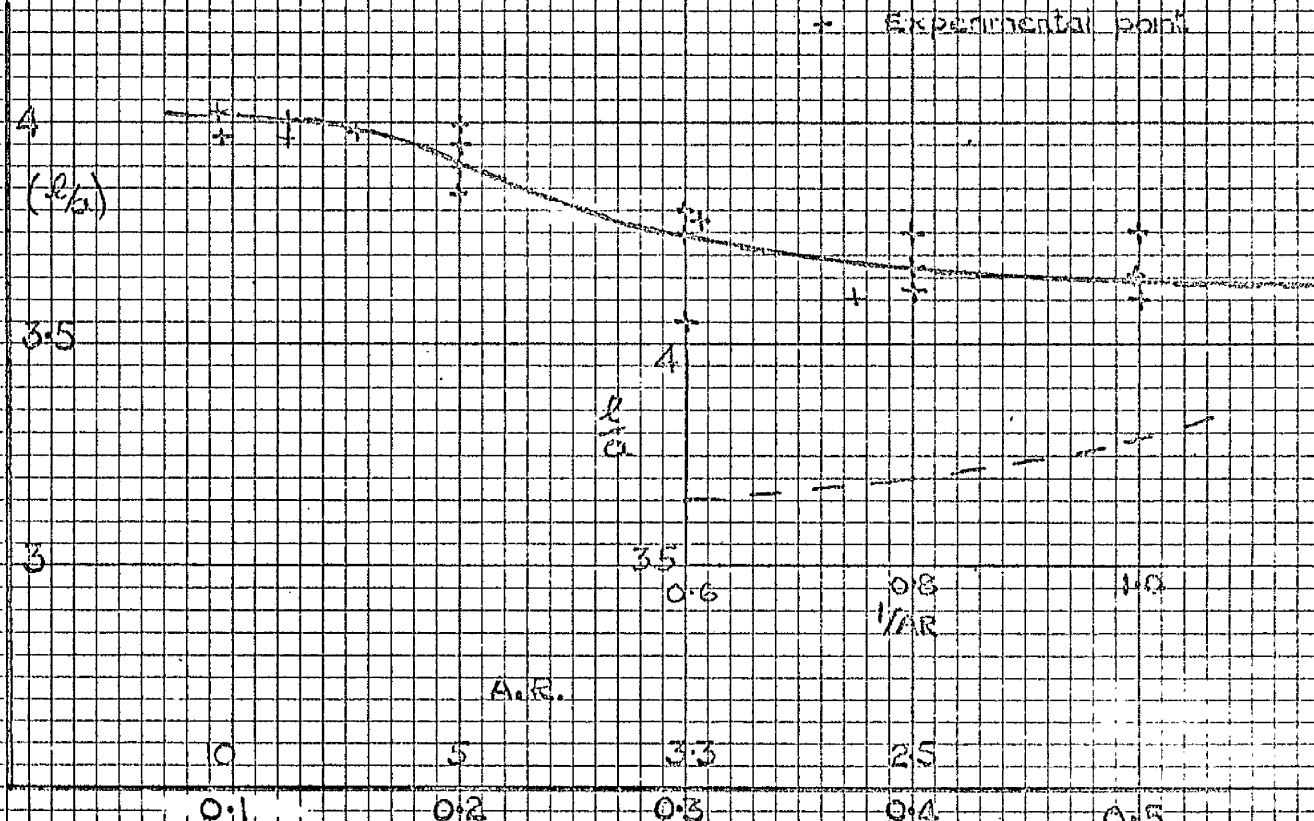

BUBBLE LENGTH / VALVE OPENING a

INVERSE ASPECT RATIO

VARIATION OF BUBBLE LENGTH WITH CLEARANCE RATIO.

FIGURE 3.8.a

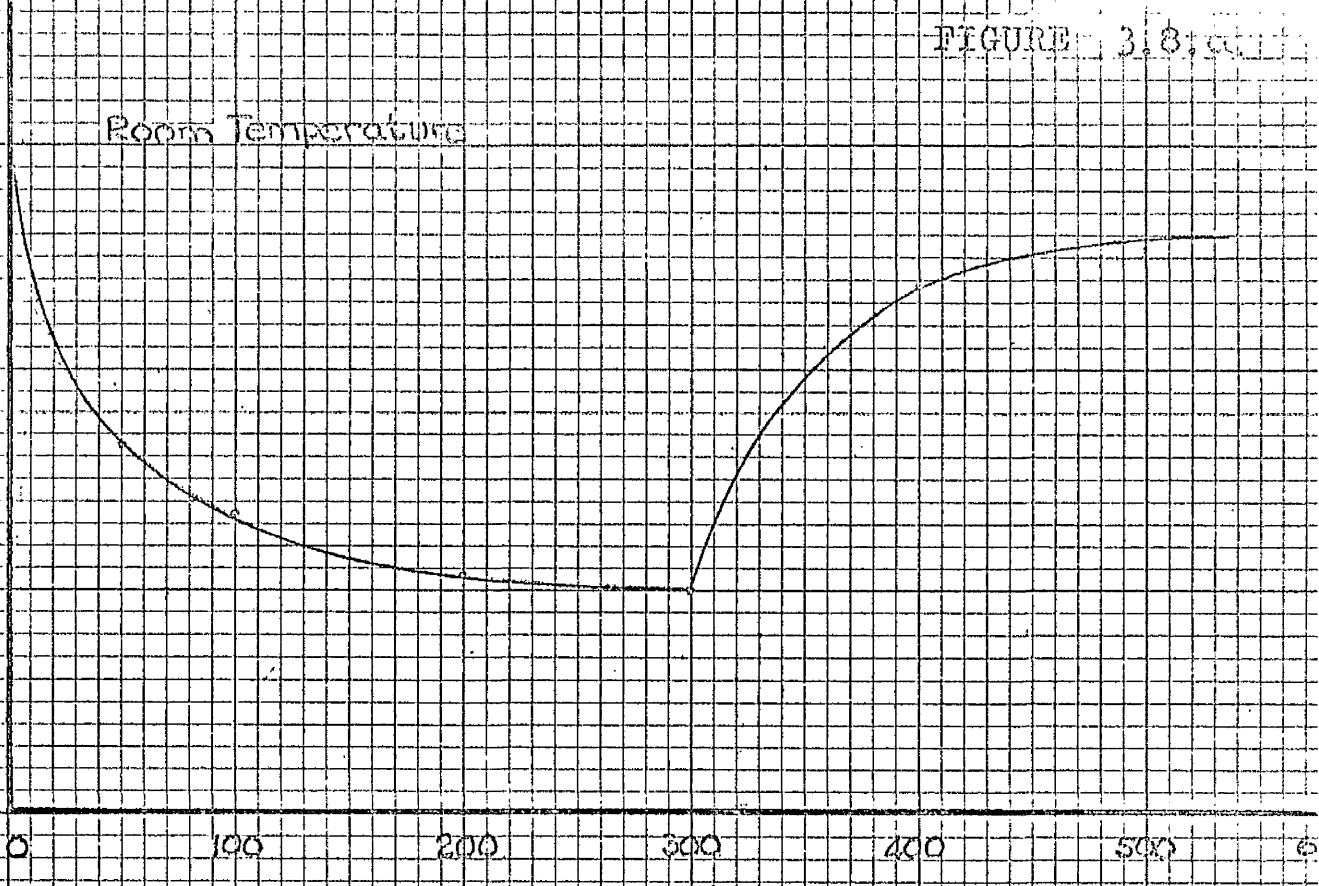

PISTON COOLING CURVE.

FIGURE 3.8.b

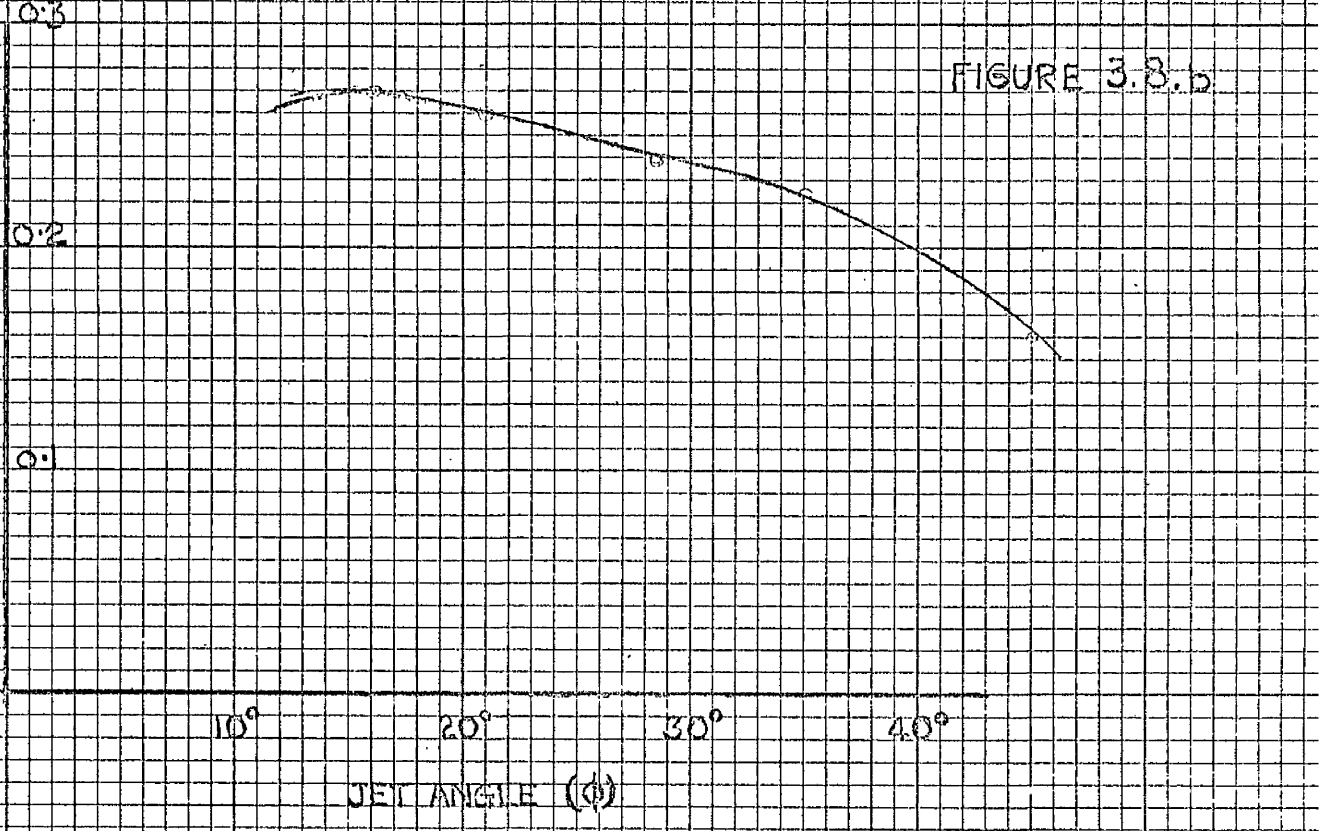

VARIATION OF BUBBLE MINIMUM PRESSURE WITH JET ANGLE.

FIGURE 3.9.

COMPARISON OF PREDICTED JET ANGLE WITH EXPERIMENTAL MEASUREMENTS.

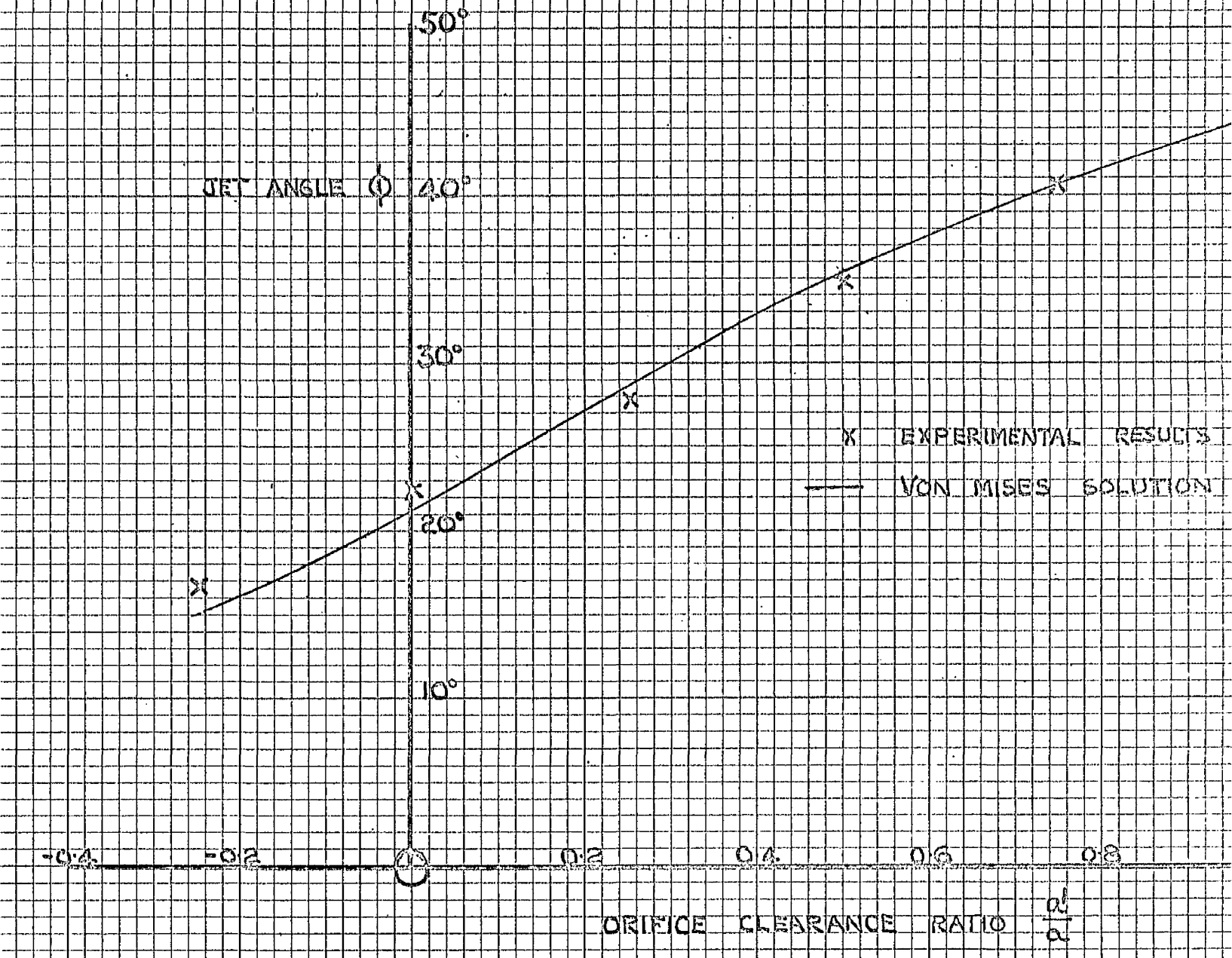

Chapter 4.

Theoretical study of compressible flow.

4.1. Theoretical prediction of jet – an attempt at a potential solution.

4.2. Norwood's relaxation method applied to the flow through the valve geometry.

4.3. A solution for jet angle using force defect coefficients.

4.1. Theoretical prediction of jet - an attempt at a potential solution.

In the investigation of incompressible flow through the valve geometry it was found possible to divide the flow into two separate regions. One was the highly convergent upstream flow which was treated by an ideal potential solution, and the other the downstream region where turbulence and viscosity played a large part in determining the mode of flow. This same subdivision was continued in the investigation of compressible flow.

To obtain a complete solution for the upstream region, a compressible potential map was required to correspond to the Von Mises solution used in chapter 2. No such solution could be traced and it was necessary either to complete one or obtain some of the desired information by other means.

Three types of solution were considered to calculate the jet angle and thickness at the vena contracta; the first was an analytical potential solution, the second was a relaxation method to give a potential map by an iterative arithmetical procedure and the third an analysis to allow compressible values to be calculated from the existing Von Mises solution without a potential map, but incorporating certain further assumptions.

The flow in the downstream chamber, consisting of the reattachment of a compressible jet, was also unrecorded. Only

one attempted solution was traced, that of Olson(37) who evaluated predictions of bubble length by an arithmetical method using constants derived from Rouse's (1) experimental investigation of incompressible jets. Although the analysis produced predictions which were approximately confirmed by experimental measurements, it was felt that a more basic investigation of the variation of the entrainment into compressible jets was preferable to calculations based on incompressible figures.

The control valve geometry is not the ideal configuration to use to investigate compressible reattachment as the jet inlet position is so poorly defined. Both the size and position of the vena contracta and the jet angle change with increasing Mach No. (Morley(35)), so that there is considerable difficulty in making even an estimate of the inlet plane. However when the jet angle is 45° that is when the orifice is symmetrical, only the jet thickness, alters with increasing gas velocity, and changes in the bubble length can be attributed only to this and to a change in the entrainment into the jet. Since the contraction coefficient of a symmetrical orifice can be found from the incompressible value, using the works of Jobson (26) or Bragg (7), the change in entrainment can be found.

Thus no theoretical predictions were attempted for the downstream flow, but an attempt was made to use the experimental results obtained from the measurements described in chapter 5 to outline the effect of gas velocity on entrainment.

Potential solution.

The first attempt to obtain a stream function map of the upstream region was made along lines suggested in a report by C.C.Chang (9). This involved substituting in the general compressible stream function equation as found by Chaplygin,

$$\frac{\partial^2\psi}{\partial\nu^2} + \frac{(1-M^2)}{\rho^2}\frac{\partial^2\psi}{\partial\vartheta^2} = 0 \quad \left(\frac{d\nu}{dq} = -\frac{\rho}{\rho_o}\frac{1}{q}\right)$$

, an approximation to the term $\frac{(1-M^2)}{\rho^2}$ which is an implicit function of ν.

By carefully choosing this approximation the equation can be transformed into one of a known type, and the particular series of functions chosen by Chang transform it into various forms of the generalised hypergeometric equation. The most accurate substitution was used and it led to the equation —

$$\frac{\partial^2\psi}{\partial\psi^2} + \frac{a\nu(1+b\nu)}{(1+c\nu)^2}\frac{\partial^2\psi}{\partial\vartheta^2} = 0.$$

This was shown to have a solution

$$\psi_{(\nu,\vartheta)} = (c_1\nu+c_2)(c_3\vartheta+c_4) + \sum_1^{\infty} A_n W^{(n)}_{k,m}(Z)\sin(n\lambda\vartheta+\alpha_n)$$

where $Z = 2n\lambda\frac{ab}{c^2}(1+c\nu)$, $W^{(n)}_{k,m}(\ )$ is the Whittaker function, and $c_1, c_2, c_3, c_4, A_n, \lambda$ and α_n are all constants to be determined from the boundary conditions.

The problem in the present investigation was therefore to define the boundaries of the flow in the ψ,ϑ plane, and to attempt to find the values of the various constants by applying these constraints.

Figure 4.1.a shows the problem on the physical plane at jet speeds below sonic (parallel – sided jet emerging tangentially to the upstream walls). When this is translated to the hodograph plane (u and v as the velocities in the x and y directions) the boundaries are completely defined. The lines AB and CD in (b) represent the acceleration of the fluid from stagnation (infinity upstream) points A and C to the final jet speed achieved at B and D. After B and D no further change in velocity is possible so that DFEB is a quarter of a circle representing the formation of the vena contracta, and the points F and E represent the final jet angle and speed.

When this is changed to the ν, ϑ plane the accelerations AB and CD are at constant ϑ then the formation of the contraction takes place at constant velocity i.e. at constant $\nu = \nu_{final}$ representing the final speed.

Substituting these boundary conditions into the general solution yields –

$$\psi_{(\nu,\vartheta)} = -\frac{2Q}{\pi}\vartheta + \frac{Q}{\pi}\sum_{n=1}^{\infty}\frac{1}{n}\,\frac{W^{(n)}_{k,m}(Z)}{W^{(n)}_{k,m}(Z_o)}\,(2 - 3\cos n\pi)\sin 4n\pi$$

This equation can be transferred back to the physical plane by complex variable techniques using the complex number $z = x + iy$. The differential dz can be found in terms of the solution for $\psi_{(\nu,\vartheta)}$ and thus the derivative $\frac{dz}{d\vartheta}$ which can be integrated to give z. The integration constant is found by differentiating z w.r.t. ν and equating this to the $\frac{dz}{d\nu}$ part of the differential.

The labour involved in these manipulations is great and the final expressions for x and y are large. Figure AO shows these expressions for x and y.

The solution is obtained using the method by assuming a value for ψ and velocity (i.e. ν), substituting these in the complete solution to find ϑ, then finally substituting ϑ and ψ to get x and y, the coordinates of the point ψ, ϑ, ν on the physical plane.

The complexity of this procedure, involving complex Whittaker functions in series and their derivatives, is obvious. By reducing the accuracy of the original approximation for the term $\frac{(1-M^2)}{\rho^2}$ it is possible to reduce the complex Whittaker fns. to complex Bessels functions (of complex order) about which more has been written, but much more simplification would be needed to make the method in any way possible.

A more complete exposition of the analysis is contained in Appendix 2.

4.2. Norwood's relaxation method applied to the flow through the valve geometry.

When the attempt at an analytic potential solution, which was described in the previous section, proved to be too complex to evaluate, it was decided to attempt a relaxation solution along the lines suggested by Norwood (36.a.). A solution of this type was tried by Mitchell but was not completed.

A relaxation solution involves assuming an approximate distribution of a field and then adjusting it systematically to make it conform to the known boundary conditions and field equations The difficulties associated with this type of solution for compressible flow is very great if the operations are carried out in the physical plane, but Norwood has devised a means whereby the relaxation process can be carried out in the hodograph plane where the boundaries are more often known and where the field equations are linear. Having obtained an accurate solution in the hodograph plane it is a relatively simple procedure to transfer it back to the physical plane.

To justify his method Norwood carried out the process and obtained a series of flow maps for supersonic flow through a flapper type of control valve. He then built a two – dimensional model of the valve and obtained experimental confirmation of his predictions.

Subsonic solution.

Figure 4.2.a shows the physical conditions existing as compressible fluid flows at subsonic speed through the valve confi-guration and 4 2.b the same flow pattern transferred to the v—ϑ hodograph plane, where v is the fluid velocity and ϑ is the angle which the velocity vector makes with the X —axis in the physical plane.

The velocities along the walls AB and CD are represented on the hodograph diagram by ab and cd respectively. At B and D the pressure is p_a and the velocity cannot increase further if the flow is subsonic. Thus the circular arc befd represents the two edg velocities as the vena contracta is formed while angle eab represen the final jet angle and ae the finaljet velocity. Unlike the incom-pressible flow the jet angle varies as the fluid velocity changes.

If the jet edge ABE is defined by $\psi = 0$ and the edge CDF by $\psi = Q$, then the intermediate streamlines and the position of the point e,f can be guessed approximately as shown. A net of constant velocity circles and equiangular rays can then be drawn with a,c as centre. The cross points in the net can be given app — roximate values of ψ except the point a,c which has two values 0 and Q. This can be overcome in several ways but the easiest is to assume that ψ is uniformly distributed around the periphery of the innermost circle which then becomes one of the boundaries. Since the distribution of ψ is known exactly around the edges of the known hodograph diagram, the relaxation process can be used to

correct the intermediate values of ψ to provide increased accuracy.

The final accurate map showing the distribution of ψ within the boundaries can then be used to plot the streamlines back onto the physical plane. This allows the free boundaries of the jet to be established thus providing information regarding the jet angle and thickness which is required in the investigation of the flow in the downstream chamber.

A separate solution has to be made for each pressure ratio across the orifice which makes the process of establishing a plot of angle against ratio very lengthy. However a high speed computer can be programmed to perform the operations quickly and such a method is quite feasible.

Supersonic solution.

Figure 4.3.a shows the flow pattern existing when the gas velocity is supersonic and Figure 4.3.b the flow transferred onto the hodograph plane.

A gas can be accelerated beyond sonic speed only by first reducing the area of the flow until the speed of sound is reached and then increasing the area again to allow supersonic expansion. In Figure 4.3.a the cross-sectional area of the jet reduces from A to B and from C to D so that the velocity at B and D cannot be supersonic. Assuming an isentropic expansion, which is already assumed for potential flow, the static pressure at B is a fixed

ratio of the pressure difference across the orifice and is higher than the atmospheric pressure into which the jet discharges. Thus there is a sharp pressure discontinuity at B (and at D) causing an instantaneous change in the size and direction of the velocity at these points. In addition the direction of the gas as it leaves the edges of the orifice is not tangential to the upstream wall.

On the hodograph plane the lines ab and cd represent the expansion of the gas (increase in velocity) from A to B and C to D. At B and D the velocity is sonic so that the velocity distribution along the sonic line is the circular arc bd.

The discontinuities of the pressure distribution at B and D are the focal points of two expansion waves allowing the gas to expand from the sonic line into the supersonic jet. For a given pressure ratio (which can be found from the parameters of the configuration) the angle through which the velocity changes and the size of the increase in velocity can be calculated. This locates the points b' and d' , while the lines bb' and dd' represent the action of the expansion waves. The pressure at both B' and D' is equal to the downstream pressure and no further expansion takes place, so that the velocity at the edge of the jet remains constant in magnitude thereafter. However the direction of the velocity can change and these changes are represented by the circular arc b'd'.

If C is a point on the jet edge downstream of B', then the flow between C and the sonic line is supersonic and any disturbance at C will be propagated along a characteristic line as

shown. The effects of the disturbance are only felt at points downstream of the line, but if the line cuts the sonic line the whole subsonic region is affected. As the pressure ratio across the orifi increases the characteristic from C makes a more acute angle with the general direction of flow until a condition is reached where even if C coincides with B' , the characteristic does not touch the sonic line. Under these 'choked' conditions no disturbance of the jet or lowering of the downstream pressure has any effect on the flow upstream of the sonic line, on the distribution of ψ along that line or on the total mass flow through the orifice.

Thus the analysis of the supersonic condition has two possibilities, depending on whether the orifice is choked or not. In either case it is necessary to assume a distribution of ψ along the sonic line and then to relax the areas on either side of it, changing the initial distribution of ψ until the final flow maps match on either side. When the orifice is fully choked it is only necessary to perform this operation once, since the potential map of the subsonic region is constant, but if it is not choked the solution has to be completed each time.

Relaxation in a supersonic flow is not carried out using an externally imposed net, the net lines are formed from characteristic lines at arbitrary spacings. It is also necessary to change the process slightly to allow for the fact that only points downstream of the characteristic lines emanating from an intersection are affected by changes in that point.

Relaxation downstream of the sonic line must therefore be carried out in areas bounded only by characteristic lines or free boundaries; the sonic line is the first characteristic line. In Figure 4.3.b if e is a point on the sonic line, the characteristics from e intersect the edges of the jet at g and h. Considering the boundaries of the area bb'he, bb'h is the streamline $\psi = 0$, eh is a characteristic as is the sonic line be, so that if the distribution of ψ along be is assumed the area can be relaxed and an accurate map obtained for that initially assumed distribution. The area edd'g can be similarly treated. These two areas make up the total super - sonic region in contact with the subsonic flow region. Thus to find the streamline map of the area it is necessary to carry out the relaxation process in all three regions, adjusting the initial distribution of ψ along the sonic line until the streamlines are continuous across the line.

From this point the solution can be progressively extended downstream by considering the area cut off by the characteristics from g and h, and continuing in this way as far as desired.

In the case of a supersonic jet the sides of the jet are not parallel but the thickness oscillates as the expansion wave at the exit from the orifice is reflected downstream. Since there is no external influence on the jet the variation in the jet shape is exactly repeated in each cycle, and the diagrams on the hodograph plane are coincident. A solution up to the lines mln is all that is needed to represent the jet flow to infinity.

This summary shows that a relaxation solution is a possible means of obtaining the characteristics of the flow through the simple valve configuration. Such a method would require a fast digital computer to make it feasible – Norwoods rather simpler con – figuration took some three hours per pressure ratio using an I.B.M. 709 computer, and although modern machines are much faster, the additional complexity of the valve configuration would offset this improvement.

4.3. A solution for jet angle using force defect coefficients.

Before the relaxation solution described in the previous section was started an alternative approach was suggested to the author. This new method enabled the jet angle and minimum thickness to be calculated from the known incompressible values without any potential solution. Accordingly the relaxation method was not completed, although future investigations into supersonic flow will possibly require that part of the calculation to be reattempted.

Force defect coefficients were first applied in attempts to derive the compressible characteristics of measuring orifices and nozzles from the values obtained using incompressible flow, since mass flow measurements are more conveniently made with fluids than with gases. The two most important analyses of the problem were made by Jobson (26) and by Bragg (7.a).

The orifices used in flow measurement are normally axi - symmetric for ease and accuracy of manufacture and to remove scaling difficulties. As fluid approaches such an orifice its velocity increases, reducing the static pressure on the upstream face of the boundary wall. The total reduction of pressure can be summed to give a force parallel to the direction of the flow which Jobson termed the Force Defect in his analysis of the problem

If the fluid is incompressible the velocity distribution remains constant for all mass flows (though the magnitudes are proportional to the jet speed) so that the size of the force is

exactly proportional to the mass flow. It is then possible to define a force defect coefficient as the force divided by the jet momentum; the size of the coefficient is determined by the velocity distribution, but is independent of the mass flow.

The incompressible force defect coefficient can be related to the compressible value provided that an assumption is made to describe the effect of compressibility on the velocity distribution upstream of the orifice.

Jobson first made the assumption that the velocity distribution upstream was independent of the mass flow. This is equivalent to equating the two coefficients, and leads to an analysis whereby the contraction coefficient can be calculated for any pressure ratio. The predictions obtained by this calculation are accurate for orifices with a contraction coefficient of less than 0.7; beyond that value they become increasingly inaccurate.

Bragg, in his published paper (7.a) improved on Jobson's analysis by changing the assumption relating the velocity profile to the mass flow. By assuming that the mass flux at any point on the upstream wall is proportional to the average mass flow through the complete section including the original point, Bragg was able to complete an analysis which was accurate for all contraction coefficients.

Recently Bragg has indicated that his method can be used for non-symmetrical two-dimensional orifices. The calculation provides a means of predicting the angle and thickness of a com-

compressible jet issuing from such an orifice, and in addition it predicts the total force acting on either upstream wall. Although ideally some information regarding the position of the vena contracta is also required, the analysis provides enough to allow the investigation of the flow downstream of the orifice to procede. In a note to the author Bragg outlined an analysis for subsonic flow through an assymetric orifice. This has been completed and a new analysis added for supersonic flow . Both analyses have been evaluated providing graphs predicting the jet angle and thickness for a range of orifice configurations and pressure ratios.

The orifice under consideration is shown in Figure 4.4; and the jet angle and thickness are known for incompressible flow by means of Von Mises theoretical solution and by direct measurement.

Asymmetric boundary walls are treated by splitting the force defect into two components perpendicular to the walls, that is in the directions (1) and (2) on the diagram. Having done this a force defect coefficient can be defined for each direction, $f_{(1)}$ and $f_{(2)}$.

By considering the equation of motion of a control area including allthe fluid upstream of the vena contracta, two equations are obtained relating the defect coefficients with the contraction coefficient and jet angle in the incompressible flow case. Then using Bragg's assumption that the mass flux past any position on a boundary wall is proportional to the average mass flux at that

section, the incompressible coefficients can be related to the compressible values in terms of the pressure ratio across the orific

Finally the jet thickness and angle can be calculated from the compressible coefficients —one equation for either direction — and the two equations solved to eliminate the jet angle and to give C the contraction coefficient in terms of the pressure ratio and the incompressible values. Solving C into either equation allows the jet angle to be calculated.

As in Bragg's original analysis the relationship between the compressible and incompressible coefficients is a function of C which cannot be eliminated. It is therefore necessary to solve the latter half of the analysis using an arithmetical reiterative method.

The analysis is slightly changed for supersonic flow since the conditions at the vena contracta are not the same as the down-stream conditions. In supersonic flow the conditions there correspond to sonic velocity and there is a further expansion after the minimum section.

A summary of the new supersonic analysis is given in the Appendix in which the argument and principal equations are more fully indicated, and this is followed by a summary of the equations for the subsonic analysis.

The solution was carried out for five orifice geometries (w = 0, 0.25, 0.5, 0.75, and 1.0 .) with the pressure ratio varied between 1.0 and 0 (M = 0 to M = infinity). The graphs of

the results of these calculations are shown on Figures 4.5 and 4.6.

In these graphs the jet angle and thickness are plotted on a base of pressure ratio across the orifice. Figure 4.7 shows the per unit increase in the jet thickness (over the incompressible value) plotted against the pressure ratio. This graph was used extensively in the analysis of the experimental results of the next chapter to adjust measured bubble lengths for increase in jet thickness.

Figure 4.5 shows that the variation in jet angle due to compressibility changes with the degree of asymmetry of the orifice When $w = 1$ ($\varphi = 45^{\circ}$) the orifice is symmetrical and there is no change in angle which makes this the only geometry in which there is no change in reattachment bubble length due to a change in angle Thus any changes in bubble length which do occur are due entirely to an increase in jet thickness (allowed for using 4.7.) and to the effect of compressibility on the entrainment.

Normal operating conditions in a control valve correspond to $w = 0$ and the jet angle is 21°, but it can be seen from 4.5 that the angle is much reduced at high pressure differences. In terms of the physical length of a reattachment bubble under these circumstances, the effect (of reducing the length) would be almost cancelled out by the increase due to the thicker jet.

Using Figure 3.6 to relate bubble length to the jet angle and 4.5, the bubble length can be calculated at any pressure ratio allowing for both the decrease in jet angle and increase in thick-

—ness. The results of these calculations are shown on Figure 4.8 which indicates that for the valve configuration the two effects almost cancell out, for angles less than 38°. This prediction is examined in the next chapter in the light of the experimental measurements. (Note – Fig. 3.6 assumes constant entrainment.)

The variation of the contraction coefficient of Figure 4.6 is similar to that of a symmetrical orifice as reported in Bragg's paper, with the increase in jet thickness due to compressibility almost constant at all geometries.

FIGURE 4.1.

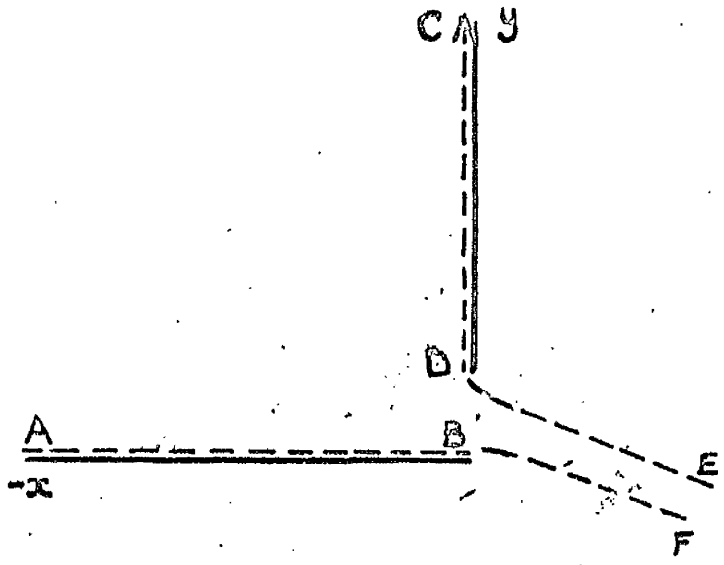

a) Physical plane

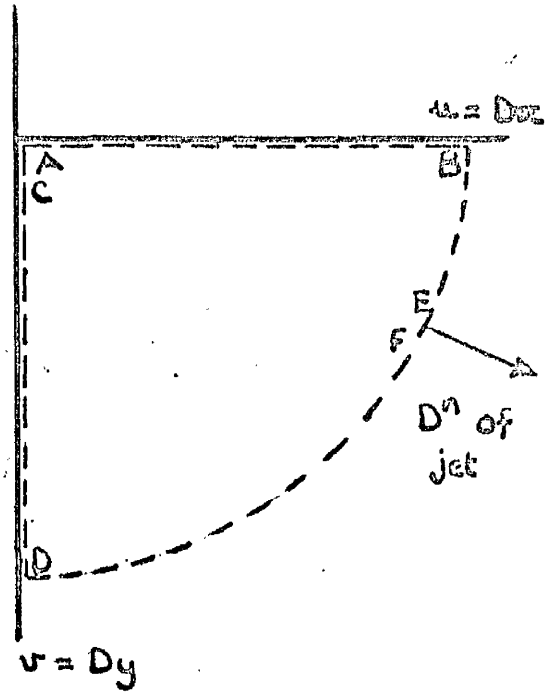

b) u,v hodograph plane

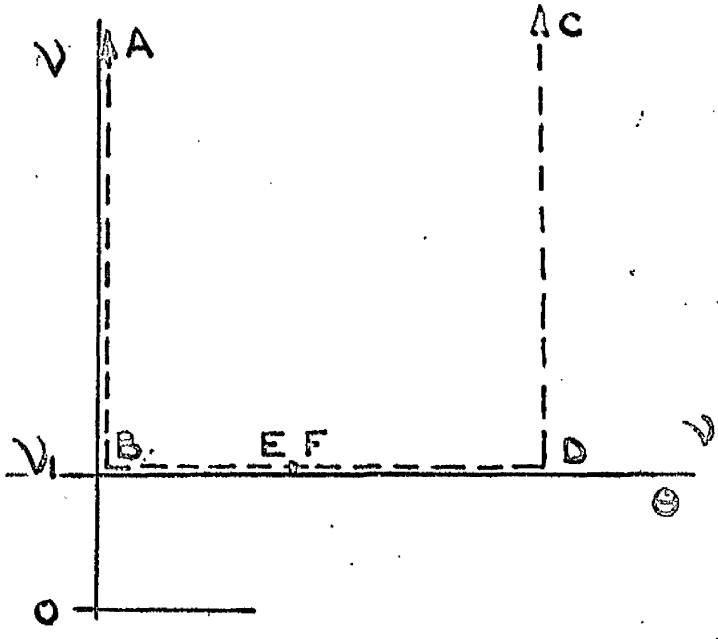

c) V,Θ hodograph plane.

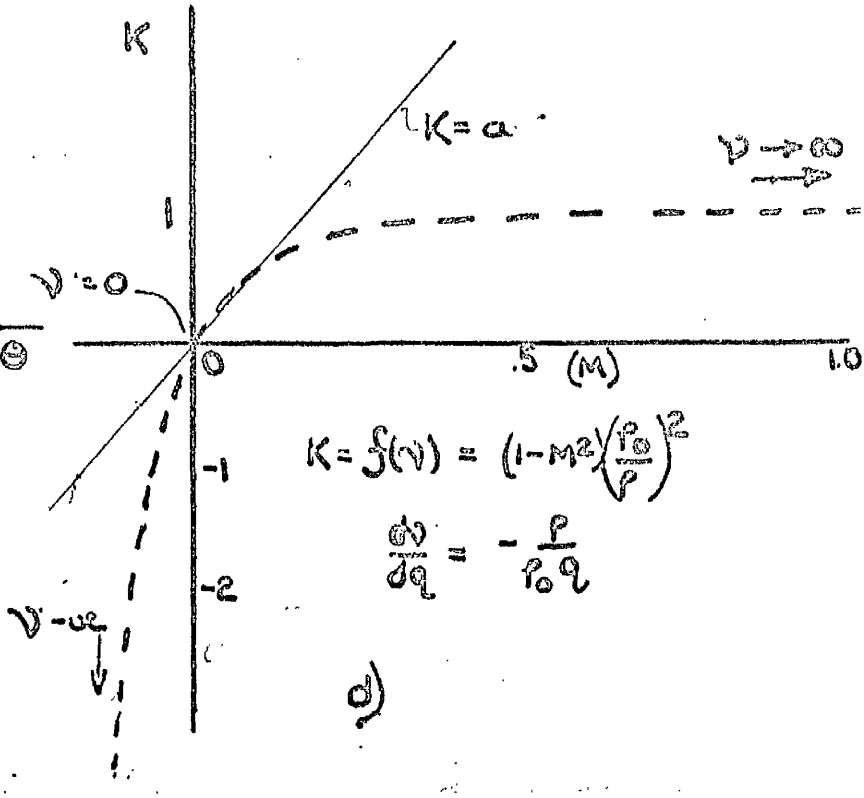

FIGURE 4.2.

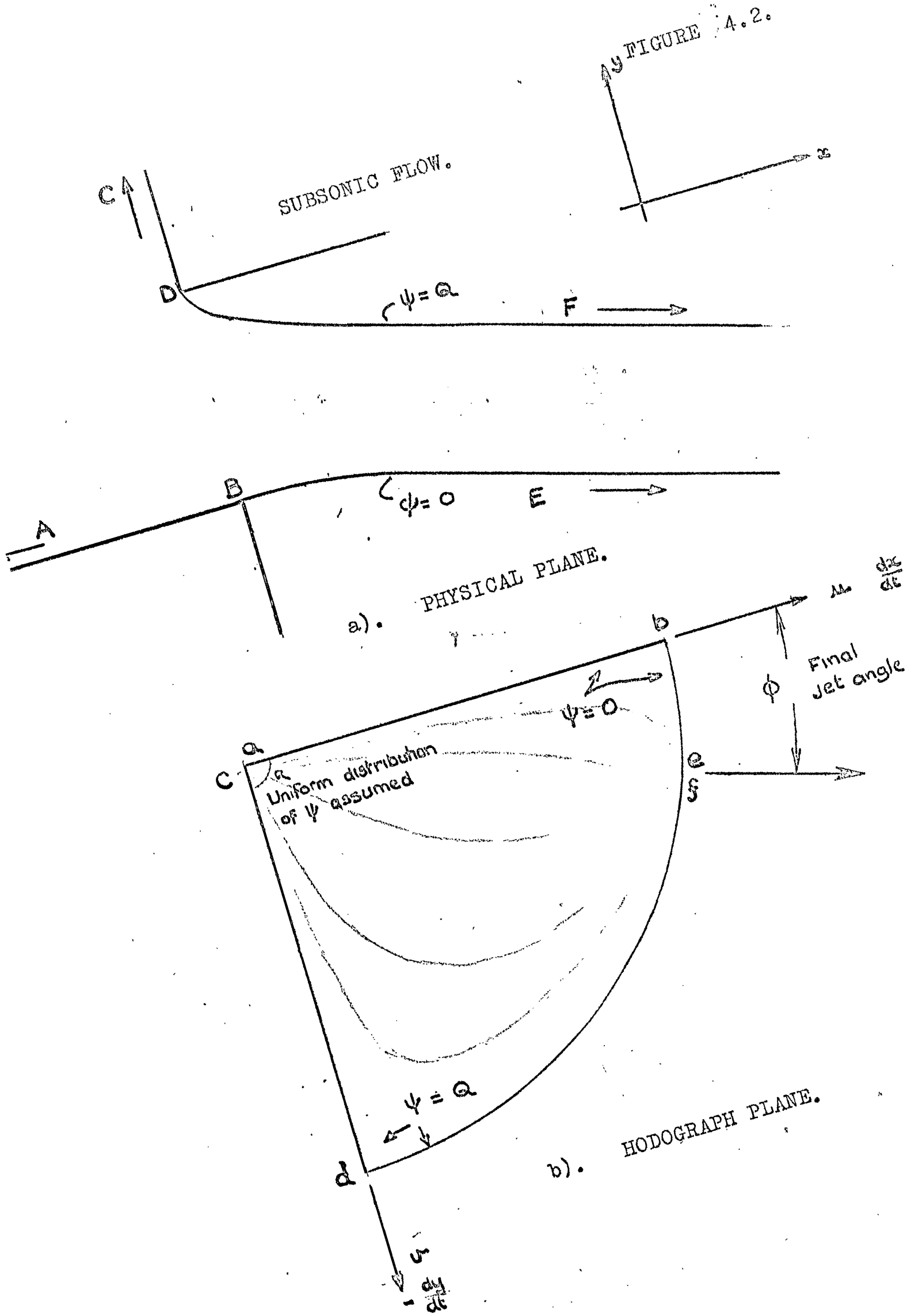
y
x
SUBSONIC FLOW.
C
D
ψ = a
F
A
B
ψ = 0
E
a). PHYSICAL PLANE.
y
b
M. dx/dt
Final Jet angle
φ
Z
ψ = 0
a
C
Uniform distribution of ψ assumed
e
f
ψ = Q
d
b). HODOGRAPH PLANE.
u
- dy/dt

FIGURE 4.3.

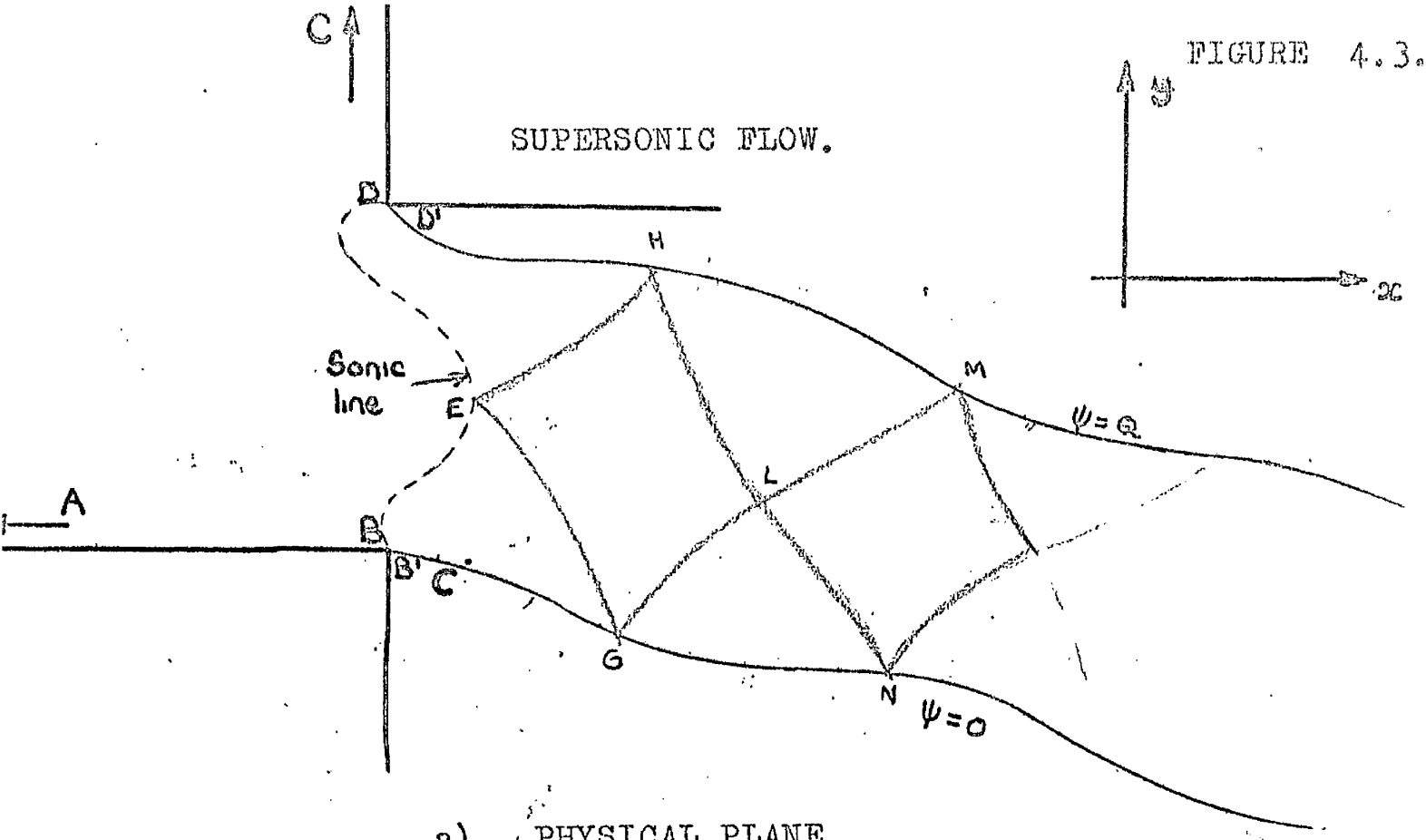

a). PHYSICAL PLANE.

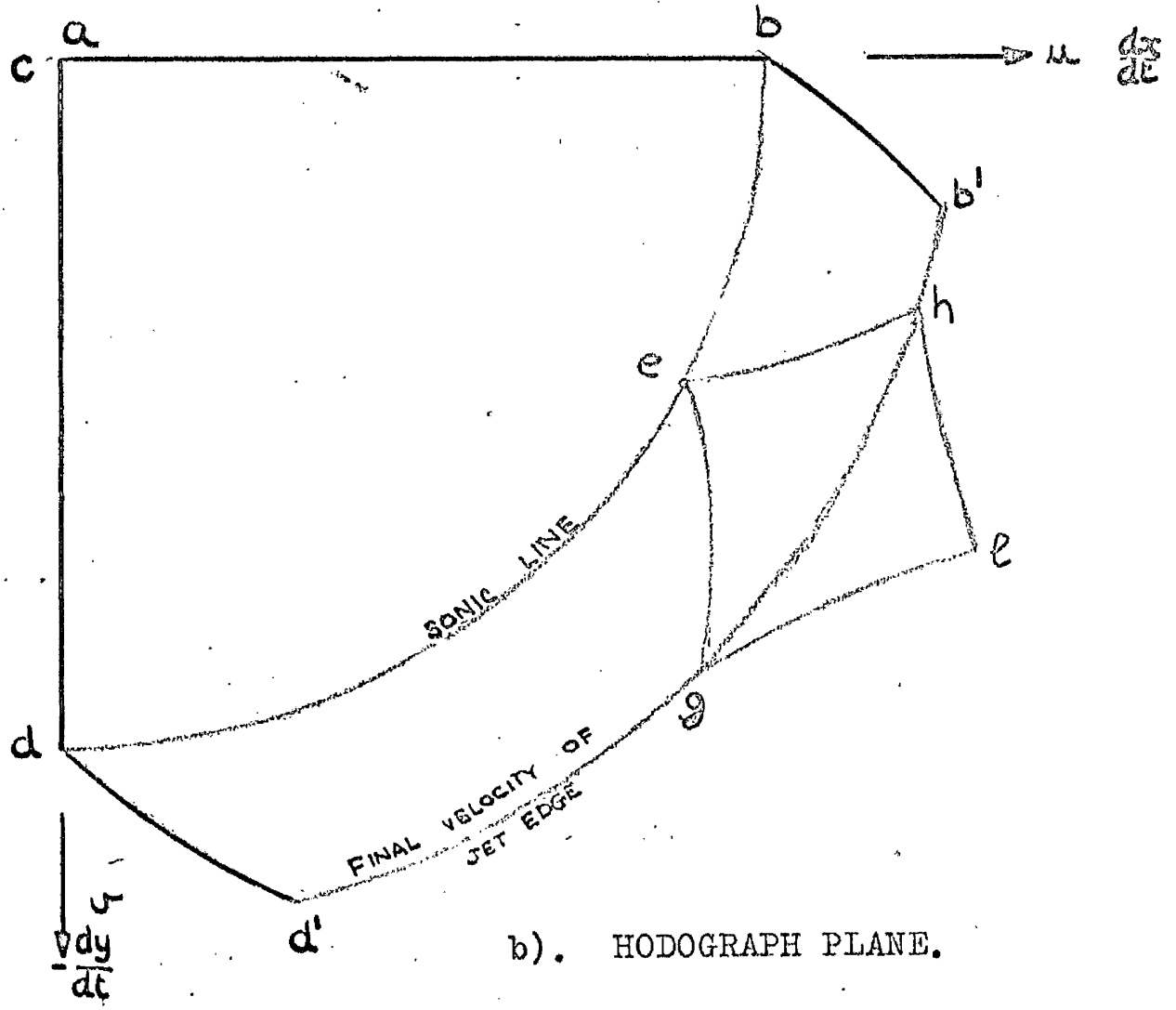

b). HODOGRAPH PLANE.

FIGURE 4.4.

FORCE DEFECT ANALYSIS APPLIED TO FLOW THROUGH VALVE.

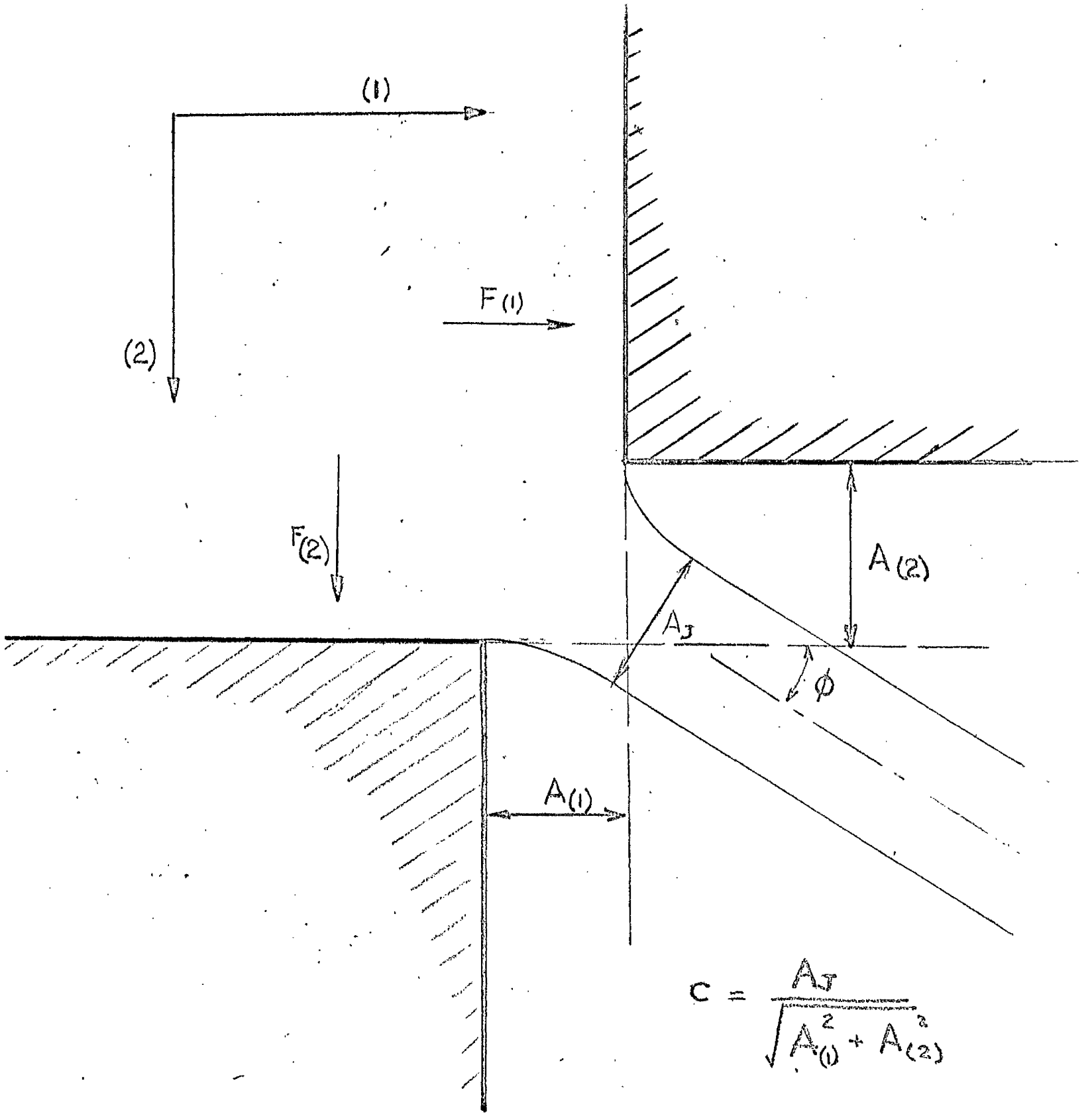

$$C = \frac{A_J}{\sqrt{A_{(1)}^2 + A_{(2)}^2}}$$

FIGURE 4.5.

VARIATION OF JET ANGLE WITH PRESSURE RATIO.

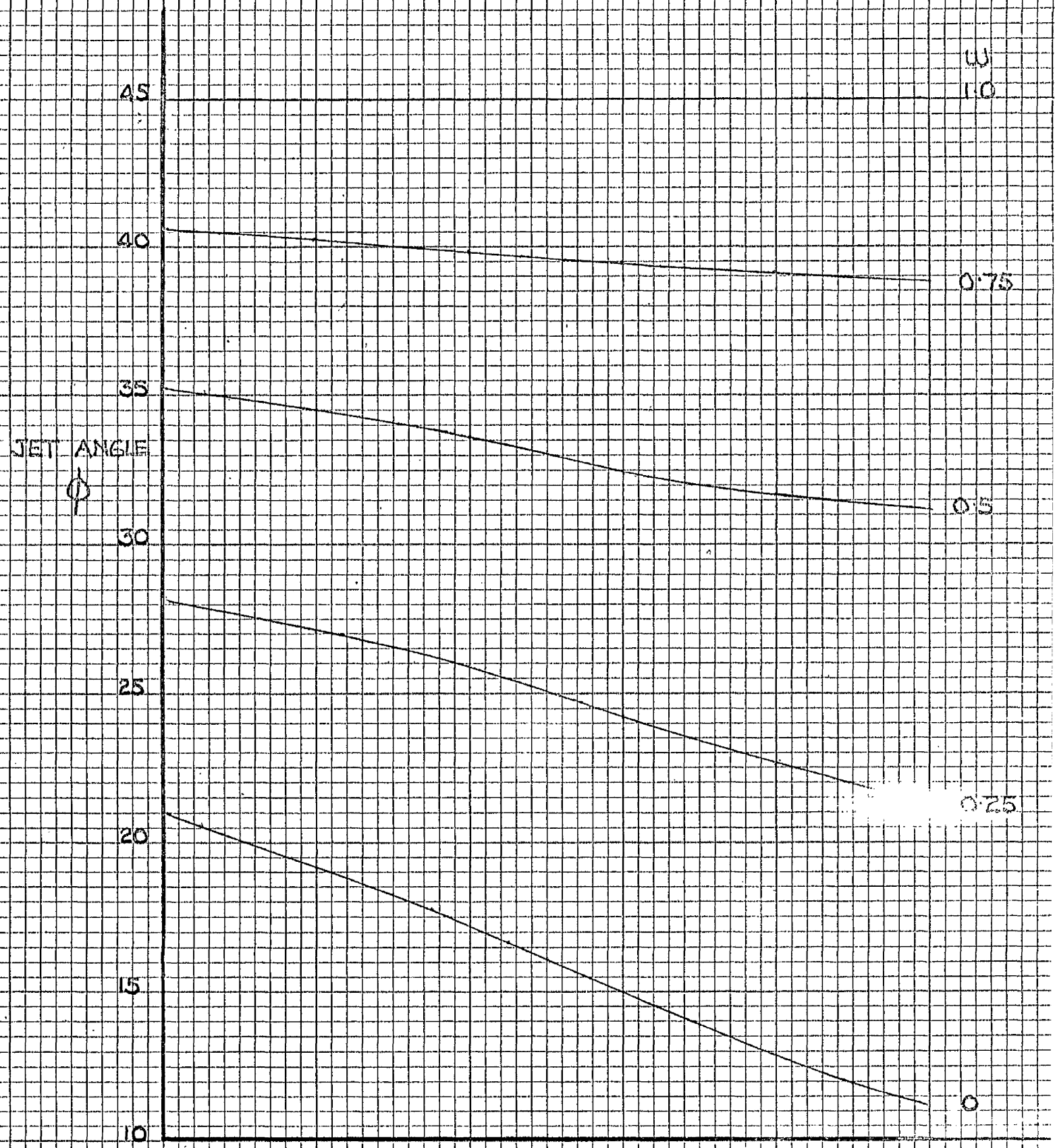

FIGURE 4.6.

VARIATION OF JET CONTRACTION COEFFICIENT WITH PRESSURE RATIO.

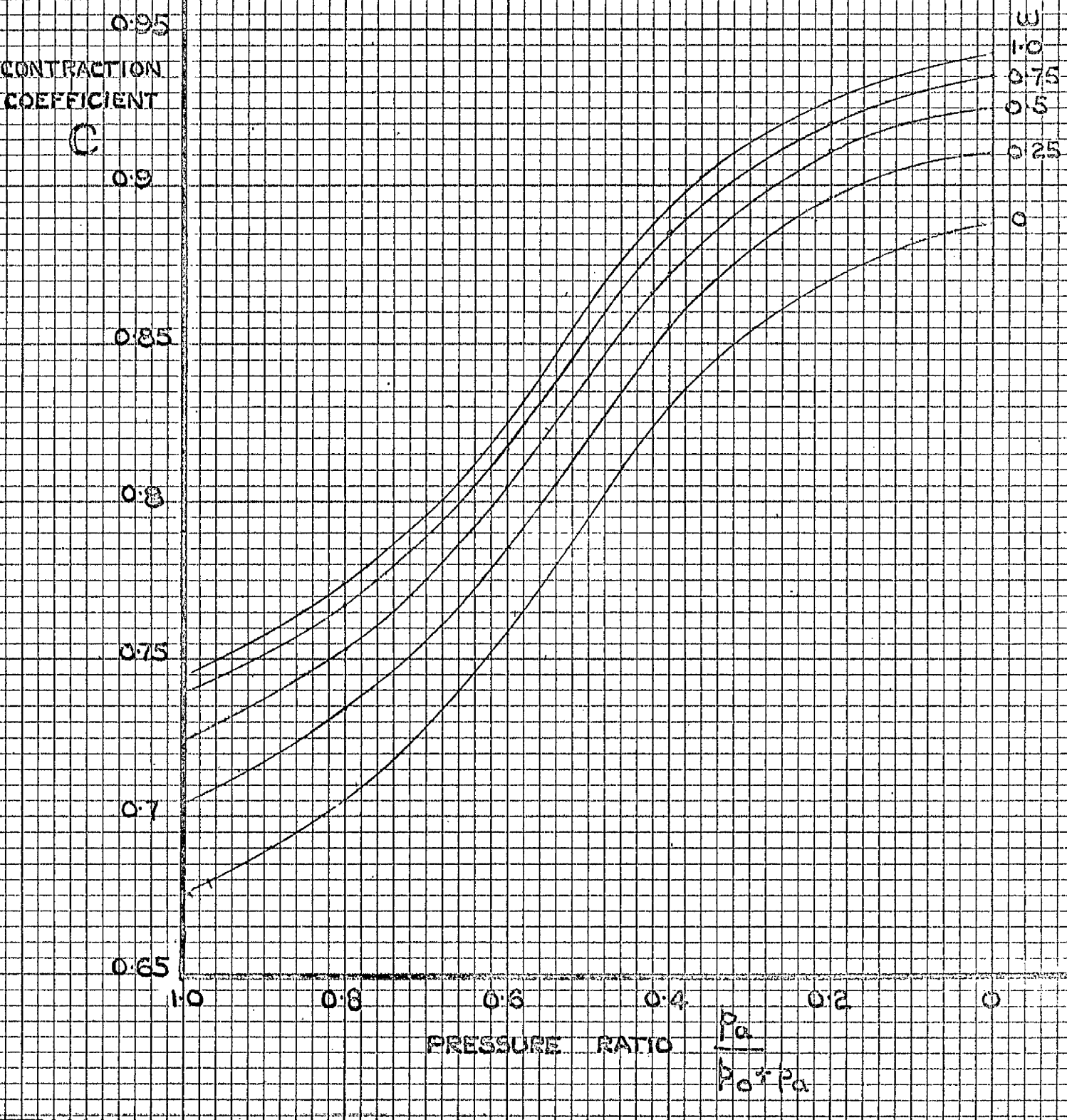

FIGURE 4.7.

INCREASE OF CONTRACTION COEFFICIENT DUE TO CHANGE OF PRESSURE RATIO.

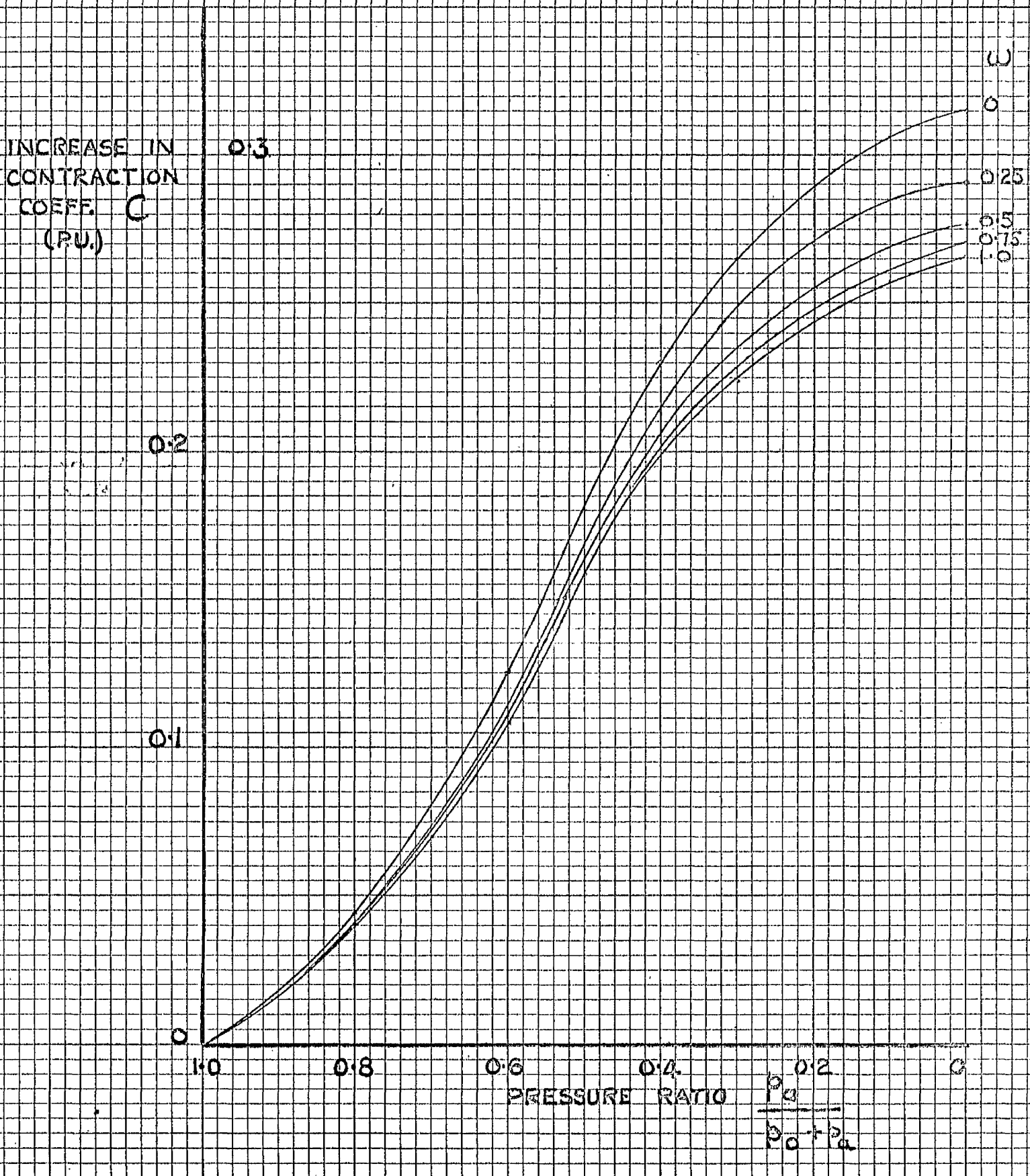

FIGURE 4.8.

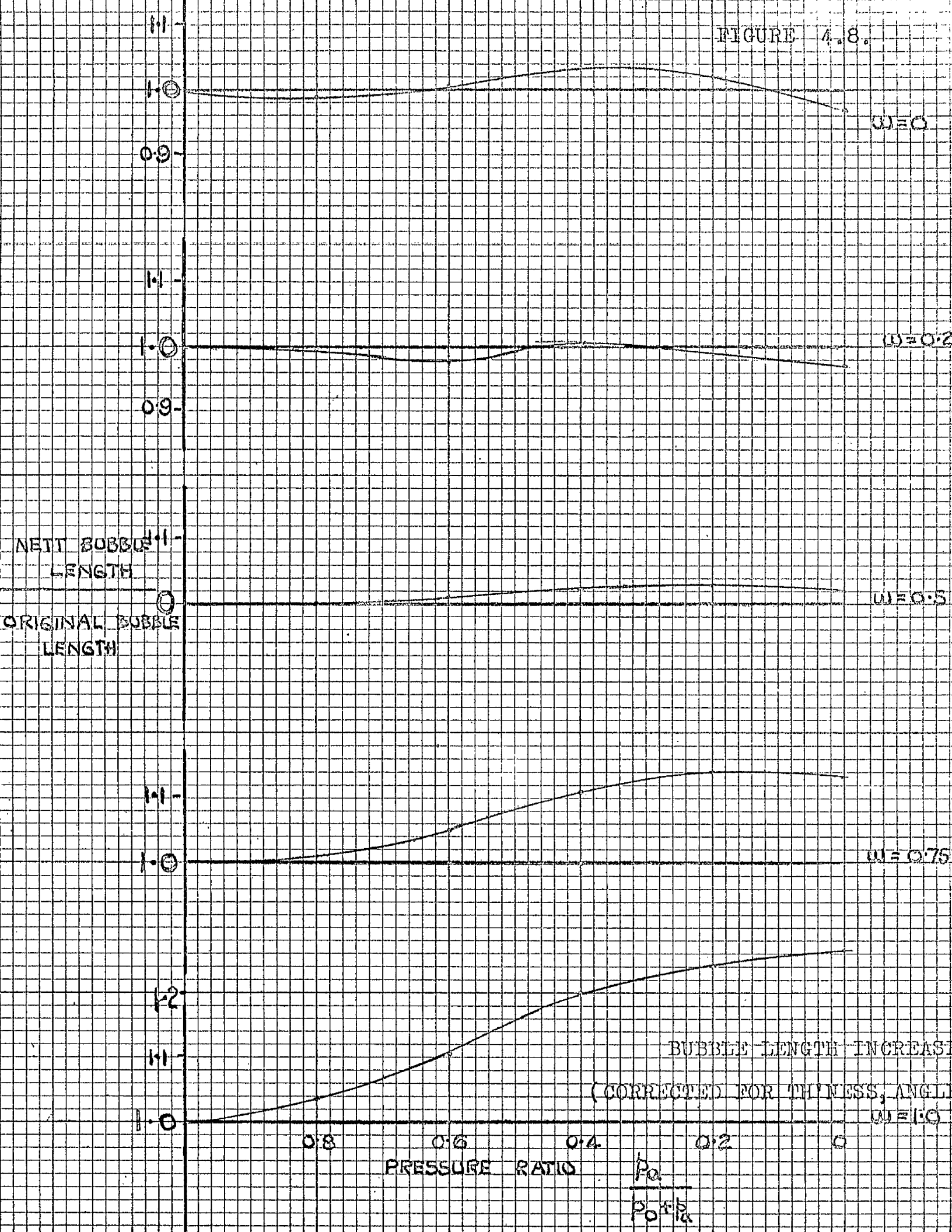
1·1
1·0
0·9
W=0
W=0·2
W=0·5
W=0·75
W=1·0
NETT BUBBLE LENGTH
ORIGINAL BUBBLE LENGTH
1·2
BUBBLE LENGTH INCREASI
(CORRECTED FOR THINESS, ANGLI
0·8
0·6
0·4
0·2
0
PRESSURE RATIO
Pa / Po + Pa

Chapter 5.

Experimental study of compressible flow.

5.1. Modifications to apparatus.

5.2. Experimental work and results.

5.3. Discussion of results.

5.1. Modifications to the apparatus for the compressible flow measurements.

Before the measurements of compressible flow could be made it was necessary to modify the apparatus to withstand the high gas pressures involved in accelerating the jet to supersonic speed and to provide means to allow a flow visualisation system to be installed, since much can be learned from the shock – wave patterns of supersonic flow.

Figure 5.1 shows the changes which were made. The most important modification was to machine a circular hole in both perspex plates and cement a plate glass disc into either hole as shown. The discs were one inch thick to withstand the pressure, and this necessitated machining the steel backing plates to fit round them. In order to strengthen the walls in the region of the orifice so that the gas pressure would not deflect the perspex away from the pistons and allow gas to leak across the corners inside the seals, the discs and the backing plates were reinforced by two heavy steel beams which were clamped together by four steel bolts passing completely through the apparatus. These bolts passed between the struts of the pistons outside the sealed high pressure chamber to allow the pistons to be moved to alter the orifice dimensions. Due to the high pressure exerted by the beams the pistons could not be moved without first slackening the bolts, which reduced the ease of positioning of the pistons, but the effect was not serious.

To prevent the beams from exerting too great a load on the glass discs and cracking them against the edges of the pistons before the gas pressure reduced the load, the bolts were progressivel tightened as the gas pressure was increased. This was only necessary at the higher pressures (above two atmospheres). The load distri - bution between the discs and the backing plate was controlled by varying the thickness of hard rubber packing beneath the beam.

The glass discs were necessary to allow a Schlieren flow visualisation system to be used. Perspex itself is not suitable for this purpose as it introduces additional light patterns due to flow lines and internal stresses which cannot be removed by heat treat- ment. The glass discs chosen were of optically tested plate glass polished to very fine tolerances of flatness and smoothness.

Figure 5.2 shows the arrangement of the Schlieren system. Two optical benches were fixed in line perpendicular to the plane of the apparatus as shown and two smaller benches parallel to it. Mounted on these benches were the optical elements of the system and the camera to record the patterns.

The light source used was a mercury vapour lamp mounted on the lower bench. A plane mirror reflected the light upwards through a condensing lens which was focussed on a fine slit at the focal point of one of the two main lenses. This produced a parallel beam of light through the working section illuminating the gas flow around the orifice and reattachment bubble. The beam was then re - focussed onto a knife - edged mirror (by the second main lens) and the image reflected horizontally onto a ground glass screen mounted

on the upper bench. Those portions of the beam of light which passed through the working section were partially refracted by the severe changes of density ocurring at the jet edges and at shock waves so that they did not refocus onto the mirror, and the image on the screen had unilluminated zones corresponding to the density changes.

The flow patterns displayed on the screen were recorded by a 35mm. camera fitted with a portrait supplementary lens to obtain a suitable size of image, and the lighting was sufficient to allow slow fine – grain film (F.P.3) to be used. This was a considerable advantage, since the negatives could be analysed using a projection microscope with a magnification of 25X. Tracing paper was placed on the screen and marked off to allow more permanent records to be obtained without the necessity of printing.

Conduction of heat through the boundary layer to the cold high–velocity gas (and the consequent cooling of the wall in contact with the gas) caused considerable condensation on the surface of the glass discs although, as predicted from the earlier tests, no moisture appeared on the metallic walls. This condensation, along with small traces of oil vapour carried over from the compressor, obscured some of the intricacies of the flow patterns and it was necessary to dismantle the apparatus at frequent intervals to clean the surface of the glass. Latterly some improvment was effected by wiping the discs with a demisting fluid and by making a specially shaped cleaning pad on a stick to wipe the inside without dismantling.

At the high mass flows involved in supersonic tests the air supply pressure could not be maintained by the compressor, and the reservoir pressure varied considerably. Since there were more than thirty static pressure tappings in the piston faces which had to be measured, some quick method had to be devised to monitor the pressures. The automatic recording system described in the appendix was not fully developed at the time and was only suitable for pres - sures up to 10 p.s.i. so that another method was needed.

Finally it was decided to use a 60 tube mercury manometer and to photograph the mercury levels, thus obtaining a permanent record which could be analysed at leisure. This method proved very satisfactory except for a few tappings where the pressures seemed to be oscillating and unstable. In these cases the photographic record could not be relied on to give any accuracy, and such points were noted and ignored. Again the lighting was arranged to allow Ilford F.P.3 to be used, and a projection microscope provided a means of analysing the negatives accurately.

The pressure difference across the orifice was measured by a 100 inch mercury column at the lower values, and by an accurat pressure gauge at high pressures.

Pressures were read to the nearest $^1/_{10}$ of an inch of mercury using the manometers, and to the nearest 0.2 p.s.i. on the gauge.

5.2. Experimental work and results – compressible flow.

1. To determine the variation in jet angle due to change of pressure ratio across the orifice.

This measurement was made to test the predictions of Chapter 4.3 which are shown on Figure 4.5. The jet angle was measured by using the Schlieren system to show the edges of the jet at various orifice geometries. The lowest speed at which the method could be used corresponded to a pressure ratio of around 0.9. Above this the density gradient at the jet edge was too small to show clearly on the screen, although measurements could be made at higher ratios using smoke to show up the jet. At ratios below 0.25 the jet was also indistinct due to the large expansion wave immediately after the orifice. Between these two limits the measurements were satisfactory.

To allow the jet to stream from the orifice in a straight line it was necessary to stop it from reattaching to either of the downstream boundaries. In the earlier tests this was achieved by allowing the downstream chamber to empty so that the water jet flowed out into an air filled space, and the surface tension of the water stopped all entrainment. The jet of air could not be treated in this way and it was necessary to remove the wall to which the jet would reattach if allowed.

For this purpose a special piston was constructed (which is described in the appendix and illustrated in Figure A.4) with

the appropriate wall missing. It was not necessary to remove both walls since (as Bourque measured (6.)) a jet will not reattach to a plane which makes an angle of more than 60° with the direction of the jet, and this was the case for the configurations tested.

The Schlieren pictures of the jet flow showed the jet as two straight lines emanating from the edges of the orifice and gradually becoming less distinct as the jet entrained air and the density gradients at the edges became more gradual. As the jet velocity was increased the length of distinct line became longer up to sonic speed after which shock and expansion waves tended to disperse the discontinuity. Over a considerable range the lines were sufficiently clear to allow accurate measurement of the jet angle. These measurements were found to be repeatable to within a quarter of a degree.

Typical pictures are shown on Figure 5.4. and the results of the tests are on Figure 5.5.

This experiment was carried out for orifice dimensions with clearance ratios of $w = 0$ and $w = 0.25$, at which angles the change in jet angle due to compressibility was maximum. Also at higher values of w the angle between the jet and the remaining wall was less than 60°, which would have allowed the jet to reattach to the wall. In either case the pressure ratio was varied between 0.9 and 0.25.

During the course of the experiment it was found that an error in aligning the benches of the optical system resulted in angles being distorted on the screen. This error was measured by

placing a perspex protractor on top of the working section and measuring the distortion in the angles shown on the screen, thus permitting appropriate corrections to be applied. The maximum error measured was $1^{1}/_{2}^{o}$.

2. To measure the effect of compressibility on bubble length.

This test was to measure the length of bubble for varying inlet jet angles, at varying Mach numbers. To obtain the graphs of Figure 5.6 the clearance ratio was varied in steps of 0.25 from 0.0 to 1.0. At each setting the bubble length was measured (taking the pressure maximum as indicating the reattachment point) at pressure ratios between 1.0 (the incompressible case) and 0.25, or as near to this ratio as was possible before the flow broke down.

This breakdown in the flow pattern occurred at lower values of w; the pressure ratio at which it happened was approxim - ately 0.43 with w = 0.0 but decreased markedly as the jet angle increased until at w = 0.5 the effect did not happen within the rang used. Later an attempt was made up to an upstream pressure of over 120 p.s.i. but no breakdown occurred.

Schlieren pictures (Figure 5.3.a) confirmed that the flow above these critical pressures was in the form of a series of expansion and shock waves round the corner. Under these conditions the manometers connected to the static tappings showed wildly changing pressure readings around the corner which became a regularly varying pressure profile, corresponding to the principal shock being reflecte

from the jet boundaries at top and bottom.

The static pressure distributions found in these tests were recorded using the photographic method described in a previous section of the report.

3. To measure the static pressure distribution along the boundary wall at various jet velocities.

The changes in bubble length which were found in the previous experiment were so complex (as illustrated in Figure 5.6) that some explanation was sought in the static pressure changes along the boundary wall. The photographs of 2. above were there - fore analysed andaugmented where necessary by taking Schlieren pictures at what seemed to be critcal conditions.

Figure 5.10. shows the variation of the static pressure profile along the reattachment wall as the pressure ratio reduces to breakdown for w = 0.0, Figure 5.10.b the variation in minimum bubble pressure, and Figure 5.3 some of the Schlieren pictures corresponding to these tests.

4. To measure the effect of the second downstream wall on the reattachment bubble at low pressure ratios.

The photographs of Figure 5.3.a. confirm the predictions of chapter 4 that at low pressure ratios the jet expands laterally after the vena contracta. At the lower ratios this expansion is quite large and the jet approaches the downstream walls on the out - side as well as on the inside.

The proximity of the inner edge to the wall is a necessary part of the reattachment process, but the outer edge is supposedly free and it was felt that the extra expansion of the jet after the orifice might enlarge effects not shown up in the previous incompressible tests.

To determine the effect of the wall, the auxilliary piston was replaced by the special piston with the downstream wall removed, (Appendix 4) and measurements and photographs taken of the flow patterns in the bubble.(w varied between 0,1)

A comparison of the readings and photographs showed no evidence of any effect, but again it must be noted that in fluid logic elements, with smaller angles between jet and plane, a sizeable difference can be measured. (21)

5. To determine the limits of flow breakdown at low pressure ratios

Since the breakdown of jet flow is obviously very important to the designer of valves, a series of tests were carried out to determine at what jet angles and pressure ratios the effect occurred, and whether there was any hysteretic action which would prevent an unstable condition.

The tests consisted of slowly increasing the jet speed until breakdown occurred, then reducing it again until the jet flow was re-established.

Some of the findings are show on Figure 5.6,where the region in which breakdown could be achieved is indicated. It was found that the change could occur over a range of pressure ratios and a reduction in jet speed was needed to reform the jet.

flow again. Thus there is no possibility of an oscillating flow from these causes alone, but accompanying the change is a very considerable reduction in total pressure on the boundary wall which might be more serious from the point of view of stability.

6. To investigate jet flow with negative clearance ratios (w less than 0.).

In an attempt to provide more information on the change of flow pattern described above, tests were carried out to investigate the breakdown of jet flow with low jet angles. This involved negative clearance ratios (an impractical condition) since the jet angle is 21° for w = 0.0.

These tests involved very short bubble lengths, and in order to get measurable lengths (in terms of the number of tappings included within the bubble) it was necessary to lower the aspect ratio from about 5 to as low as 2. Although this gave a qualitative result as regards behaviour, the limits measured for the two types of flow were false, being affected by three-dimensional effects. However the tests generally confirmed the previous results and some points are included on Figure 5.6.

5.3. Discussion of results.

The results of the experiments which were carried out to measure the jet angle at various Mach numbers agree quite closely with the calculated values from Chapter 4.3 (Figure 4.5), and the graphs can be compared on Figure 5.5. Since the predictions of the jet thickness (Figure 4.6) were obtained from the same analysi and assumptions as the angles, they are taken to have similar accuracy and are used in the following analysis of the measurements of the bubble length.

The only remaining difficulty, as in the incompressible study, lies in the assumption regarding the position of the vena contracta. This is increased in the compressible case by the position changing with M. (Stanton (51)). Initially the position will be assumed constant, and the effects of changes discussed later.

Figure 5.6 shows the bubble lengths as a function of the valve opening a, and there appears to be a reduction in the ent - rainment due to compressibility especially at the higher jet angle When the graph is corrected to express the length as a multiple of the calculated jet thickness and the curves are plotted to a base of M. the reduction in entrainment at higher angles is re - duced and there appears to be a slight increase at the lower angle This is without any allowance for the decrease in jet angle due to M. which affects the lower angles most. (Figure 5.7).

To make some allowance for this effect a series of graphs

can be drawn, one for each value of M., plotting bubble lengths against calculated jet angle. From these the bubble lengths at constant inlet angles can be derived, and the results are shown on Figure 5.8. This still indicates an overall decrease in entrainment with M., again most marked at the larger angles, but the range of variation is reduced – ranging from some 8 percent. at 21° to 60 percent at 45°, compared to minus 20 percent to plus 60 without the allowance for jet angle.

Figure 2.10 (for incompressible flow) shows that if the value of $\underline{\sigma}$ changes from 20 to 25 with an inlet angle of 21° then the bubble length increases by 22 percent, whereas the same increase in $\underline{\sigma}$ at 45° causes an increase of 37 percent, almost twice This increased sensitivity to changes in $\underline{\sigma}$ also affects the graphs of Figure 5.8, and reduces the apparent decrease in entrainment to 37 percent from 60.

At this point the variation of the position of the vena contracta can be considered. In Stanton's experiments he showed that the position varied with the pressure ratio across an orifice and that the amount of the movement might be almost a jet thickness (for a symmetrical orifice) Although the present orifice is asymmetric a change of half this amount seems possible and a change of this size would increase the bubble length by 19 percent at 45° inlet, and by 33 at 21°. (derived from Figures 2.10 and 2.11 These figures could further decrease the apparent effect of M. on entrainment, but since the location and change of the contraction are unknown, no useful figures can be derived.

This rough analysis, however, is sufficient to show that the increase in bubble length of Figure 5.6 does not represent a large change in the apparent value of σ with M at subsonic flows and that the apparent difference between the effects at high and low inlet angles is due more to the configuration of the apparatu rather than any fluid flow changes. On average the entrainment appears to diminish by some 25 percent between M = 0 and M = 1.

One fact that emerges clearly from the tests is that the valve geometry is most unsuited for compressible flow work. Further investigations with simplified entry conditions such as were used by Sawyer and Bourque will be necessary before an accu rate knowledge of the effect of M on entrainment can be obtained and the graphs of Figure 5.6 explained.

At transonic and supersonic speeds the jet showed some remarkable phenomena — the bubble breaking down into a wall jet at the smaller angles and behaving in an oscillatory manner at others.

The first supersonic effect to be noted occurred at the pressure ratio giving M = 1 in the contraction. Due to the low pressure existing within the bubble the streamline at the inner edge of the jet reaches sonic speed before the others. By the time the outer streamline reaches sonic speed the inner edge is supersonic and no longer emerges tangentially to the upstream wall. Instead it expands outwards at the corner so that the inner edge turns towards the plane (see Figure 4.3.a, the point D). When the outer streamline becomes supersonic it also expands outwards, this time

turning away from the plane. Over the range of pressure ratio between the inside becoming sonic and the outside doing the same the average velocity vector of the jet swings towards the plane, thus shortening the bubble.

This effect is opposed by a change of jet angle caused by the differential pressure existing across the downstream side of the orifice, which increases the momentum of the flow along the upstream boundary at the side with the bigger pressure dif - ference, and this increased momentum pushes the jet away from tha side, only to have the effect reduced by the curvature of the flow before the contraction.

The relative sizes of these effects almost certainly changes with jet angle, Mach no., bubble pressure and position of the contraction so that no estimation of the overall effect can be made. As previously stated experiments with simpler inlet conditions are needed to separate the various aspects of the problem.

Schlieren photographs taken of the flow patterns corres- ponding to these phenomena showed little apparent difference and a much larger apparatus may be needed to distinguish the various effects. The photographs are shown on Figures 5.4, 5.3 and 5.9. and are discussed later.

Tests on the pressure distribution along the boundary wall within the bubble showed the pressure minimum gradually moving towards the separation point from its incompressible position some one third of the way along the length (Figure 5.10) When the inner edge became sonic the corner of the orifice (the

centre of the expansion wave at lower pressure ratios) was the position of the minimum, and the edge expanded inwards as described previously. At low jet angles, decreased further by the effects of compressibility, the bubble flow persisted until the accelerations within the bubble became too great and the reattachment flow broke down to become a wave expansion round the corner followed by a supersonic wall jet with a strong shock wave pattern as shown on Figure 5.3.

Figure 5.10.a shows that as the pressure ratio across the orifice was increased the pressure gradient at the point of reattachment slightly diminished. This was an adverse gradient so that it appears that the mechanism whereby the breakdown occurs is at the opposite end of the bubble, that is at the separation end.

In order to establish a criterion for the breakdown, therefore, an exact knowledge of conditions and dimensions at the separation point is necessary. Since this was not available no accurate analysis can be made —several approximate calculations were attempted but no satisfactory solutions could be found.

At higher jet angles another form of instability was isolated involving a sudden decrease in the bubble length of some 20 percent accompanied by no apparent change in either the shape of the pressure distribution curve along the plane or of the Schlieren photographs. This is shown on Figures 5.6, 5.7 and 5.9.

This instability showed no hysteretic effect, and the bubble length varied abruptly between the two values with an apparently random period. The variations were measured using the

multitube mercury manometer which had a time constant of 8 secs and the recorded fluctuations exhibited the same rate of response. Thus the changes in pressure distribution must have been rapid in comparison to the manometer response.

Readings were taken at various values of Reynolds' No., Aspect Ratio and with different downstream boundaries (other than the reattachment plane) to try to dissociate the phenomenon from the dimensions of the apparatus, but no change was found in either the size of the effect or in the pressure ratio at which it occurre

At first it was thought that the instability was caused by the finite number of pressure diamonds between the separation point and the reattachment, but the Schlieren photographs (Figure 5.9) showed that the bubble was so long that the shock patterns did not extend up to reattachment, and any increase in the length of the diamonds would not result in a smaller number. Since the flow at reattachment is subsonic it does not seem likely that the instability can be caused by the downstream half of the jet, and an explanation must be sought in the complex flow at the inlet. Further tests on compressible reattachment will show whether the effect is a function of the inlet configuration or of compressible flow in general.

The tests conducted to find whether the the downstream wall opposite the bubble had any effect on it indicated that there was n change over the range of pressure ratios covered in the tests. This does not rule out the possibility of an effect appearing at very low ratios as was found in a similar configuration (Norwood(36.b)).

The region in which either the bubble or the supersonic wall jet can exist is shown on Figure 5.6 by the lightly shaded area. Operation of a valve in the range would be just as unsatis - factory as under the conditions with the jet reattaching to either downstream wall. No attempt was made to determine an upper limit of angle at which the effect ceased to occur since the value found would have been function of the Aspect Ratio and would be of little practical use since the jet angle is fixed at 21° ($w = 0$) in a normal valve.

Similarly the tests at negative clearance ratios only served to indicate the general trend, showing the flow patterns to be unsuitable for accurate control purposes above sonic speed.

Figure 5.10.b (showing how the minimum bubble pressure varies as the clearance ratio is increased) indicates, as expected, that the negative pressure diminishes with Mach no. However the effect whereby the pressure rises again at $M = 1$ was observed only for $w = 0$ and 0.25, roughly the same range at which the bubble breakdown was seen. Since it has been argued that this particular instability is due to an effect at the orifice end of the bubble, it may be that the increased negative pressure at the separation point is a primary cause of the breakdown. As previously discussed a much larger apparatus would be needed to investigate this.

FIGURE 5.1.

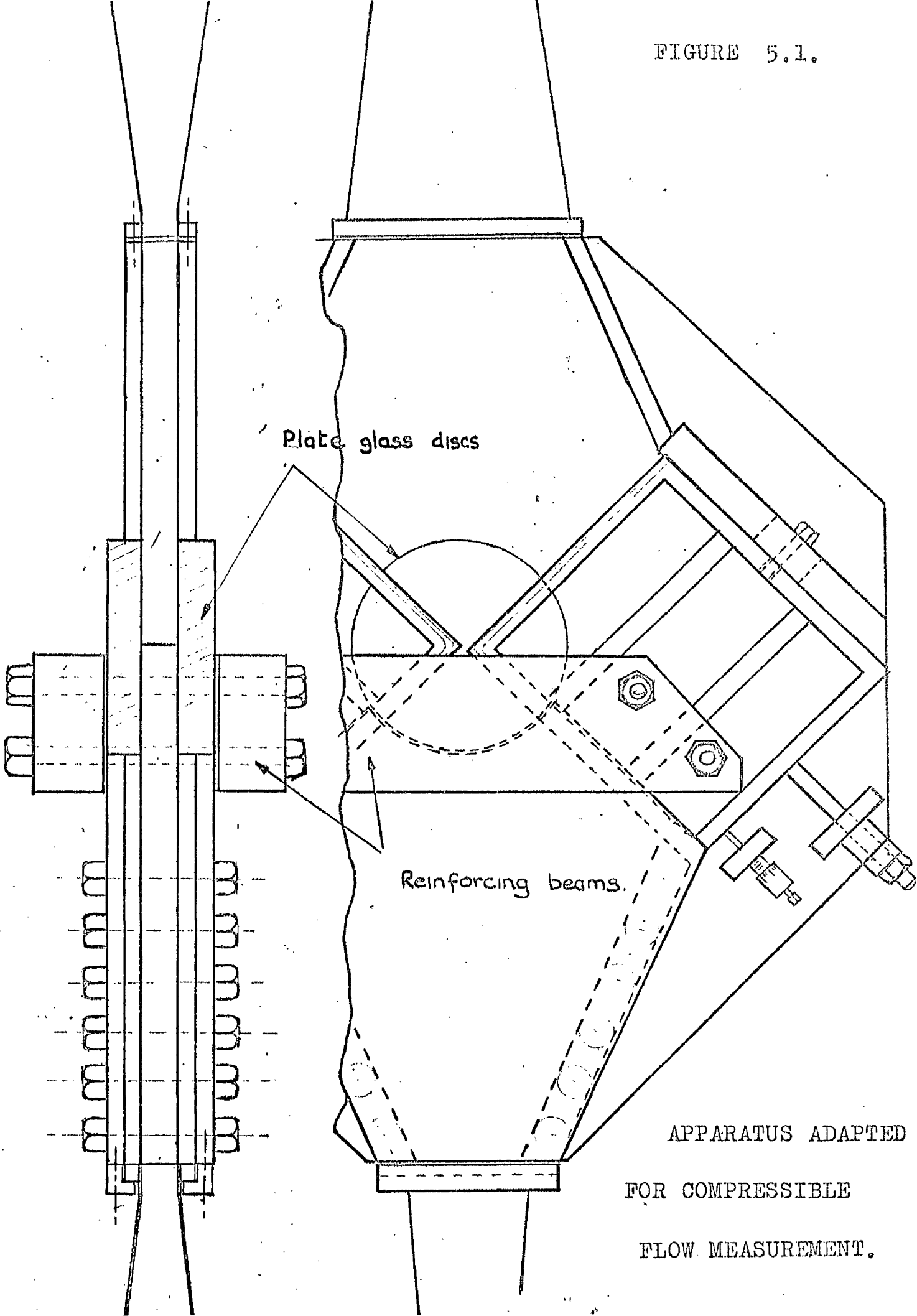

APPARATUS ADAPTED FOR COMPRESSIBLE FLOW MEASUREMENT.

FIGURE 5.2.

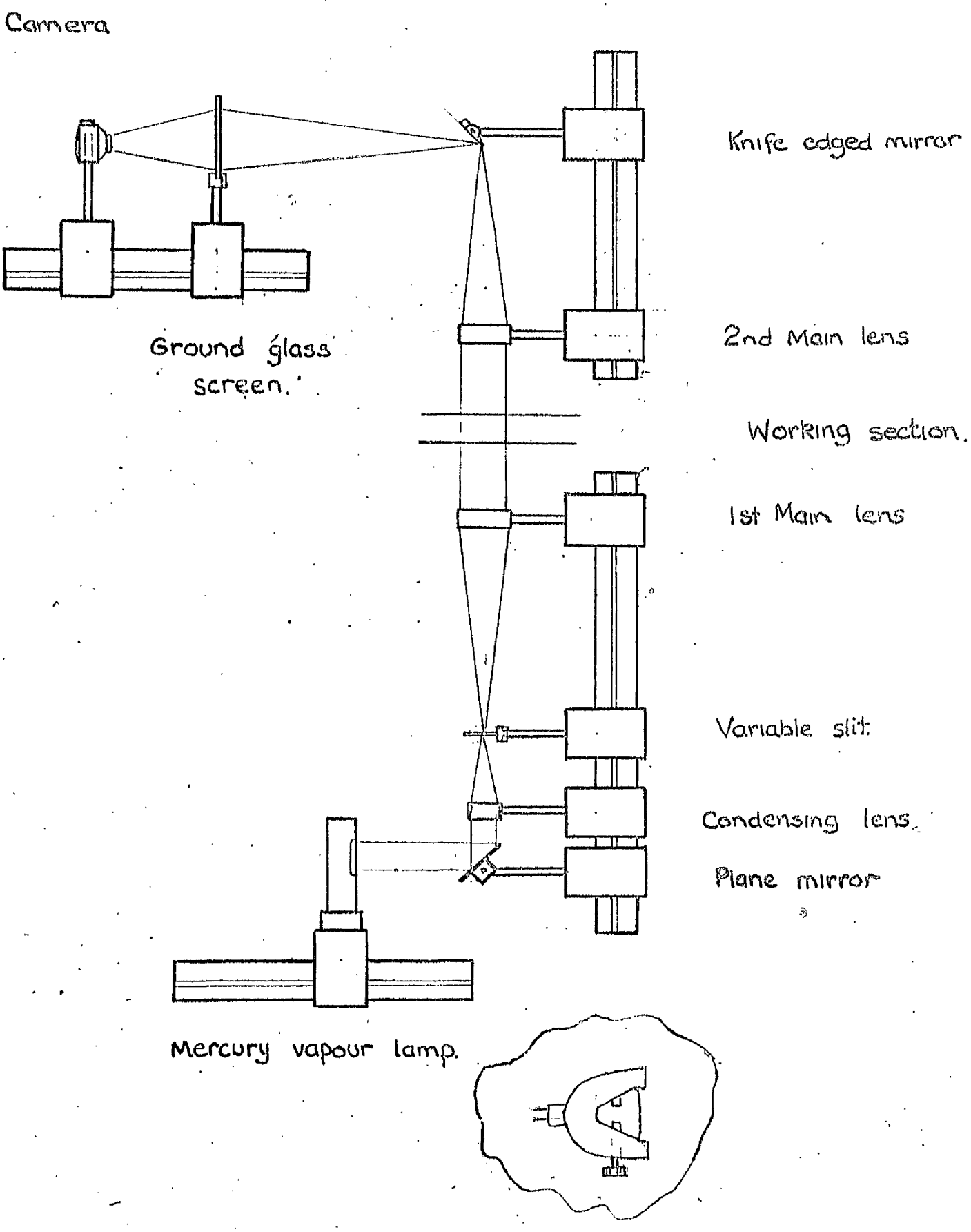

SCHLIEREN SYSTEM FOR FLOW VISUALISATION.

FIGURE 5.3.

SCHLIEREN PHOTOGRAPHS OF BUBBLE INSTABILITY AT LOW JET ANGLES.

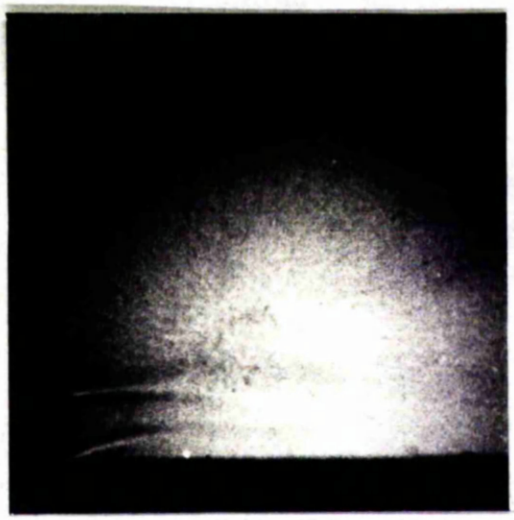

W = 0, Press. Ratio=0.76.

W = 0, P.R.= 0.57.

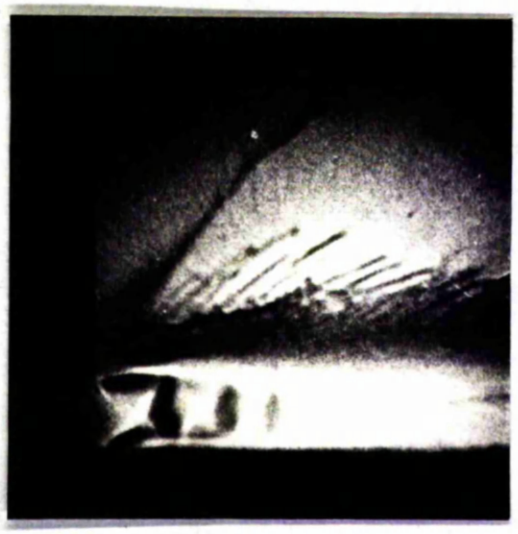

W = 0, P.R.=0.48.

W = 0, P.R. = 0.43.

FIGURE 5.4.

SCHLIEREN PHOTOGRAPHS USED IN MEASUREMENT OF JET ANGLE.

W = 0, Press. Ratio=0.75.

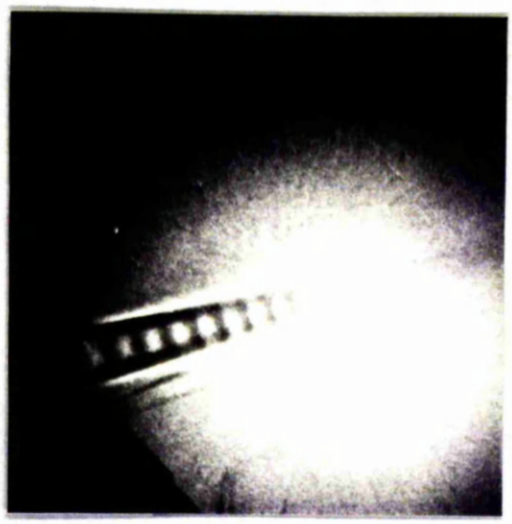

W = 0, P.R.= 0.49.

W = 0, P.R. = 0.23.

FIGURE 5.5.

VARIATION OF JET ANGLE WITH PRESSURE RATIO.

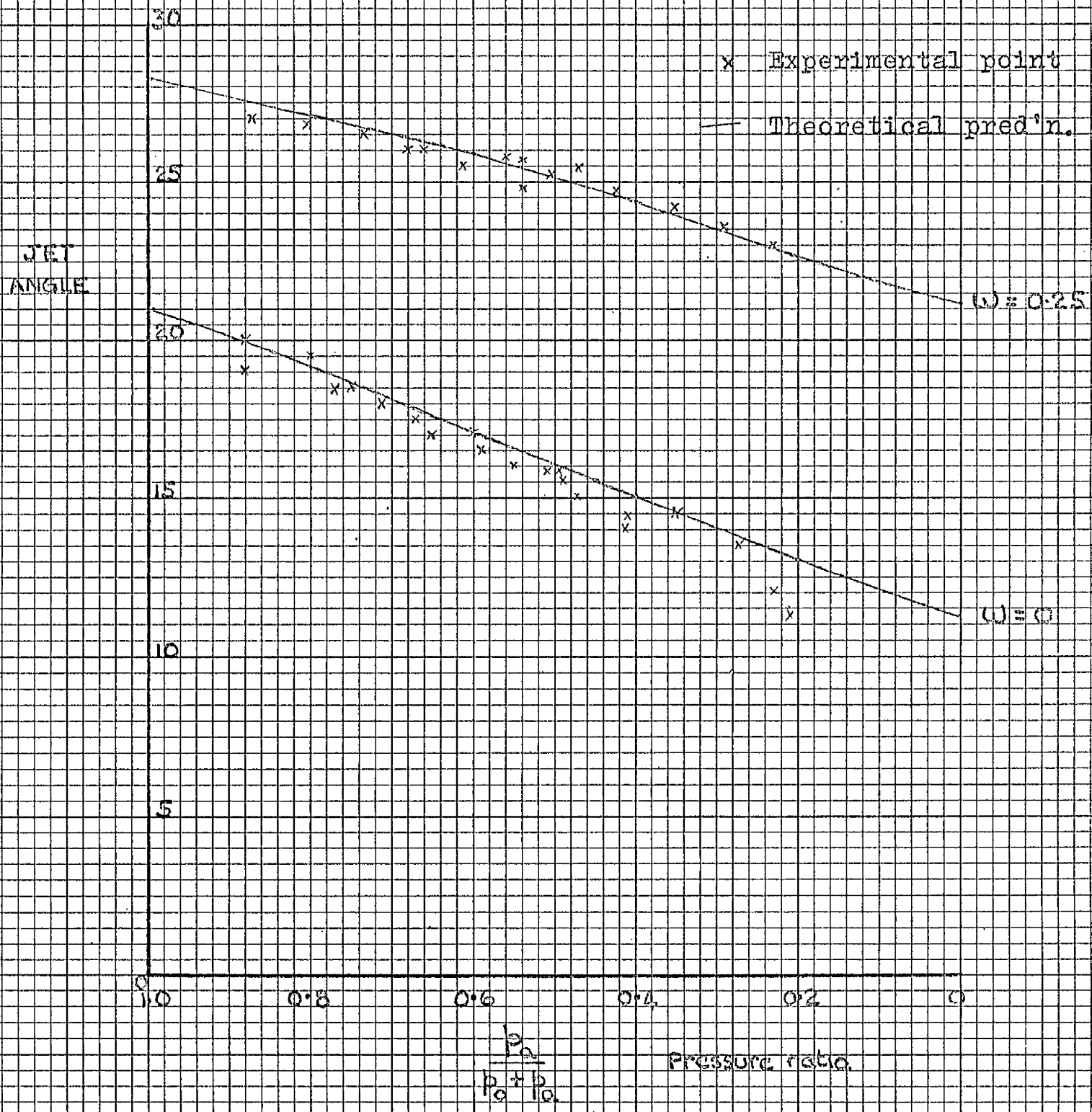

FIGURE 5.6.

VARIATION OF BUBBLE LENGTH WITH PRESSURE RATIO.

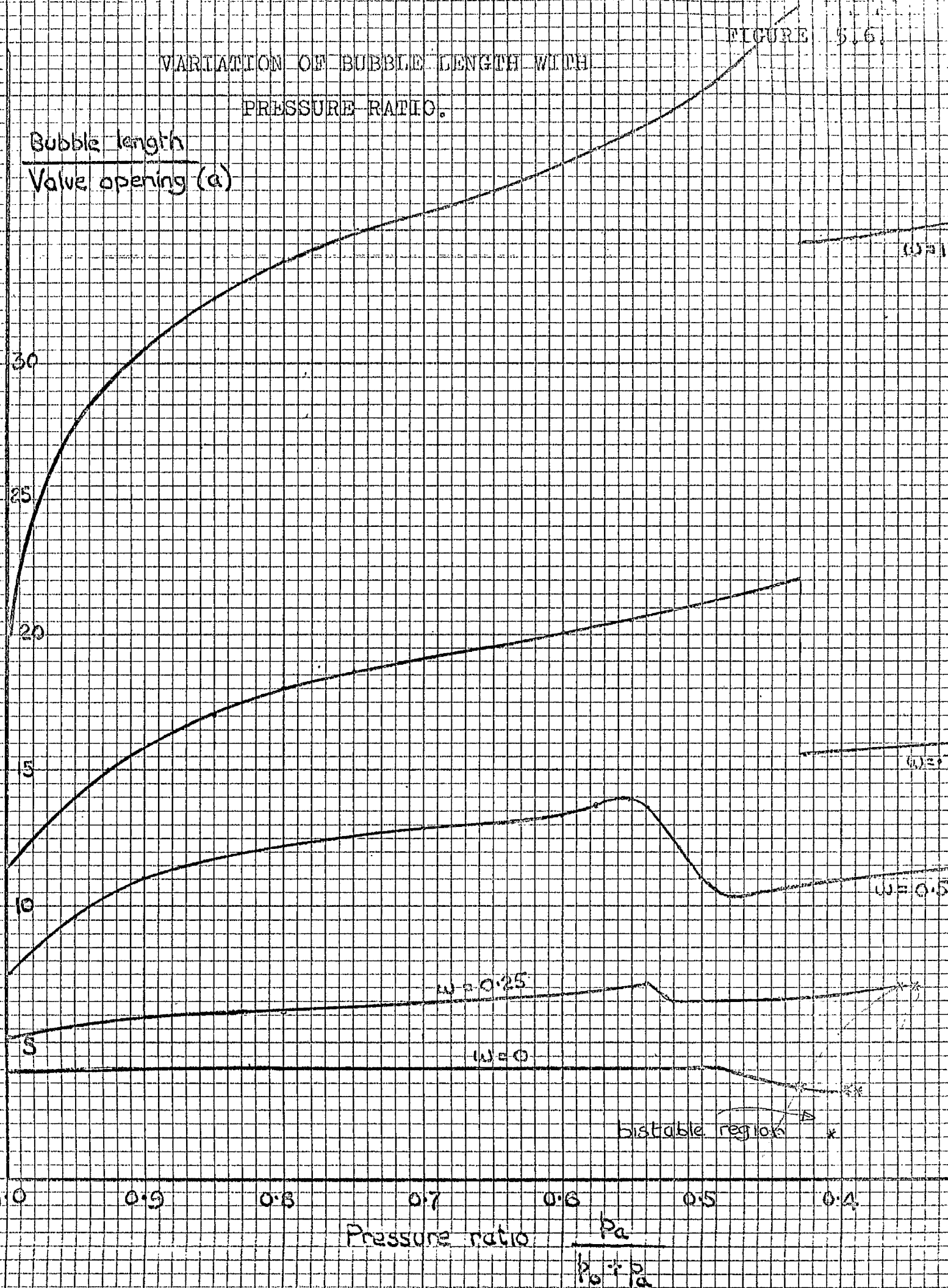

VARIATION OF BUBBLE LENGTH WITH MACH NUMBER.

(corrected for jet thickness)

FIGURE 5.7.

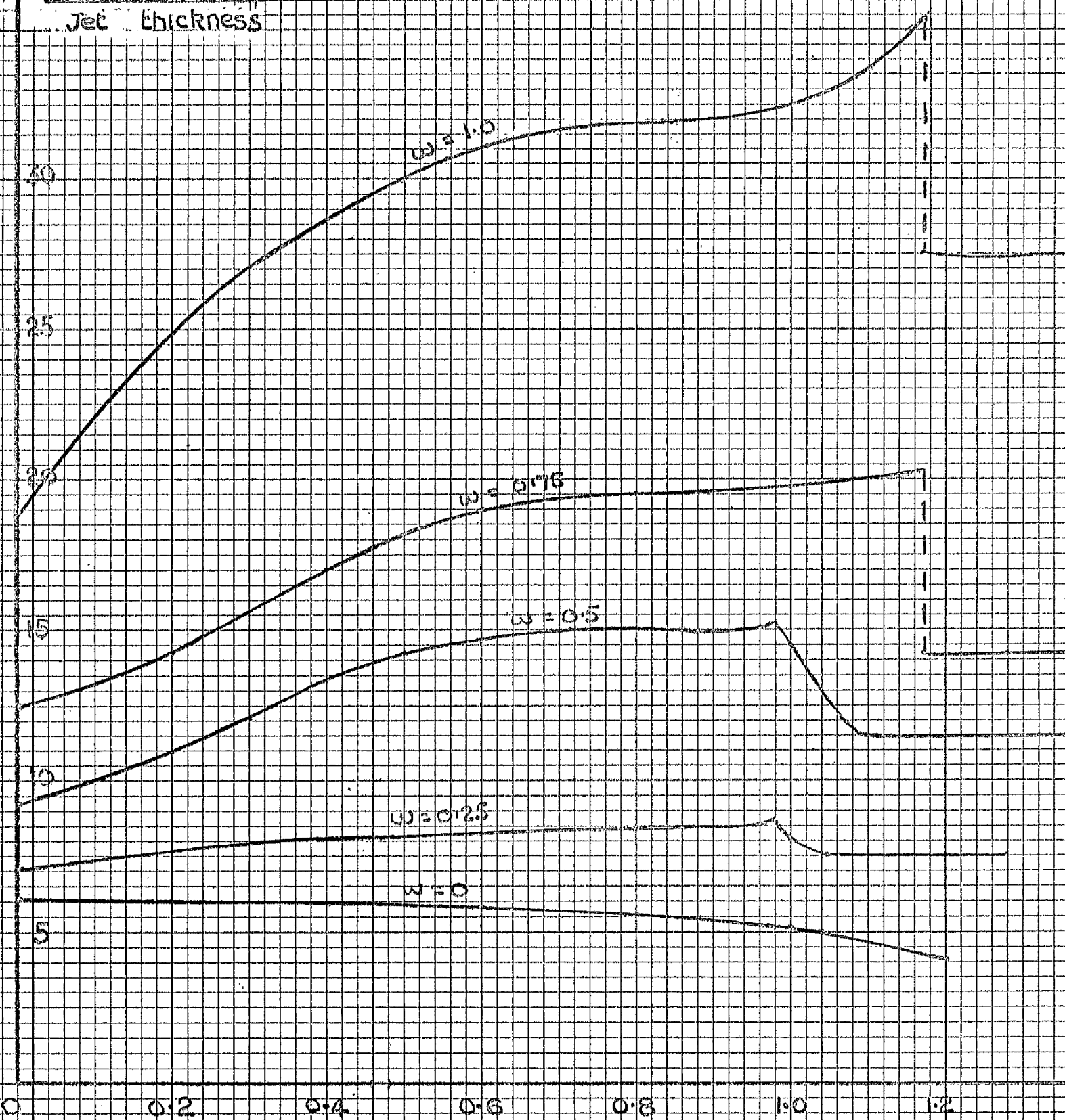

FIGURE 5.8.

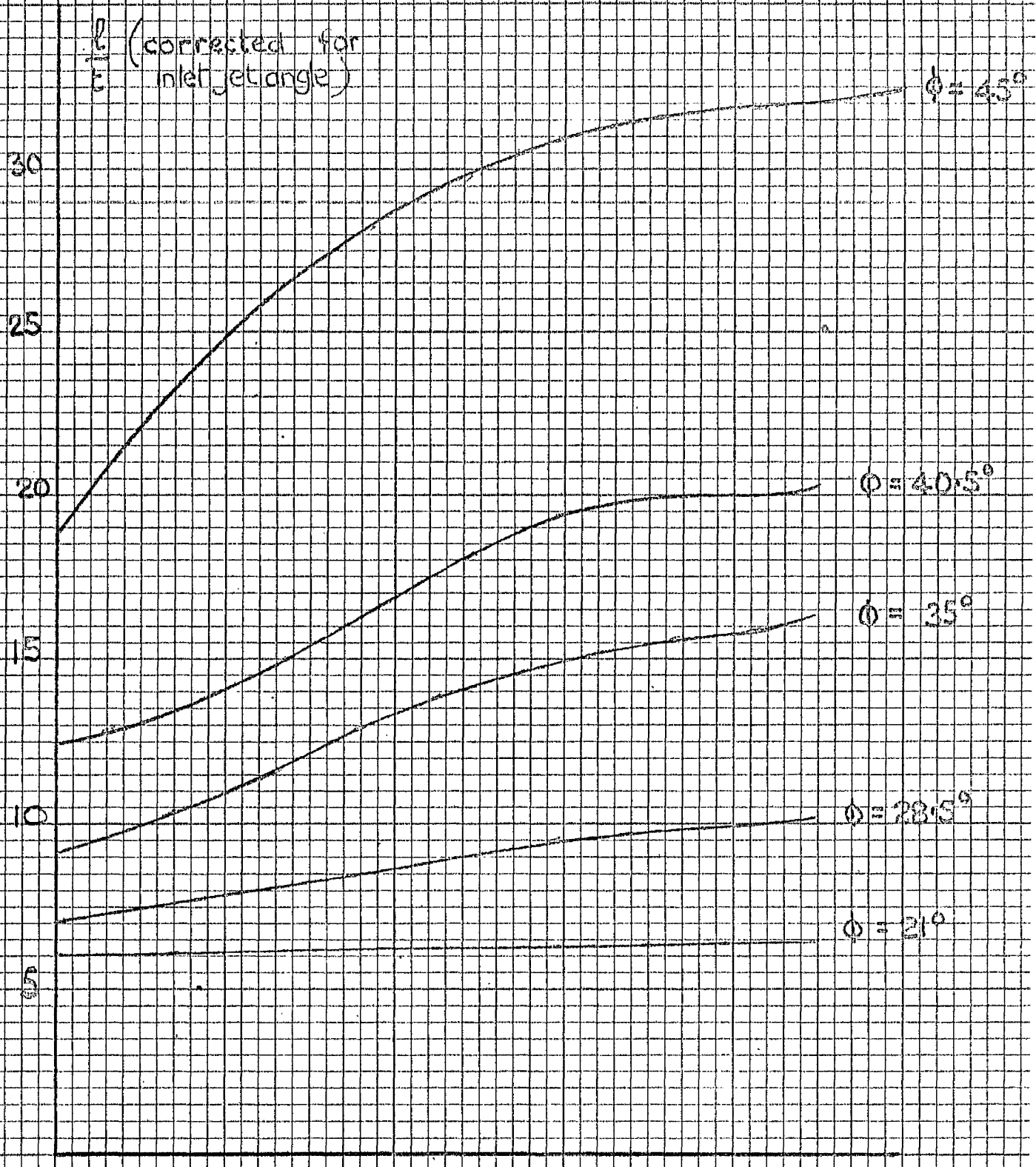

VARIATION OF BUBBLE LENGTH WITH MACH NO. (CORRECTED FOR INLET ANGLE).

FIGURE 5.9.

SCHLIEREN PHOTOGRAPHS OF BUBBLE INSTABILITY AT HIGH JET ANGLES.

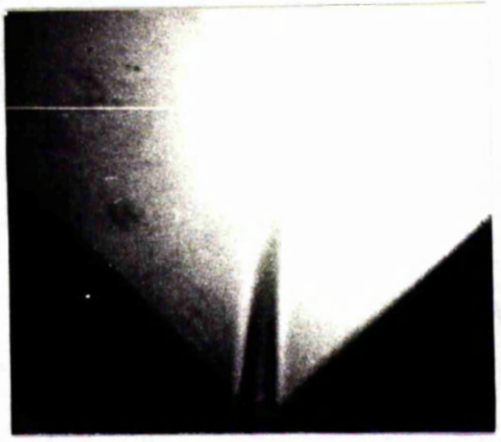

W = 1, Pres. Rat.= 0.55.

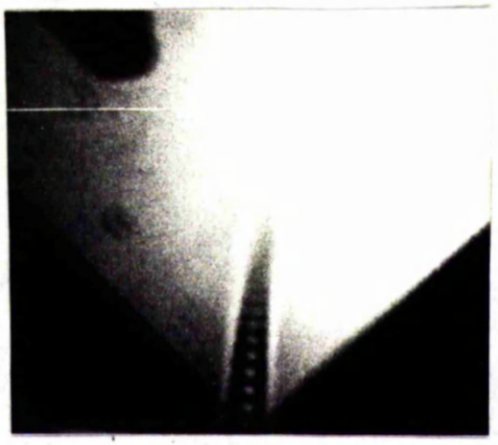

W = 1, P.R.= 0.50.

W = 1, P.R. = 0.43.

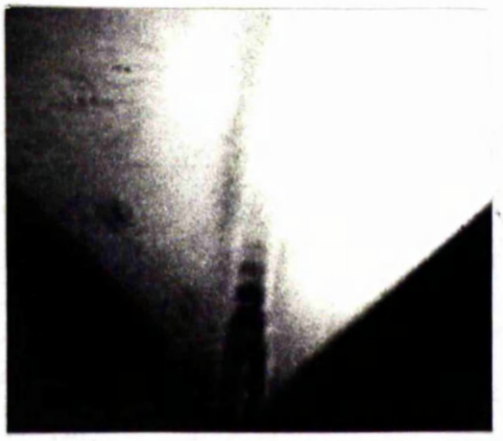

W = 1, P.R. = 0.41.

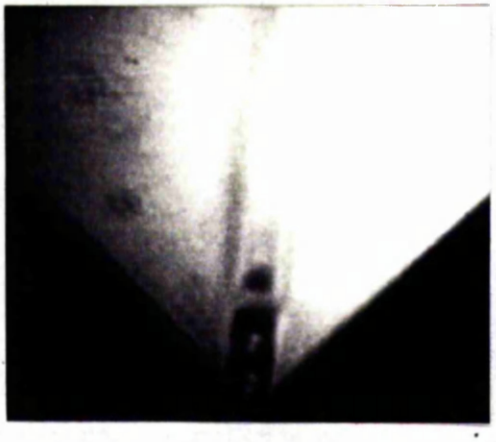

W = 1, P.R. = 0.36.

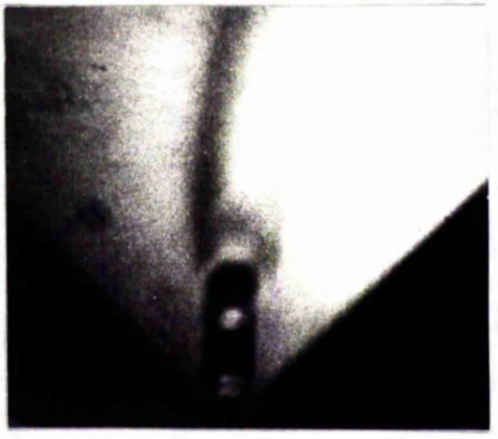

W = 1, P.R. = 0.26.

FIGURE 5.10.a.

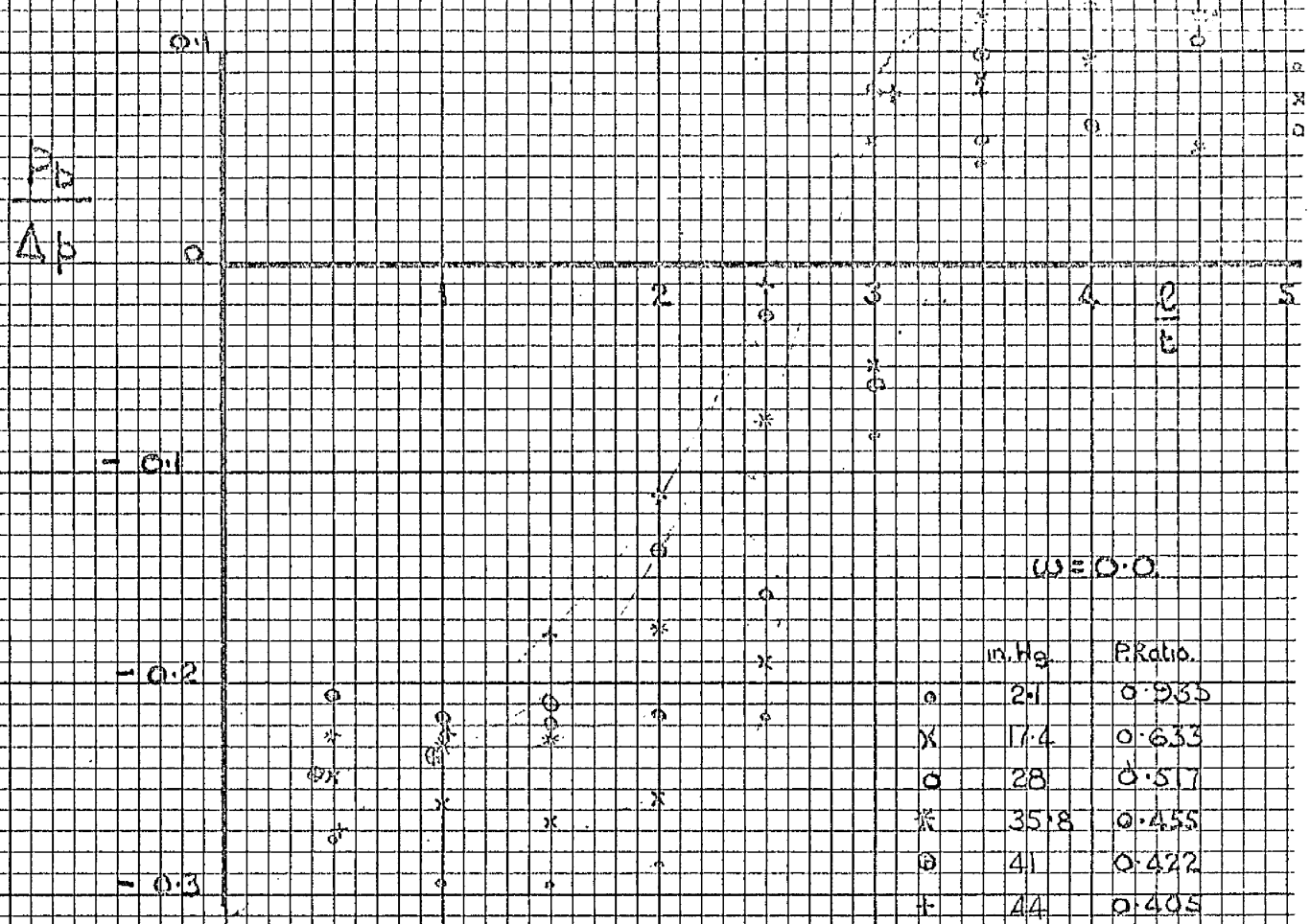

VARIATION OF PRESSURE PROFILE WITH PRESSURE RATIO.

FIGURE 5.10.b.

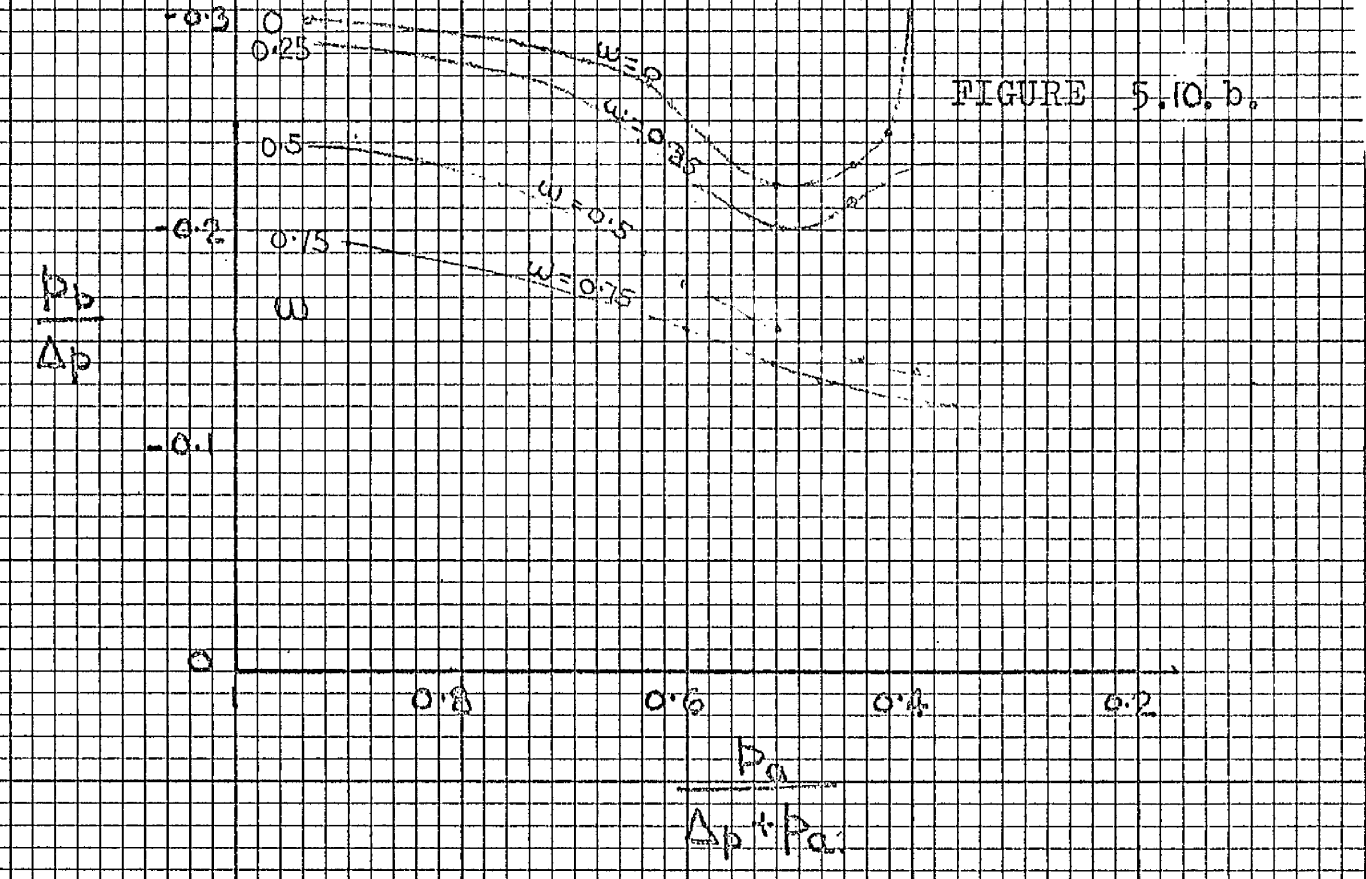

VARIATION OF MINIMUM BUBBLE PRESSURE WITH PRESSURE RATIO.

Chapter 6.

Conclusions and suggestions for further study.

6.1. General discussion and conclusions.

6.2. Some suggestions for future investigations.

6.1. General discussion and conclusions.

The investigation described in this report was aimed at increasing understanding of the various flow phenomena found in piston valves, and in applying this knowledge to the design and prediction of performance of these valves. In order to achiev this the flow patterns were subdivided into regions in each of which a particular effect was of paramount importance, and the regions were studied separately by theoretical models and exper - imental measurement.

Although the Aspect ratio of the apparatus was too smal to allow truly two - dimensional flow, sufficient accuracy was achieved in the study of incompressible flow to let an analysis be made to predict the flow patterns. This analysis was then show to agree with two previous attempts once all three had been put on a common basis. Subsequent experiments have shown that some of the assumptions used were accurate, and that the values of entrainment(derived from the experimental results)for the inside edges of curved jets were reasonably correct.

The theoretical method developed in this section is suitable for the prediction of reattachment phenomena in other configurations; the upstream treated as inviscid streamline flow, and the downstream in terms of the new entrainment model. More importantly the analysis can be used to design valves with known characteristics,and changes in reaction force and flow coefficien can be predicted.

As well as providing design data the investigation con -

confirmed that the separation and reattachment flow in valves can either be prevented or controlled. Reattachment can be pre — vented by a cut — back piston or a shaped spool (Figure 1.4.b.), and in either instance the flow is stable under steady — state conditions, though dynamic instabilities may yet be found.

If jet flow is accepted, then bistability may be avoided over a certain range of valve opening by choosing the downstream chamber dimensions so that the jet can have only one stable position, which is calculable.

Although the investigation has suggested no new ways of removing the problem, it has provided a model which can be used to explain many of the previous findings and to limit its effect.

The study of the compressible flow patterns did not yield such an exact analysis or such definite conclusions. The difficulties encountered were threefold. Firstly the jet inlet position into the downstream chamber varied in an unknown way with gas speed, secondly no previous quantitative measurement of the variation of entrainment with Mach no. could be found and thirdly there were no other investigations of similar compressible jet flows, (c.f. those of Sawyer and Bourque.). Under these circumstances, to calculate the flow patterns in the lower chamber proved impossible, but during the investigation of the flow upstream of the orifice a method was found for finding the angle and thickness of the issuing jet. This method is app — licable to alltwo — dimensional asymmetric orifices with plane

upstream walls, and has application in similar instances when any other form of solution is impracticable or lengthy.

In the experimental investigation of the downstream flow several phenomena were isolated which were partly explained in terms of measured and calculated effects, but lack of accurat inlet information prevented further analysis. These effects woul be seriously detrimental to the operation of piston valves with gas speeds greater than sonic.

The breakdown of the bubble flow into a wall jet occur red at low jet angles, and the normal valve geometry ($w = 0$, $\varphi = 21^{\circ}$) was affected at speeds just above sonic. Slightly larger angles were similarly affected at higher speeds (up to an angle of 30°) and all angles showed changes of bubble length around $M = 1$, with similar changes in the flow coefficient and pressure distribution.

At larger jet angles the breakdown was replaced by ano- ther form of instability which was found to be self – oscillatin with no hysteretic effect. Finally reports were found of further bistable behaviour at high supersonic speeds in a geometry not unlike that tested, and the nature of these flows and their dependence on complex shock patterns indicated that they would be most undesirable in any control system.

Therefore it would seem that the piston valve port is satisfactory for compressible flow up to sonic speed. Though variations in both the flow coefficient and the reaction force may be as high as 20 percent over the range, no instabilities

are found other than those of incompressible flow. At higher gas speeds other effects appear, and the changes in the flow patterns and characteristics make the system nonlinear, bistable and liable to instability.

6.2 Some suggestions for future investigations.

In the course of the tests it was established that the flow in the valve model was not truly two – dimensional, and as a result accurate measurement of bubble length and flow coef - ficient was not possible. A model with an Aspect Ratio of at least 30 would be necessary for such measurements, and the figure obtained could then be compared directly with those of the other reports. The tests would also provide accurate values for the flow coefficient which has not so far been measured.

It would also be useful if the new model was capable of operation over a wide range of A.R. – from 30 down to 0.3 say- which would allow all the previous results to be correlated (al - though the existing accuracy is reasonable)

The method developed by Spalding and Ricou (40) to measure the quantity of fluid entrained into a jet (axisymmetric) could be adapted to a two – dimensional jet. Thus it would be possible to directly measure the entrainment on the inside and or the outside of a curved jet. The results of such a test would be extremely useful since they would allow Gortler's hypothesis of uniform turbulent mixing across a jet to be modified for the case of a curved jet, and would enable the values of the entrainment parameter σ to be realistically compared with that of a straight jet. Figure 6.1.a shows a possible arrangement.

A test on these lines was carried out by J.H.T.Carter since the present tests were completed. The results showed

clearly that entrainment is markedly reduced on the inside of a curved jet and increased by about the same amount on the outside, making the total almost constant. Velocity profiles were also plotted which showed that this differential entrainment had little effect on the jet's velocity distribution in the axial direction, but that there was a considerable flow across the jet centreline radially inwards to make up for the reduced entrainment. Graph - ical integration of this radial velocity distribution showed the total flow across the centreline to be almost exactly equal to the difference in entrainment.

Unfortunately the design of theapparatus did not permit very small radii of curvature to be tested, but the results did indicate that the method is satisfactory for two - dimensional flow, and that considerable accuracy is possible.

Conditions existing at the point of reattachment are not yet well defined and tests to find the variation in the position of zero flow with respect to the static pressure maximum would aid correlation of various reports.

Another study which would aid further tests on the valve geometrywould be a potential solution with a pressure difference acting across the jet on the downstream side. Analytically this is difficult, but a relaxation solution would present no undue problems,and it would give accurate knowledge of the jet angle under the true entry conditions.

Foster has shown that the flow patterns in valves under dynamic conditions are considerably different from those existing

in the steady state. It seems therefore that an investigation into the dynamic properties of jets will be essential before understanding of the flow in valves is complete. Such an investigation would have to include sudden, continuous and even sinusoidal movement of the piston and would require considerable instrumentation. Initially this investigation should not be carried out using the valve geometry, with its uncertain inlet conditions, but in either of the two other geometries described in Chapter 2.

The effect of the extra downstream walls (CD in Figure 1.1.b) was well tested by Mitchell (32.a) but if these walls were included in the examination of the velocities at the reattachment point more light might be shed on the problem of reattachment with an adverse pressure gradient. (Figure 6.1.b.)

Although a solution was found giving the contraction coefficient and jet angle for compressible flow, a series of potential maps at various Mach numbers and with differential pressure across the downstream jet would be useful, especially at supersonic speeds. These could be obtained using Norwood's relaxation method which is described in Chapter 4.

The supersonic maps would show the change in jet angle due to compressibility and also the effects caused by the different expansion angles on either side of the jet immediately after the orifice.

In subsonic flow the most immediate necessity is a test to determine exactly the bubble lengths at various angles and Mach numbers. Such a series of tests would require an appar-

apparatus similar to that of Bourque or Olson with a sizeable fan or compressor, but without a knowledge of the effect of compres - sibility on bubble length and entrainment little further progress can be made. These tests might be complemented by measurement of the actual volumes entrained into the jet using the system describ for incompressible flow earlier in this section.

FIGURE 6.1.

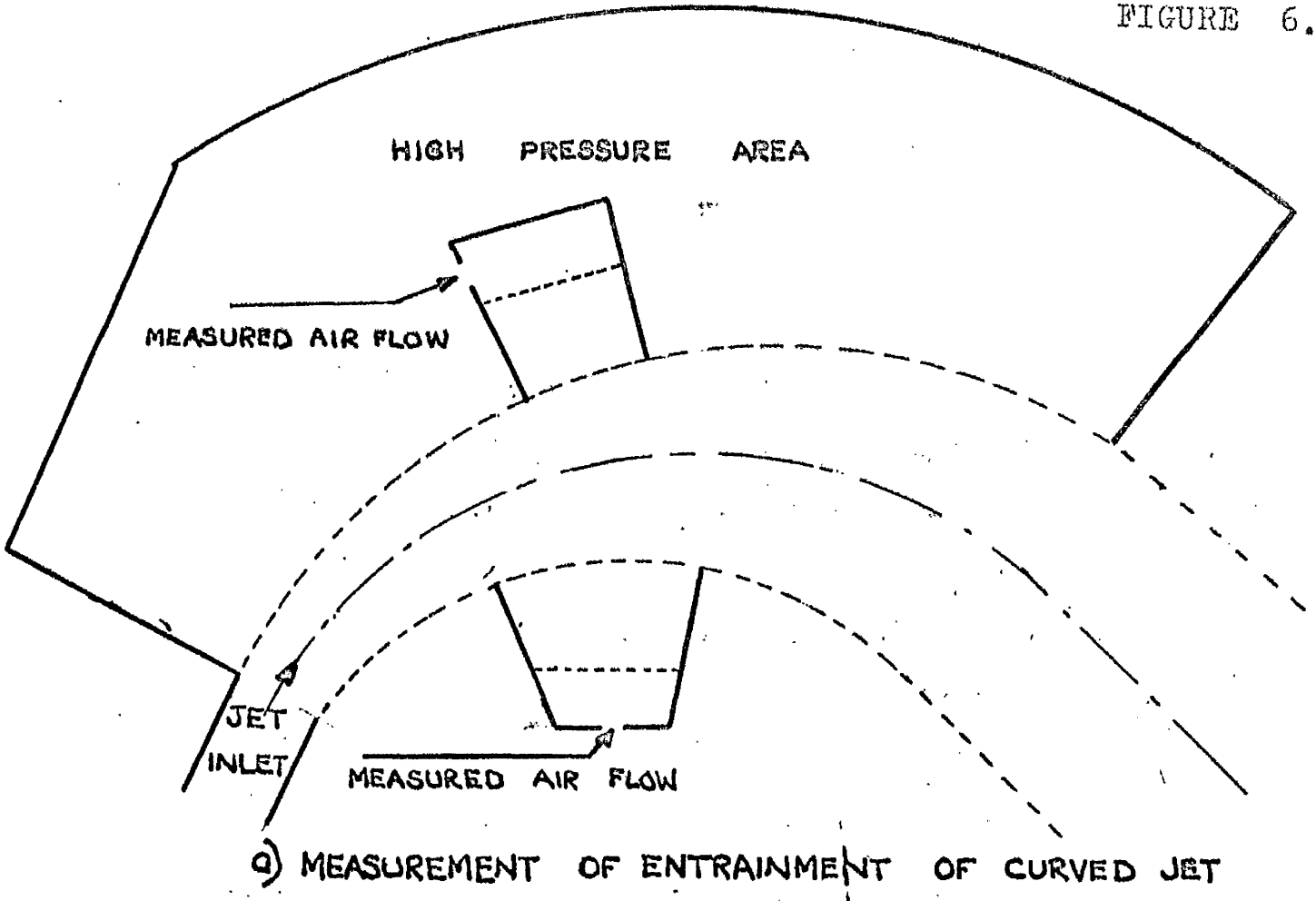

a) MEASUREMENT OF ENTRAINMENT OF CURVED JET

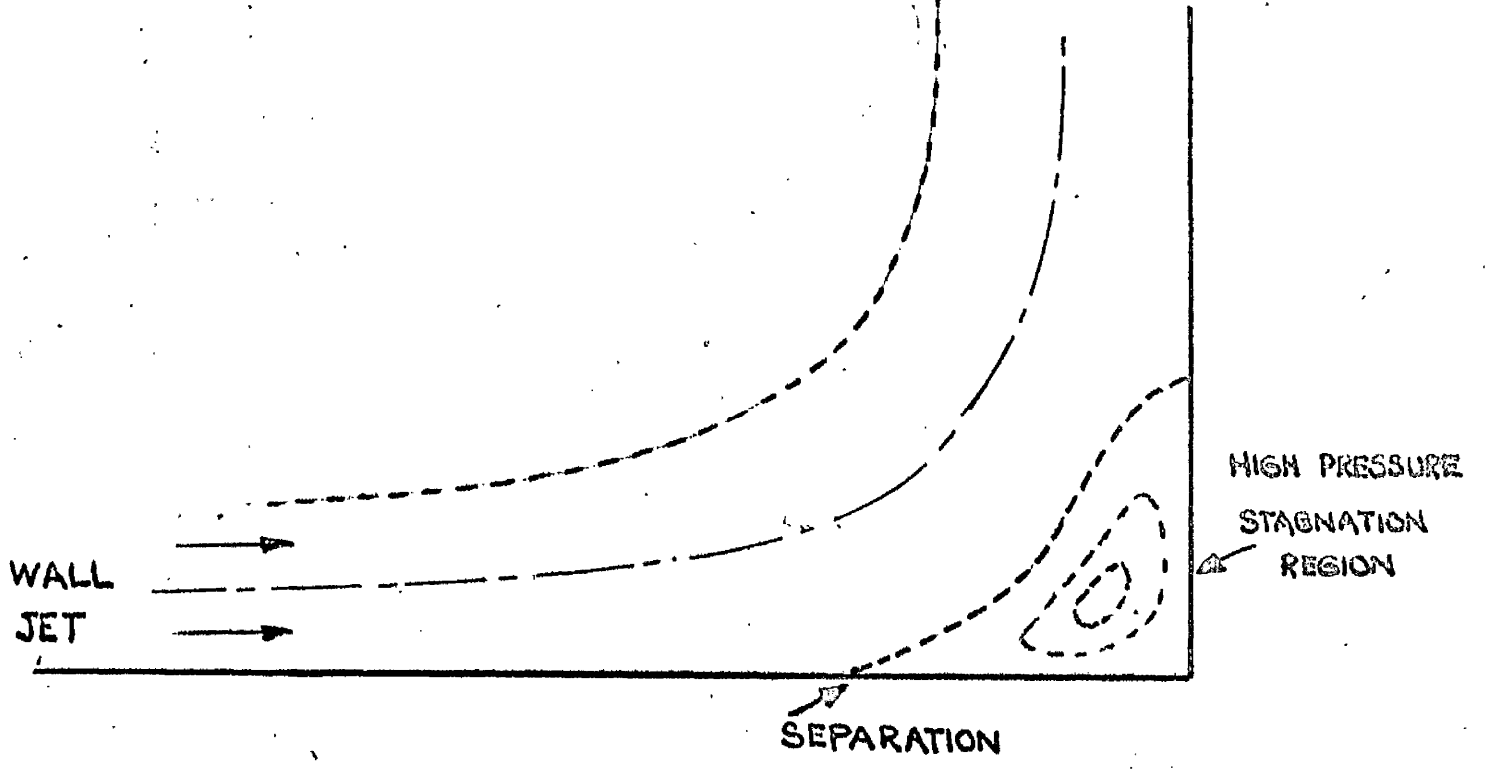

b) SEPARATION DUE TO ADVERSE PRESSURE GRADIENT.

List of references used in the study of flow through valves.

1. Albertson M.L., Dai Y.B., Jenson R.A., Rouse H. 'Diffusion of submerged jets.' Proc. A.S.C.E., Vol. 74., 1948.

2. Benson R.E. 'Experiments on a piston controlled port.' The Engineer, Nov. 25th., 1960.

3. Backe W. 'On the stability of hydraulic control valves under flow conditions.' Thesis to Aachen Tech. Inst., 1960

4. Bakké P. 'An experimental investigation of a wall jet.,' Jl. of Fl. Mechs., Vol.2., 1957.

5. Blackburn J.F., Reethoff G., Shearer J.L. 'Fluid power control.' John Wiley and Co.

6. Bourque C., Newman B.G. 'Reattachment of a 2—D. incompressible jet to a flat plate.' Aero. Quart., Vol. 11, 1960.

7. Bragg S.L. a) 'The effect of compressibility on the discharge coefficients of orifices and convergent nozzles.' Jl. Mech. Eng. Sci., Vol. 2, 1960.
   b) Private communication.

8). Buckingham E. 'Contraction coefficients of jets of gas!' Jl. of Research, Vol. 6, 1931.

9). Chang C.C. 'General consideration of problems of compressible flow using the hodograph method.' N.A.C.A. T.N. 2582.

10). Caille C. 'The even distribution of air emerging at right angles from a duct'.

10). cont. Sulzer Tech. Review, No.1., 1956.

11). Corrsin S. Kistler A.L. 'The free stream boundaries of turbulent flows.' N.A.C.A. T.N.3133.

12). Crabtree L.F. 'a) 'The effect of leading edge separation on thin wings.' Jl. of Aero. Sci., Vol.24.

b) 'Formation of regions of separated flow on wing surfaces.' A.R.C. R. and M. 3127.

13). Dodds J.I. 'The use of suction or blowing to prevent separation of a turbulent boundary layer.' Cambridge Ph.D. thesis, 1961.

14). Donald M.B. Singer H. 'Entrainment in turbulent fluid jets.' Trans. Inst. Chem. Eng., Vol.37, 1959.

15). Emmons H.W. 'The numerical solution of compressible fluid flow problems.' N.A.C.A. T.N. 932., 1944.

16). Eynon G.T. 'Developments in high performance electro-mechanical servomechanisms.' Sym. on Auto. Control, I.Mech. E., 1960.

17). Forstall W. Gaylord E.W. 'Momentum and mass transfer in a submerged water jet.' Jl. of Applied Mechs., 1955.

18). Forthman E. 'Turbulent jet expansion.' N.A.C.A. T.M.789 , 1936.

19). Foster K. Private communication.

20). Frankl F.I. 'The flow of a supersonic jet from a vessel with plane walls.' Trans. Acad. Sci. U.S.S.R., Vol.58, 1947.

21). Glaettli H.H. Private communication.

22). Glauert M.B. 'The wall jet.' Jl. of Fluid Mechs., 1956.

23). Harrison P. 'Tests on a 2–D. model of an oil control valve.' M.E.R.L. Fluids report No. 50.

24). Head M.R. 'Entrainment in the turbulent boundary layer.' A.R.C. R.and M. 3152, 1960.

25). Ishigaki Y. 'Self excited oscillations of a hydraulic control valve without load.' Jl. Jap. Soc. Aero. Space Sci., Dec. 1961.

26). Jobson D.A. 'Flow of compressible fluid through orifices.' Proc. Inst. Mech. Engs., Vol.169, 1955.

27). Lachman G.V. 'Boundary layer and flow control.' Pergamon.

28). Lee S.Y. Blackburn J.F. 'Contributions to hydraulic control.' Trans. A.S.M.E., Vol.74, 1952.

29). Longbottom G. Private communication.

30). MacLellan G.D.S. Turnbull D.E. MitchellA.E. 'Flow characteristics of piston type control valves.' Symp. on auto. control,I. Mech. E. 1960.

31). Mathieu J. Tailland A. 'Study of a plane jet directed tangentially to a wall.' C.R. Acad. Sci., Paris, 252, 1961.

32). Mitchell A.E. a) 'Some characteristics of incompressible flow through piston slide valves.' Cambridge Ph.D. Thesis, 1960.

b) Private communication.

33). Mitchell A.E. Comparin R.A. Muller H.R. Glaettli H.H. 'The limitations and special phenomena in fluid amplifiers.' I.B.M. Research report R.Z. 92 , 1962.

34). Moore C.A. Kline S.J. 'Some effects of vanes and turbulence in 2–D. wide angled subsonic diffusers.' N.A.C.A. T.N. 4080.

35). Morley T.B. 'Flow of air through nozzles.' Proc. I.Mech.E., 1916.

36). Norwood R.E. a). '2-D. transonic jets.'
Thesis to M.I.T. for D.Sc., 1961.
b). 'A flapper valve study.'
Thesis to M.I.T. for M.S., 1959.

37). Olson R.E. 'Reattachment of a 2-D compressible jet to an adjacent plate.'
Symp. of A.S.M.E. on fluid jet devices, 1962.

38). Owen P.R.
Klanfer L. 'Laminar boundary layer separation from the leading edge of a thin aerofoil.'
A.R.C. T.R.16576.

39). Pai S.Y. a)'Introduction to the theory of compressible fluid flow.')
b)'Fluid dynamics of jets.') Van Nostrand.

40). Ricou P.P.
Spalding D.B. 'Measurement of entrainment of axisymmetric jets'
Jl. of Fluid Mechs., Vol. 11, 1961.

41). Rouse H.
Abul-Fetough A.H. 'Characteristics of irrotational incompressible flow through axisymmetric orifices.'
Trans A.S.M.E., Vol. 72.

42). Sawyer R.A. 'The flow due to a 2-D. jet issuing parallel to a flat plane.'
Jl. of Fluid Mechs., 1960.

43). Schaeffer J.W. 'An electrically operated hydraulic control valve.'
Bell System Tech. Jl., 1957.

44). Schlichting H. 'Boundary layer theory.' McGraw – Hill.

45). Schwartz
Cosart 'The 2-D. wall jet.'
Jl. of Fluid Mechs., 1961.

46). Sears W.R. 'Transonic potential flow of a compressible fluid.'
Jl.of Applied Physics, 1950.

47). Shapiro A.H. 'The dynamics and thermodynamics of compressible fluid flow.' Ronald Press.

48). Shearer J.L. 'Resistance characteristics of control valve orifices.'
Sym. on Auto. Control, I.Mech.E., 1960.

49). Sigalla A. 'Measurements of skin friction in a plane turbulent wall jet.'
Proc. R. Ae. Soc., 1958.

50). Spikes R.H.
Pennington G.A. 'Discharge coefficients of small submerged orifices.'
Proc. I.Mech. E., 1959.

51). Stanton T.E. 'On the flow of gases at high speeds.'
Proc. R.Soc., 1926,(A3).

52). Stenning A.H. 'An experimental study of 2-D. gas flow through valve-type orifices.'
A.S.M.E., 1945.

53). Tanaka K. 'Air flow through a suction valve with a conical seat.'
Aero. Res. Inst.,Tokyo Uni., Vol.4(50,51)

54). Tu Y.-O.
Cohen H. 'A theoretical model for separation in fluid jet amplifiers.'
I.B.M. Res.Paper, R.C.816, 1962.

55). Turnbull D.E. 'Some characteristics of hydraulic piston-type control valves in relation to their use as components in a feedback position control system.'
Ph.D. thesis to Cambridge, 1956.

56). Turnbull D.E.
Noton G.J. 'Some factors influencing the stability of piston-type control valves.'
Proc. I.Mech.E., Vol.172,1958.

57). Von Mises R. a) Zeit verein. Deutch Ing., Vol. 61,1917.
b)'Mathematical theory of compressible fluid flow.' Academic Press Inc.

58). Whittaker E.T. 'Generalised hypergeometric functions.' Bulletin of Am. Math.Soc.,Vol.10,1903.

59). Williams H. 'Effect of oil momentum forces on the performance of electro-hydraulic servomechanisms.' Symp. on Auto. Control, I.Mech.E. 1960.

Appendices.

1. Entrainment analysis.
2. Potential solution.
3. Solution for jet angle.
4. Further description of apparatus.

1. Entrainment analysis – prediction of the length of a reattachment bubble in terms of an entrainment parameter σ.

As explained in Chapter 2.2 the entrainment analysis was based on an assumption of the position of the vena contract Two alternative positions were tried, illustrated in Figures 2.8.b and 2.9.b. The latter is the most accurate since the jet must have a short length to contract inwards to its final thickness (Figure 1.3), but the former was included to test the sensitivity of the resulting predictions to small changes in th inlet assumptions.

Referring to Figure 2.9.b, the vertical distance from O to the reattachment plane = $a/2$ and on Figure 2.8.b it is $a/2 + a/2(\sin\varphi)$

Then OG, the distance from O along the radius of curvature to the surface as shown is

$$\frac{a}{2\cos\varphi} \quad \text{or} \quad \frac{a}{2\cos\varphi}(1 + \sin\varphi)$$

$$\text{Thus GO} = \bar{R} - \frac{a}{2\cos\varphi} \quad \text{or} \quad = \bar{R} - \frac{a}{2\cos\varphi}(1 + \sin\varphi)$$

Then from the diagrams –

$$\frac{DG}{DE} = \frac{\cos\vartheta}{\cos\varphi}, \quad \text{where DE} = \bar{R} - \frac{\delta_R}{2}, \text{ giving}$$

$$\frac{\cos\varphi}{\cos\vartheta} = \frac{\bar{R} - \frac{\delta_R}{2}}{\bar{R} - \frac{a}{2\cos\varphi}} \quad \text{or} \quad = \frac{\bar{R} - \delta_{R/2}}{\bar{R} - \frac{a}{2\cos\varphi}(1 + \sin\varphi)} \quad \text{------ *}$$

The edge of the jet is defined as the locus of points where the axial velocity is 0.1 of the centre line velocity on the same normal plane. Thus half the jet width, for a jet with a velocity profile given by $u = U_{max}\,\mathrm{sech}^2 \frac{\sigma Y}{X}$, can be shown to be given by –

$$\frac{\delta_{(\ )}}{2} = \frac{1.818}{\sigma} \cdot X_{(\ )} = kX_{(\ )}$$

In the analysis the jet is assumed to originate from an infinitesmal slit at a distance X_o from the plane of the vena contracta, so that by equating momentum at the inlet plane

$$X_o = \frac{\sigma t}{3} \quad \text{and for the point P,} \quad \frac{3X_P}{\sigma t} = \frac{1}{\tanh^2 \frac{\sigma Y_P}{X_P}}$$

Also using – $\dfrac{X_R - X_o}{\vartheta + \varphi} = \bar{R}$ the equation * becomes

$$\frac{\cos\varphi}{\cos\vartheta} = \frac{X_R - X_o - \frac{(\vartheta+\varphi)}{\sigma} kX_R}{X_R - X_o - \frac{(\vartheta+\varphi)}{\cos\varphi} \frac{3T_R^2}{2\sigma} \frac{a}{t}}$$

or –

$$\frac{\cos\varphi}{\cos\vartheta} = \frac{X_R - X_o - \frac{(\vartheta+\varphi)}{\sigma} kX_R}{X_R - X_o - \frac{(\vartheta+\varphi)(1+\sin\varphi)}{\cos\varphi} \frac{3T_R^2}{2\sigma} \frac{a}{t}}$$

X_o and X_R can then be eliminated to give –

$$T_R^2 = \frac{\cos\vartheta - \cos\varphi - k(\vartheta+\varphi)\cos\vartheta}{\cos\vartheta - \cos\varphi - (\vartheta+\varphi) \cdot \frac{3a}{2\sigma t}} \quad \text{or}$$

$$T_R^2 = \frac{\cos\vartheta - \cos\varphi - k(\vartheta+\varphi)\cos\vartheta}{\cos\vartheta - \cos\varphi - (\vartheta+\varphi) \cdot \frac{3a(1+\sin\varphi)}{2\sigma t}}$$

The other equations linking T_R and ϑ are obtained by making an assumption about the momentum in the region where the jet splits (at reattachment). This is described fully in Chapter 2.2 and the equations are –

$$T_R = 1 - 2\frac{(1 - \cos\vartheta)}{(1 + \cos\vartheta)} \qquad \text{equation (A)}$$

$$\cos\vartheta = \tfrac{3}{2}T_R - \tfrac{1}{2}T_R^3 \qquad (B)$$

$$\cos\vartheta = \tfrac{3}{4}(\tfrac{2}{3} + T_R - \tfrac{1}{3}T_R^3 \qquad (C)$$

Solutions were obtained by solving either (P) or (Q) with one of these, the operation being carried out graphically but the calculations necessary to achieve accuracy in the graphs themselves required seven figure working. This was necessary because of the high sensitivity of equations (P) and (Q) to small changes in ϑ at the points of intersection with the other curves.

An expression for the bubble length can be found from the geometry of the figure in terms of the two parameters T_R and ϑ thus enabling the extent of the bubble to be predicted for any value of entrainment parameter σ.

2. An attempt to obtain a potential solution by an analytical method.

The equation governing the stream function in compressible flow is:-

$$\frac{\partial^2\psi}{\partial x^2}\left(1 - \frac{q_x^2}{a^2}\right) - 2\frac{\partial\psi^2}{\partial x\partial y}\cdot\frac{q_x q_y}{a^2} + \frac{\partial^2\psi}{\partial y^2}\left(1 - \frac{q_y^2}{a^2}\right) = 0$$

with a similar equation for the potential function.

These equations are non-linear and great simplification can be effected by changing the variables x and y into their time derivatives $\frac{dx}{dt}$ and $\frac{dy}{dt}$ (u and v respectively)

In polar coordinates the equations become:-

$$\frac{\partial^2\psi}{\partial q^2} + \frac{1 - M^2}{q^2}\frac{\partial^2\psi}{\partial\vartheta^2} + \frac{1}{q}(1 + M^2)\cdot\frac{\partial\psi}{\partial q} = 0$$

again with a similar equation for the potential function.

Further transformations are possible to obtain even simpl equations, one due to Chaplygin introduces a variable ν , where ν is defined by:-

$$\frac{d\nu}{dq} = -\frac{\rho}{\rho_o}\cdot\frac{1}{q}$$

This transforms the stream function equation into:-

$$\frac{\partial^2\psi}{\partial\nu^2} + \frac{(1 - M^2)}{\rho^2}\cdot\frac{\partial^2\psi}{\partial\vartheta^2} = 0$$

The term $F(\nu) = (1 - M^2)\frac{\rho_o^2}{\rho^2}$ is an implicit function of q and the solution can be simplified by approximating to this function.

Chaplygin's first method of solution (the tangent gas approximati effectively replaced the function $F(\nu)$ by its value at $q = 0$, that is by 1. The method was later improved by von Karman and Tsien to allow the numerical value substituted for $F(\nu)$ to be chosen to suit the particular value of q (gas velocity) at the point of interest.

Such a solution is only suitable for flows well below sonic speed, which was of very little use in the present study since pneumatic valves work at quite high pressures, and the gas speeds are high.

Chang however suggested that closer approximation to $F(\nu)$ would allow the flow to be predicted at almost sonic speeds, and went on to analyse successively more accurate substitutions for $F(\nu)$

Replacing $F(\nu)$ by $a\nu$ is applicable in the region around $M = 1$, as is shown on Figure 4.1.d, and the stream function equati becomes a well known type (Tricomi's equation.)

A more accurate substitution is $F(\nu) = \frac{a\nu}{1 + b\nu}$, and an even more accurate one, (which was the case most closely studied by Chang) is $F(\nu) = \frac{a\nu(1 + b\nu)}{(1 + c\nu)^2}$

Both of these change the equation into forms of the generalised hypergeometric equation, and in particular into Whittaker's equation.

The last substitution yields:-

$$\frac{\partial^2\psi}{\partial q^2} + \frac{a\nu(1 + b\nu)}{(1 + c\nu)^2}\frac{\partial^2\psi}{\partial \vartheta^2} = 0$$

This can be shown to have a general solution:-

$$\psi(\nu,\vartheta) = (C_1\nu + C_2)(C_3\nu + C_4) + A_n W^{(n)}_{k,m}(Z)\sin(n\lambda\vartheta + \alpha_n)$$

where $Z = 2n\lambda \frac{ab}{c^2}(1 + c\nu)$, $W^{(n)}_{k,m}$ is the Whittaker function, and $C_1, C_2, C_3, C_4, A_n, \lambda$ and α_n are all constants to be found from the boundary conditions.

Another benefit of changing to the hodograph plane is the simplification of the boundaries which comes about as a result. Figure 4.1.a shows the problem represented on the physical plane, Figure 4.1.b shows it on the u,v hodograph plane and Figure 4.1.c on the polar hodograph plane (with the velocity transformed to ν) in terms of ν and ϑ.

The problem is now to find values for the constants shown above in terms of the bounds of the flow on the ν,ϑ plane.

Figure 4.1.d shows that when the flow is subsonic the parameter $\underline{\nu}$ is never 0. Also on the streamline AB ($\psi=0$) for some distance along it $\vartheta = 0$ (Figure 4.1.a.) Thus $\psi = 0 = \vartheta$ while ν is finite.

Then either a) $C_4 = \alpha_n = 0$

or b) $C_4 = A_n = 0$

or c) $C_1 = 0$ and $C_4 C_2 = -\sum_{1}^{\infty} A_n W(Z)\sin\alpha_n$

leading to –

a) $\psi_{(\nu,\vartheta)} = (C_1\nu + C_2)C_3\vartheta + \sum_{1}^{\infty} A_n W(Z)\sin\lambda n\vartheta$

b) $\psi_{(\nu,\vartheta)} = (C_1\nu + C_2)C_3\vartheta$

c) $\psi_{(\nu,\vartheta)} = C_2C_3\vartheta - \sum_{1}^{\infty} A_n W(Z)(\sin\alpha_n - \sin\lambda n\vartheta)$

Obviously b) cannot be a solution, and since $\psi = \vartheta = 0$ over a range of ν, alternative c) is also impossible.

Considering the $\psi = Q$ streamline, ψ remains finite while $\vartheta = -\pi/2$ and ν ranges from to a finite value.

Thus either $C_1 = 0$ or $C_3 = C_4 = 0$, so that

$$C_2 C_3 \vartheta + \sum_{-\infty}^{\infty} A_n W(Z) \sin \lambda n \vartheta = \psi_{(\nu,\vartheta)}$$

or

$$\sum' A_n W(Z) \sin \lambda n \vartheta = \psi_{(\nu,\vartheta)}$$

Choosing the first as including the second,

$$\psi_{(\nu,\vartheta)} = K\vartheta + \sum_{1}^{\infty} A_n W(Z) \sin \lambda n \vartheta.$$

Since the solution is in the first quadrant only it has a period of $\pi/2$

Thus $\sin \lambda n(\vartheta - \pi/2) = \sin \lambda n \vartheta$ giving $\lambda = 4$

When $\vartheta = -\pi/2$ $\psi = Q$

Thus $K = -2Q/\pi$ and the solution is —

$$\psi_{(\nu,\vartheta)} = -2Q/\pi + \sum_{1}^{\infty} A_n W(Z)_{k,m}^{(n)} \sin 4n\vartheta$$

Finally by writing the solution as —

$$Q(1 + 2\vartheta/\pi) = \sum A_n W(Z) \sin 4n\vartheta$$

If the R.H.S. is to be a Fourier expansion of the L.H.S. it can be shown that

$$A_n W(Z_o) = 2/\pi \int Q(1 + 2\vartheta/\pi) \sin 4n\vartheta = Q/n\pi (2 - 3\cos n\pi)$$

where $Z_o = 2\pi\lambda \frac{ab}{c^2}(1 + c\nu)$

Giving as the solution

$$\psi_{(\nu,\vartheta)} = -2Q/\pi \vartheta + \sum_{1}^{\infty} Q/n\pi \cdot \frac{W(Z)}{W(Z_o)} (2 - 3\cos n\pi) \sin 4n\pi$$

3) Solution for jet angle;—application of the concept of a force defect coefficient to the flow through a two-dimensional straight sided orifice.

The geometry of the orifice being examined is shown on Figure 4.4., and the nomenclature is given at the beginning of this work.

Referring to Figure 4.4 :—

The contraction coefficient $C = \frac{A_v}{A} = \frac{\dot{m}}{Au_v\rho_v}$

For incompressible flow $\rho . \frac{u_v^2}{2g} = p_o - p_v$

thus $C_i = \frac{\dot{m}}{A\sqrt{2g\rho(p_o - p_a)}}$ — — — (A).

The total reduction in static pressure thrust on side wall (1) in direction (1) is —

$$F_{i(1)} = \int_{A_1}^{\infty} (p_o - p_{w(1)}) dA_{w(1)}$$ where $p_{w(1)}$ is the static pressure at any point $A_{w(1)}$ on the wall (1).

The force defect coefficient, which is constant for incompressible flow, can be defined as —

$$f_{(1)inc.} = \frac{F_{(1)i}}{\frac{\dot{m}^2}{A\rho g}} = \frac{\int_{A_1}^{\infty} \frac{\rho u_v^2}{2g} dA_{w(1)}}{\frac{\dot{m}^2}{A\rho g}} \quad \text{— (B)}$$

Finally by considering the equation of motion of the control area containing all the upstream fluid as far as the vena contracta —

$$F_{(1)i} + A_1 p_o - (A_1 - A_v \cos\varphi) p_a = (A_v p_v + \frac{mu_v}{g}) \cos\varphi \quad - \quad - \quad (C).$$

Combining (A) , (B) and (C)

$$\left.\begin{aligned} f_{(1)i} &= \frac{\cos\varphi_i}{C_i} - \frac{1}{2} \cdot \frac{A_1}{AC_i^2} \\ \text{and similarly} \quad f_{(2)i} &= \frac{\sin\varphi_i}{C_i} - \frac{1}{2} \frac{A_2}{AC_i^2} \end{aligned}\right\} \quad - \quad - \quad - \quad (D).$$

From the two equations (D) it is possible to calculate $f_{(1)i}$ and $f_{(2)i}$ since both C_i and φ_i are assumed to be known.

Compressible supersonic flow.

If the final jet velocity is greater than sonic, then the velocity at the vena contracta will be exactly sonic so that —

$$\frac{p_v}{p_o} = \left(\frac{2}{\gamma+1}\right)^{\frac{\gamma}{\gamma+1}} \quad \text{and} \quad \frac{\rho_v}{\rho_o} = \frac{2}{\gamma+1}^{\frac{1}{\gamma+1}} = r_s^{\frac{1}{\gamma}}$$

From these it follows that —

$$(\rho_v u_v)^2 = \gamma g p_o \rho_o \cdot r_s^{\frac{\gamma+1}{\gamma}} \quad - \quad - \quad - \quad (E).$$

and $$A_v p_v + \frac{\dot{m} u_v}{g} = A_v p_o r_s (1+\gamma) \quad - \quad - \quad - \quad (F).$$

which combine to give —

$$C = \frac{A_v}{A} = \dot{m} / A r_s^{\frac{\gamma+1}{2\gamma}} \cdot \sqrt{\gamma g p_o \rho_o} \quad ($$

The equation of motion of the control area upstream of the vena contracta is —

$$F_{(1)} + A_{(1)} p_o - (A_{(1)} - A_v \cos\varphi) p_a = A_v p_v \cos\varphi + \frac{mu_v}{g} \cos\varphi \quad - \quad ($$

The compressible force defect coefficient can be defined as in the incompressible case.-

$$f_{(1)} = \frac{F_{(1)}}{\dot{m}^2/A\rho_o g}$$

Substituting equations (H), (G) and (F) into this -

$$f_{(1)} C^2 r_s^{\frac{1}{\gamma}} - C\cos\varphi \left[1 - \frac{r_a - r_s}{\gamma r_s}\right] + \frac{A_{(1)}}{A}\left[\frac{1 - r_a}{\gamma r_s}\right] = 0 \quad - \quad (J)$$

and $$f_{(2)} C^2 r_s^{\frac{1}{\gamma}} - C\cos\varphi \left[1 - \frac{r_a - r_s}{\gamma r_s}\right] + \frac{A_{(2)}}{A}\left[\frac{1 - r_a}{\gamma r_s}\right] = 0 \quad - \quad (J)$$

Eliminating φ and solving for C -

$$C^2 = \frac{\left[P - 2r_s^{\frac{1}{\gamma}} \cdot Q\left(f_{(1)}\frac{A_{(1)}}{A} + \frac{A_{(2)}}{A} f_{2)}\right)\right] \pm \sqrt{\left[\quad\right]^2 - 4r_s^{2/\gamma}\left(f_{(1)}^2 + f_{(2)}^2\right) Q^2}}{2r_s^{2/\gamma} \cdot \left(f_{(1)}^2 + f_{(2)}^2\right)}$$

$$- \quad - \quad - \quad (K).$$

Where $P = 1 - \dfrac{r_a - r_s}{\gamma r_s}$ and $Q = \dfrac{1 - r_a}{\gamma r_s}$

Thus provided that $f_{(1)}$ and $f_{(2)}$, the compressible force defect coefficients , are known, C can be calculated from equation (K) and its value substituted back into equation (J) to obtain φ.

In order to derive $f_{(1)}$ and $f_{(2)}$ from the incompressible values it is necessary to make an assumption regarding the up - stream velocity distribution. The assumption previously chosen by Bragg was that the mass flux at the boundary walls is proportional to the flow through the orifice for all flows. In his paper on flow through

symmetrical orifices he shows that this produces accurate predictio for all orifices and nozzles (C varying from 1.0 to 0.5)

The assumption allows the ratios $\frac{f_{(1)}}{f_{(1)i}}$ and $\frac{f_{(2)}}{f_{(2)i}}$ to be expressed in terms of the incompressible values and the pressure ratios $r_{n(1)}$ and $r_{n(2)}$.

These pressure ratios are defined by

$$r_{n(1)} = \frac{\text{pressure at the corner of the (1) wall}}{p_o}$$

$$r_{n(2)} = \frac{\text{pressure at the corner of the (2) wall}}{p_o}$$

and it can be shown that –

$$r_{n(1)}^{2/\gamma}(1 - r_{n(1)}^{\gamma-1/\gamma}) = \frac{k^2\dot{m}^2}{A^2}\frac{(\gamma-1)}{2\gamma g p_o \rho_o} = 2f_{(1)i}C^2 r_a^{2/\gamma}(1 - r_a^{\gamma-1/\gamma}) \quad (1$$

with a similar equation for $r_{n(2)}$

Also – $$\frac{f_{(1)}}{f_{(1)i}} = \frac{2}{r_{n(1)}^{1/\gamma}} - \frac{(\gamma - 1)(1 - r_{n(1)})}{\gamma r_{n(1)}^{2/\gamma}(1 - r_{n(1)}^{\gamma-1/\gamma})} \quad - - \quad (M).$$

$$\frac{f_{(2)}}{f_{(2)i}} = \frac{2}{r_{n(2)}^{1/\gamma}} - \frac{(\gamma - 1)(1 - r_{n(2)})}{\gamma r_{n(2)}^{2/\gamma}(1 - r_{n(2)}^{\gamma-1/\gamma})} \quad - - \quad (M)$$

The method used to evaluate the compressible value of C is as follo

Initially C_i, φ_i and the pressure ratio r_a are known, so tha $f_{(1)i}$ and $f_{(2)i}$ can be found using equation (D). Then by assuming a value for C (somewhat larger than the incompressible value to speed up the process) an approximate $r_{n(1)}$ can be found, which when substituted in (M) gives a value for $f_{(1)}$. Similarly a figure

can be found for $f_{(2)}$ and the two substituted in (K) to get a corrected value for C. The calculation is then repeated using this value of C initially to obtain an even closer approximation to C. In practice the initial assumption for C could be made so close that only three repetitions of the cycle were necessary to evaluate correct to three decimal places. Once C has been found φ can be immediately calculated from equations (J).

This calculation was carried out(using a desk machine) for six pressure ratios at each orifice configuration, and five orifices were investigated. These were $w = \frac{A_{(1)}}{A_{(2)}} = 0,\ 0.25,\ 0.5,\ 0.75$ and 1.0, corresponding to incompressible jet angles of 21°, 28°, 35°, 40.5° and 45°.

The results of the calculations are shown on Figures 4.5 and 4.6, and are discussed in Chapter 4.

Compressible subsonic flow.

The analysis of subsonic flow was made along similar lines but the following equations are different.

Equation (E) becomes – $(\rho_v u_v)^2 = \frac{2\gamma g p_o \rho_o}{\gamma - 1} \cdot r_a^{2/\gamma}(1 - r_a^{\gamma-1/\gamma})$.

since in subsonic flow the conditions at the vena contracta do not correspond to those of a choked nozzle, and thus $r_v = r_a$.

Equation(F) becomes – $A_v p_v + \frac{\dot{m} u_v}{g} = \frac{A_v p_o}{\gamma-1}(2\gamma r_a^{1/\gamma} - (\gamma+1) r_a)$

making Equation (G) $$C = \frac{\dot{m}}{\sqrt{\frac{2\gamma g p_o \rho_o}{\gamma-1} r_a^{2/\gamma} (1 - r_a^{\gamma-1/\gamma})}}$$

Equation (H) is the same but (J) becomes –

$$f_{(1)} C^2 r_a^{2/\gamma} - C\cos\varphi\, r_a^{1/\gamma} + \frac{\gamma-1}{2\gamma} \cdot \frac{A_{(1)}}{A} \cdot \frac{1 - r_a}{1 - r_a^{\gamma-1/\gamma}} = 0$$

and $$f_{(2)} C^2 r_a^{2/\gamma} - C\sin\varphi\, r_a^{1/\gamma} + \frac{\gamma-1}{2\gamma} \cdot \frac{A_{(2)}}{A} \cdot \frac{1 - r_a}{1 - r_a^{\gamma-1/\gamma}} = 0$$

Eliminating φ –

$$C^2 = \frac{\left[1 - \frac{2f_{(1)}A_{(1)}R - 2f_{(2)}A_{(2)}R}{A}\right] \pm \sqrt{\left[\quad\right]^2 - 4R^2(f_{(1)}^2 + f_{(2)}^2)}}{2(f_{(1)}^2 + f_{(2)}^2) \cdot r_a^{2/\gamma}}$$

which is the new equation (K). (L) and (M) remain unchanged.

The arithmetical solutions were obtained by an iterative process as in the supersonic case.

4. Further description of the apparatus

Piston sealing arrangements.

A sectional drawing of a seal pressurising unit is shown on Figure A.1. It consists of a heavy brass cylinder bored out almost completely to a diameter of half an inch. The open end of the closed tube thus formed was tapped $^{3}/_{4}$'' B.S.F. to a depth of $2^{1}/_{2}$''. The piston was made from a brass rod machined to fit the cylinder and with a groove cut near the tip to hold a hard rubber sealing ring. At the closed end of the tube two holes were drilled; one in the side to allow a small pressure gauge to be screwed in (to measure the sealing pressure) and the other in the end to allow a thick walled copper tube to be brazed into the end. This tube was connected to a similar tube on the piston by an Ermeto coupling providing a joint between them which could easily be broken and remade when dismantling the apparatus.

The pressurisers were filled by removing the piston and pouring water into the barrel through the open end. Then by screwin the piston back into the cylinder a pressure of several hundred p.s.i. could easily be produced and maintained, with a reservoir volume of almost a cubic inch. The dimensions of the unit were chosen to exceed the volume of the sealing grooves around the thin walled rubber tubes.

Figure A.2 shows the arrangement of the rubber sealing tube round the edges of the pistons. The tubes lie in grooves machined

in the top two edges of each piston, then down a groove cut acros the face of the piston which is pressed against the runner and back along the bottom two edges. Thus when the apparatus is assembled the tubes are constrained inside rigid passages which allows the pressure to be raised without having to pump a large volume of flui into the tubes. Pressures of more than 300p.s.i. were easily obtain making the seal between the pistons and the perspex complete for all working pressures.

The ends of the tubes are arranged to seal the piston end faces against the ends of the upstream permanent boundary walls. The tubes terminate in holes drilled normally into the faces at the ends of the twin grooves as shown in the figure. One hole is connec ted to the pressuriser by a fine – bore copper tube, while the othe passes right through the wall and is by a metal plug. This plug can be removed to allow the tubes to be filled with water, which is necessary so that the volume of water supplied from the pressuriser is a minimum.

Schraeder pneumatic valve tubing was used and the ends were sealed with Evostick adhesive.

Details of pressure tappings.

The distribution of the tappings along the main piston face is shown on Figure A.2. Near the corner where they are closer together the diameter of the tappings was reduced in case the ratio of hole pitch to hole diameter became too small, which affects the boundary layer and gives false readings of static pressure.

The small insert in Figure A.2 shows the method used in makir the tappings. First a fine hole was drilled completely through the wall of the piston, then the hole was opened out to within $^1/_8$ in. of the outer wall. This allowed a substantial stainless steel tube to be driven into the hole, leaving an inch of tube protruding to make connection to the manometer. Thus although the tapping size was very small the length of passage with that diameter was also small ($^1/_8$in.) and the time constant not unduly large. The method used by previous investigators was to insert the tube completely through the wall resulting in a time constant of minutes, whereas the new method decreased it to a few seconds. The dimensions of the arrangement are given on the drawing.

Polythene tubing (internal diameter 2 m.m.) was used to transmit the pressure signals from the pistons to the measuring apparatus — lengths of 8 ft. being used without appreciably increas sing the time constant.

Details of extra pistons used in special tests.

Two extra pistons were used in the experiments described in Chapters 3 and 5.

The first of these (used in the incompressible experiments) consisted of the same boundary configuration but with two rows of static pressure tappings along the piston face as shown in Figure A.3. Since this piston was to be used only once, it was made of perspex and the tappings inserted by the old method described abov In this instance however the tubes inserted were of polythene and

were cut off flush with the surface using a razor blade. Great care was needed to ensure that no roughness was left at the edges of the holes since it was found that this had a considerable effect on the indicated pressure.

The second piston, shown on Figure A.4, was used in the measurement of jet angle (chapter 5) and is a simple rectangular piston with one of the downstream walls removed to prevent reattachment and to ensure free access of atmospheric air to the inner edge of the jet.

Initially the strut AB across the open end was omitted (to ensure a free flow of gas into the jet) and the deflection of the t due to the pressure of the gas in the upstream chamber caused false readings. The strut rectified this completely.

Automatic pressure recording unit.

The difficulties experienced during these tests showed that both methods used to measure static pressure traverses were unsatisfactory. Reading the manometer one tube at a time was too slow to remove errors due to fluctuations in the supply pressure, and the photographic method did not average out oscillating readings so that the 'frozen' pictures had to be processed by eye to remove spurious values. Both methods also required a great deal of human time to convert readings into useful data.

An automatic recording system was therefore designed and a diagrammatic sketch is shown on Figure A.5. The unit was made at the end of the present tests and could not be used in the main body

of experimentation.

The system consists of a Solartron pressure scanning valve capable of measuring the pressure at each of 48 tappings in turn using a transducer. The output from this is measured on a digital voltmeter and printed out on a paper strip. It is hoped that the printout can be later replaced by a tape punch suitable for direct input to a digital computer.

A control unit attached to the valve drive allows any single tapping to be monitored and recorded or any group of tappings.

Solution is :-

$$\Psi(\nu,\theta) = -\frac{2Q}{\pi}\theta + \frac{Q}{\pi}\sum\frac{1}{n}\frac{W(z)}{W(z_0)}(2-3\cos n\pi)\sin 4n\pi$$

$$d\phi = \frac{\partial\phi}{\partial x}\cdot dx + \frac{\partial\phi}{\partial y}dy = q\cos\theta\,dx + q\sin\theta\,dy$$

$$d\psi = \text{similarly} = \frac{\rho}{\rho_0}q(-\sin\theta\,dx + \cos\theta\,dy)$$

then eliminating x and y $\quad dz = \frac{e^{i\theta}}{q}(d\phi + i\frac{\rho_0}{\rho}d\psi)$

an eliminating ϕ $\quad dz = \frac{e^{i\theta}}{q}\left\{\left[K(\nu)\frac{\partial\psi}{\partial\theta} + i\frac{\rho_0}{\rho}\frac{\partial\psi}{\partial\nu}\right]d\nu + \left[-\frac{\partial\psi}{\partial\nu} + i\frac{\rho_0}{\rho}\frac{\partial\psi}{\partial\theta}\right]d\theta\right.$

Thus $\frac{\partial z}{\partial\nu}$ and $\frac{\partial z}{\partial\theta}$ can be found $\left(dz = \frac{\partial z}{\partial\nu}d\nu + \frac{\partial z}{\partial\theta}d\theta\right)$

Integrating $\frac{\partial z}{\partial\theta}$ leaves a f^n of (ν) to befound. This can be evaluated by differentiating again w.r.t. ν and equating to $\frac{\partial z}{\partial\nu}$. The $F(\nu)$ is found to be a constant.

Finally,

$$x = \frac{2Q}{q\pi}\frac{\rho_0}{\rho}\sum_1^{\infty}\left[(2-3\cos n\pi)\left(\frac{2W'(z)\frac{\rho}{\rho_0} + W(z)}{W(z_0)}\right)\cdot\frac{\cos(4n+1)\theta}{4n+1} - \cos\theta\right.$$

$$\left. + (2-3\cos n\pi)\left(W(z) - 2W'(z)\frac{\rho}{\rho_0}\right)\frac{\cos(1-4n)}{1-4n}\right]$$

$$y = \frac{2Q}{q\pi}\frac{\rho_0}{\rho}\sum_1^{\infty}\left[(2-3\cos n\pi)\left(\frac{2W'(z)\frac{\rho}{\rho_0} + W(z)}{W(z_0)}\right)\cdot\frac{\sin(4n+1)\theta}{4n+1} - \sin\theta\right.$$

$$\left. + (2-3\cos n\pi)\left(\frac{W(z) - 2W'(z)\frac{\rho}{\rho_0}}{W(z_0)}\right)\cdot\frac{\sin(1-4n)\theta}{1-4n}\right]$$

FIGURE A.1.

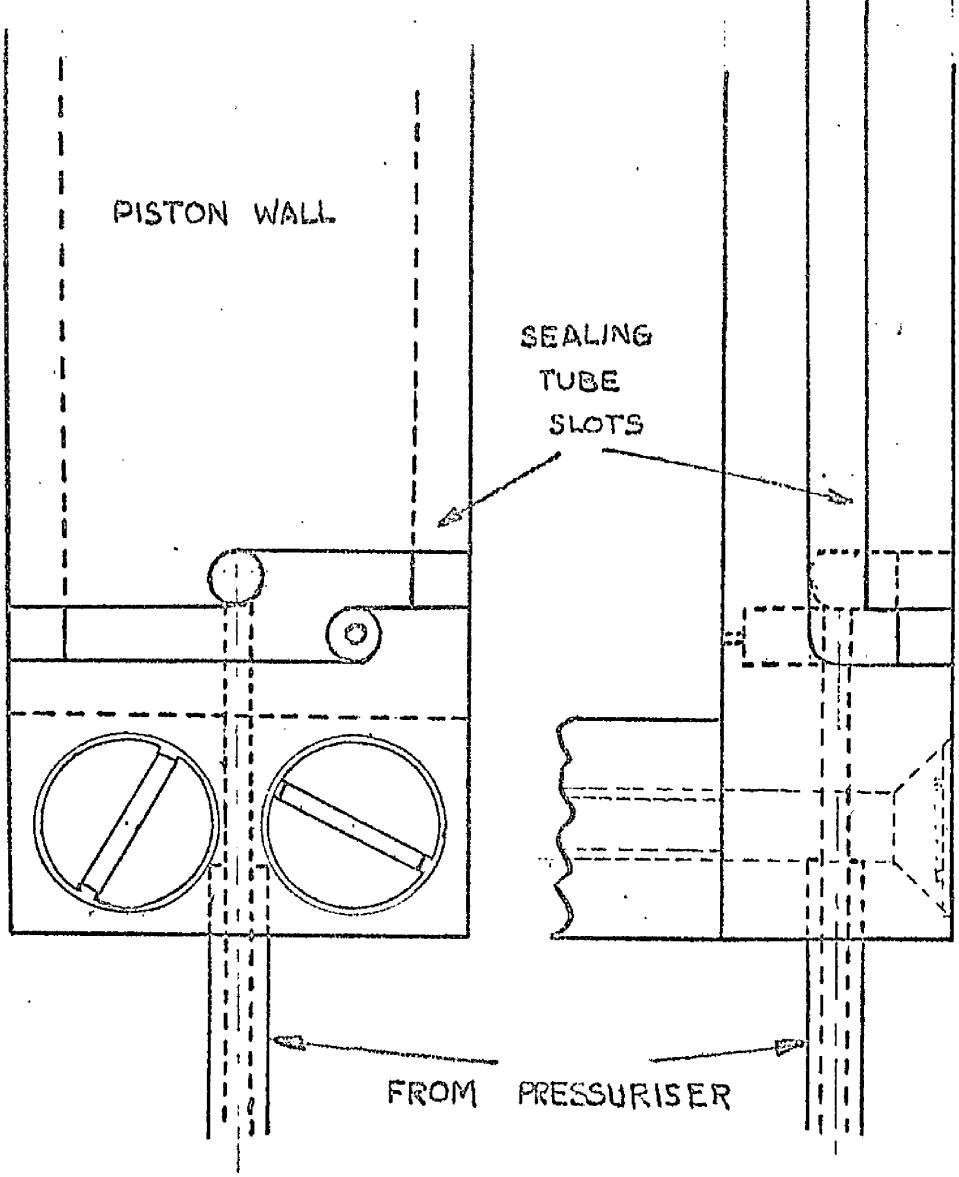

ARRANGEMENT OF SEALING TUBES.

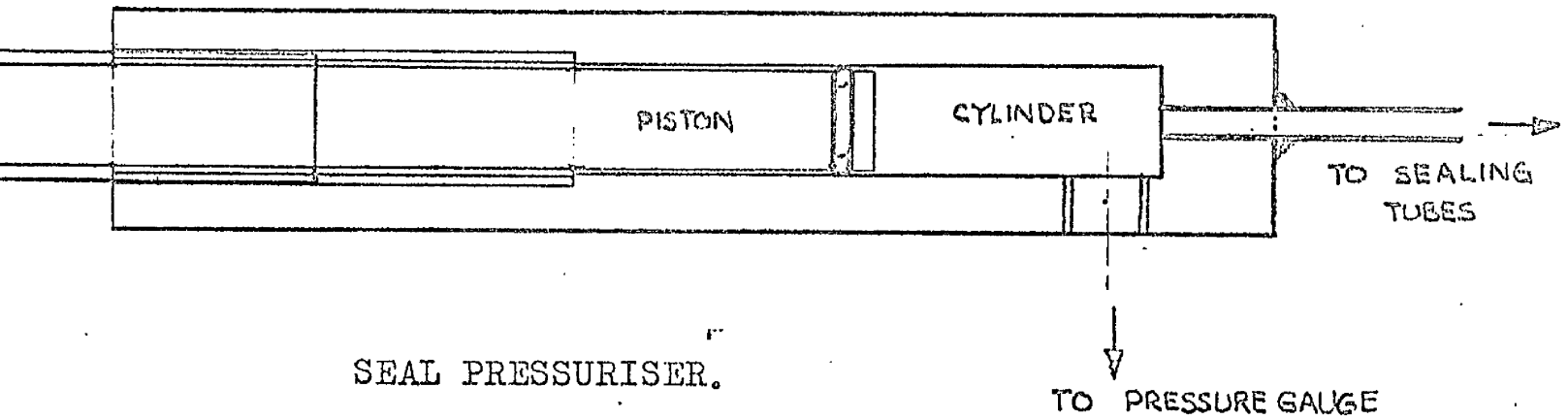

SEAL PRESSURISER.

FIGURE A.2.

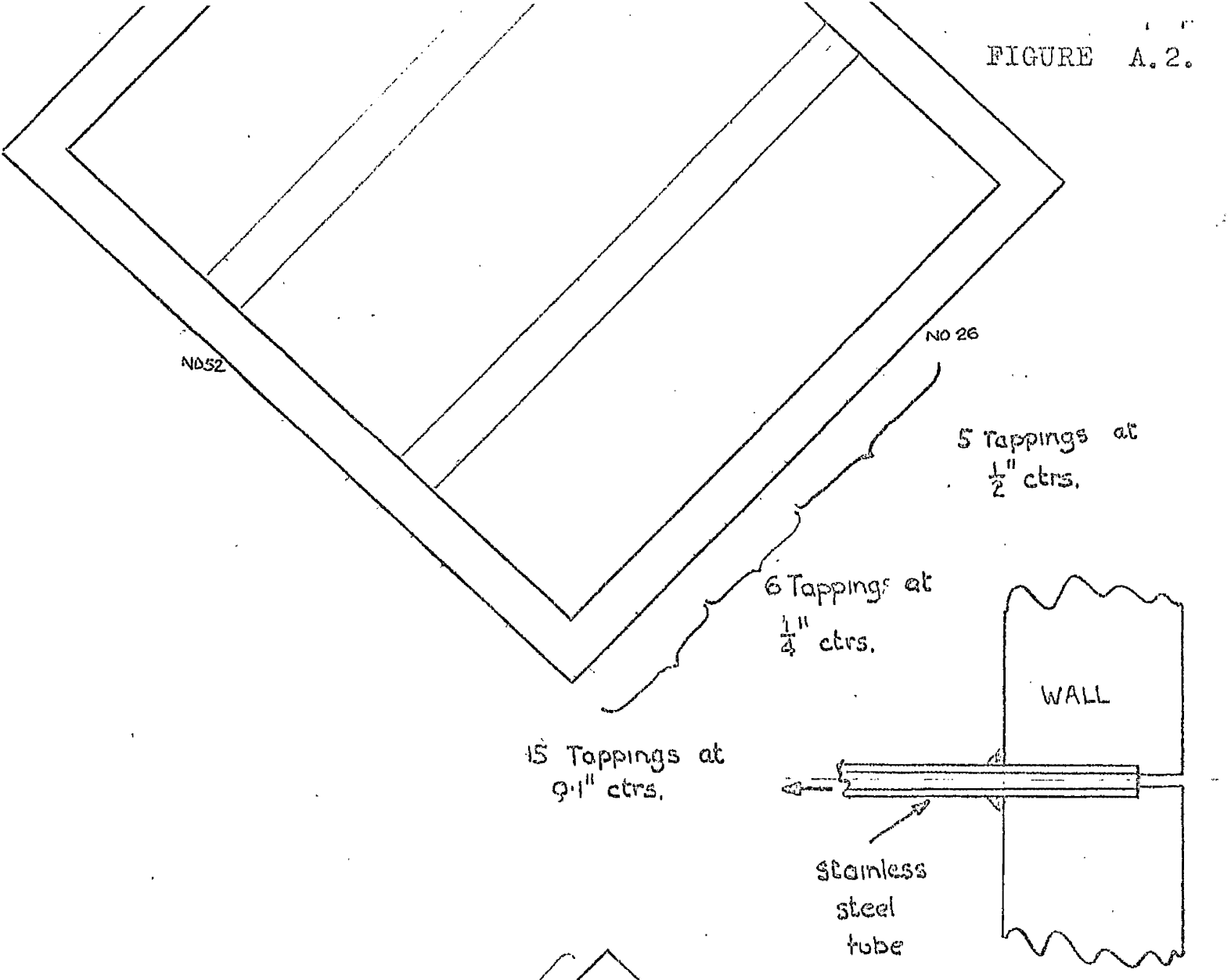

ARRANGEMENT OF PRESSURE TAPPINGS.

FIGURE A.3.

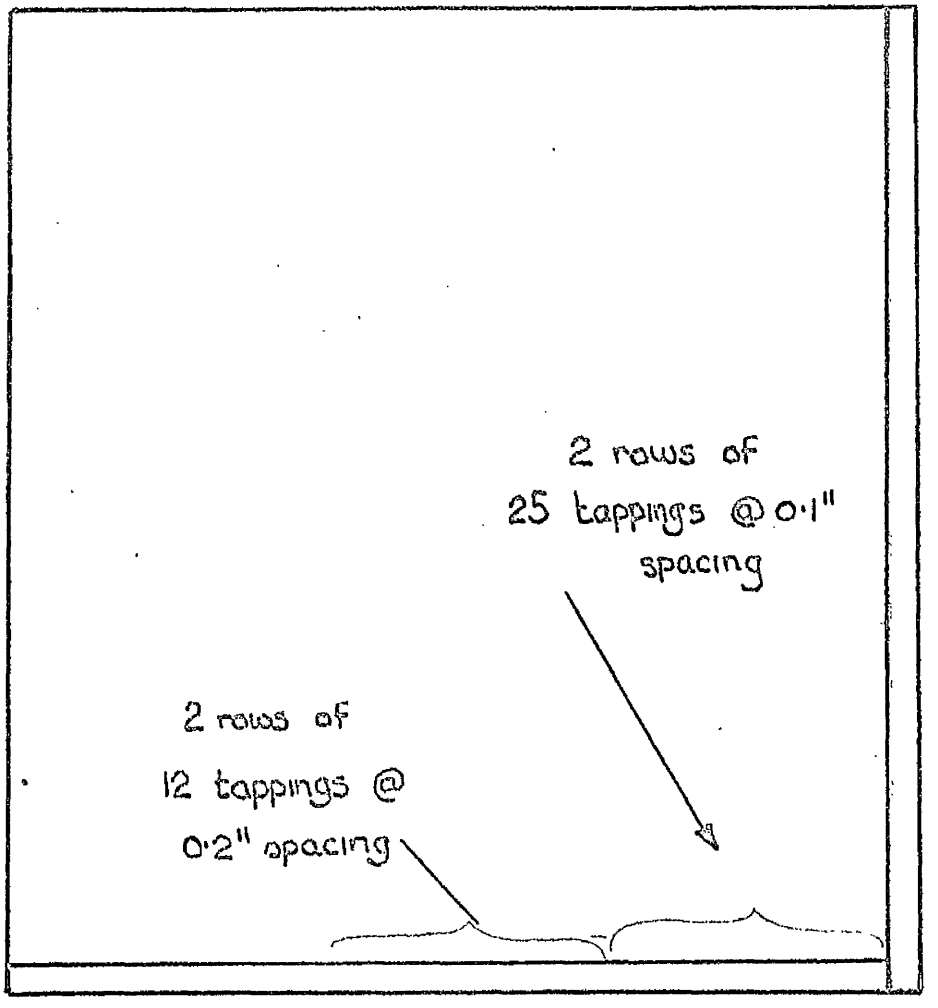

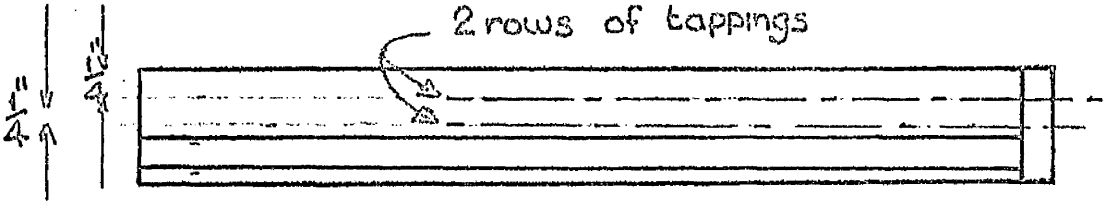

SPECIAL PISTON TO TEST THREE — DIMENSIONAL EFFECT.

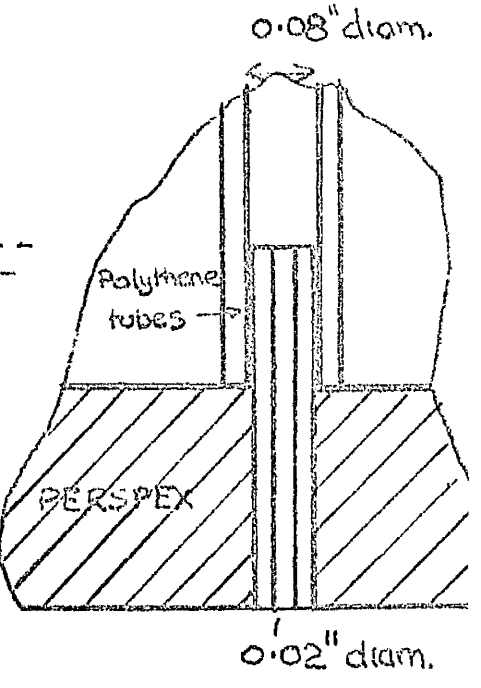

DETAIL OF TAPPING

FIGURE A.4.

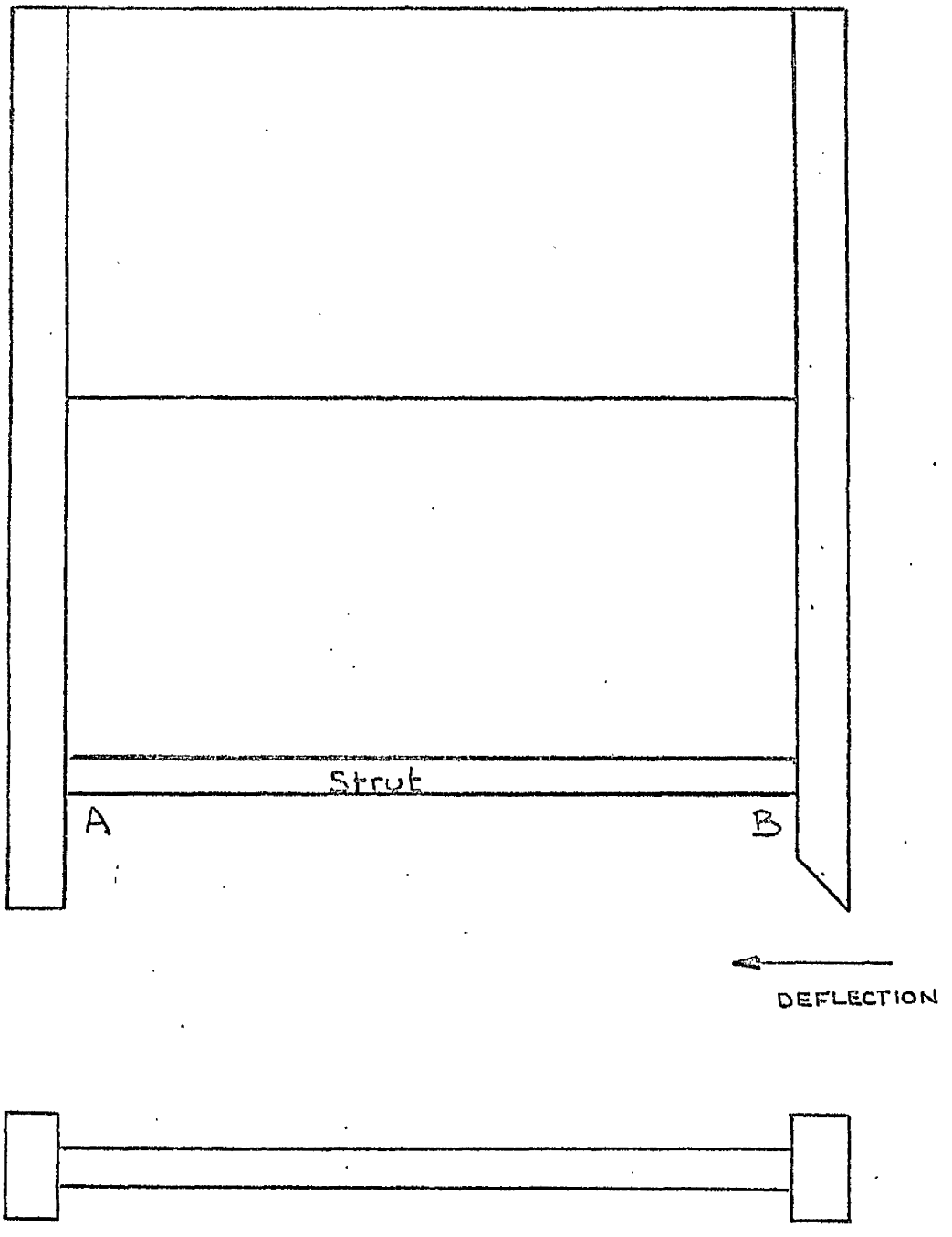

PISTON WITH DOWNSTREAM WALL REMOVED TO STOP REATTACHMENT.

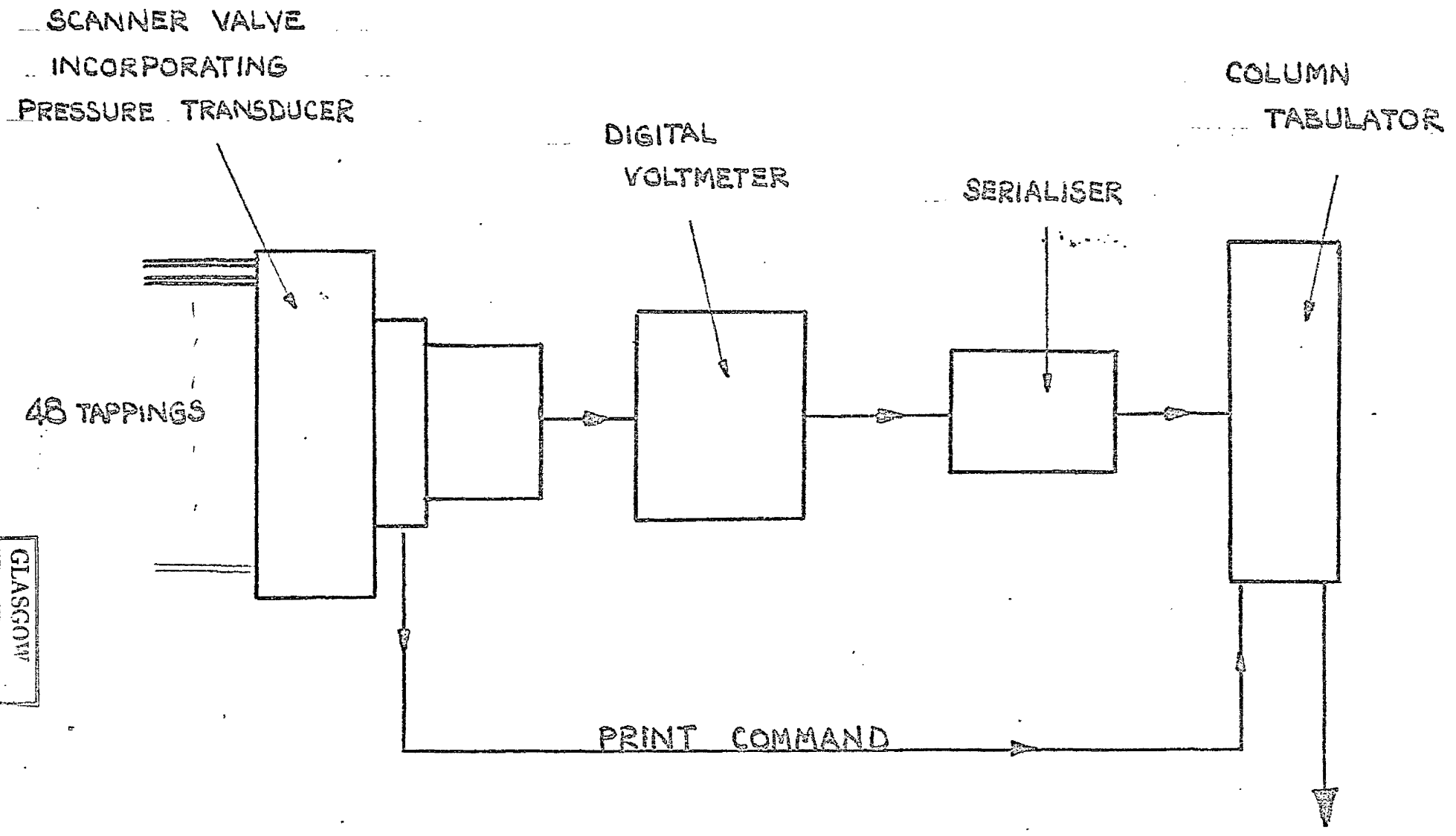

ARRANGEMENT OF AUTOMATIC PRESSURE RECORDING SYSTEM.

FIGURE A.5.